Luís Barreto

Intraspecific variation in response to marine heatwaves in two northeast Atlantic kelp species

UAlg FCT
UNIVERSIDADE DO ALGARVE
FACULDADE DE CIÊNCIAS E TECNOLOGIA

2024

Luís Barreto

Intraspecific variation in response to marine heatwaves in two northeast Atlantic kelp species

Doutoramento em Ciências do Mar,
da Terra e do Ambiente
Trabalho efetuado sob a orientação de:
Prof. Gareth Pearson
Prof. Ester Serrão
Prof. Inka Bartsch

UAlg FCT
UNIVERSIDADE DO ALGARVE
FACULDADE DE CIÊNCIAS E TECNOLOGIA
2024

Intraspecific variation in response to marine heatwaves in two northeast Atlantic kelp species

Declaro ser o autor deste trabalho, que é original e inédito. Autores e trabalhos consultados estão devidamente citados no texto e constam da listagem de referências incluída.

ACKNOWLEDGEMENTS

I want to thank my supervisors Gareth Pearson, Ester Serrão and Inka Bartsch for giving me this incredible opportunity and guide me.

To Ester, a big thank you for always supporting me when times were not so favourable.

To Gareth for always being compressive and able to find a way for me to progress.

To Inka, for the inspiring conversations and always be realistic and at the same time positive.

To BEE lab. team across my PhD: Neiva, Tania, Susana, Ana, Licinia, Cristina, Aschwin and a great thank you to Neusa!

To Jorge Assis and Eliza Fragkopoulou.

To the students that integrated their work with this project: Rasa Tverskyte, Eva Smid, Anne Davison, Raquel Torres, Laura Dennis, Hjalmar Ruud, Lennard Ypma, Fiona-Strasser

To the ones that assist during experiments and sampling: David Milla, Alexandre Jueterbock, Soukaina Kaidi and Sabour Brahim, João Franco and Myriam Valero

To Klaus Valentine for providing essential financial support for genetic analysis that will provide further knowledge enhancement of this thesis.

To my Family and friends for all the love and support, in special to my mother for always being there for and with me.

To the ones that should be here, you know.

And to Mafalda, when we started this adventure, we were only 2 now we are 4 and it could not be any better!

FUNDINGS

This study received Portuguese national funds from FCT - Foundation for Science and Technology through the PhD grant SFRH/BD/139189/2018, COVID/BD/152961/2022, FCT Cotutelas PESSOA ref 6/9, RESTORESEAS (FCT-DivRestore/0013/2020 BiodivERsA), MARFOR (FCT-BiodivERsA/0004/2015), and UIDB/04326/2020 (DOI:10.54499/UIDB/04326/2020), UIDP/04326/2020 (DOI:10.54499/UIDP/04326/2020) LA/P/0101/2020 (DOI:10.54499/LA/P/0101/2020), FCT Portugal – CNRST Morocco bilateral cooperation project 'Variation of marine-forests traits in range-edge vs core NE Atlantic upwelling refugia in a context of climatic change'. Ref. 0504/19/CNR, 2019-2021, and from the operational programmes CRESC Algarve 2020 and COMPETE 2020 through project EMBRC.PT ALG-01-0145-FEDER-022121.

Abstract

Kelp forests, one of the most productive and biodiverse ecosystems are shifting their distributional ranges due to changing environmental conditions including marine heatwaves (MHWs). We tested two kelp sister species from thermally and phylogenetically differentiated clades, *Laminaria hyperborea* (cold-temperate) and *Laminaria ochroleuca* (warm-temperate) using populations across the latitudinal gradient of the species distribution in the northeast Atlantic. We specifically selected these ecological models because *L. ochroleuca* is expanding its northern distribution poleward while outcompeting the once dominant *L. hyperborea* which in turn is contracting at its southernmost distribution limits in the Iberian Peninsula. Local thermal regimes and long-term MHW metrics were performed to characterize the thermal exposure of each population and integrate temperature in the experimental design. *L. ochroleuca*, the effects of depth were also investigated on deep (-50 m) and shallow (-4 m) populations. We performed simulated MHWs (sMHWs) with field-collected adults, *in vitro* cultured gametophytes (microscopic sexual phase), and cultured F1 juvenile sporophytes derived from gametophyte crosses. *L. hyperborea* from the South warm edge population showed 100% mortality during recovery at 23 ºC sMHW, contrasting to the other regions. We analysed for the first time the genetic structure and diversity of *L. hyperborea* across its distribution, revealing high and unique genetic diversity in the less resilient ancient South populations. *L. ochroleuca* gametophytes showed population variation as onset of mortality in the North began at 23°C, while in the remaining populations mortality was only apparent at 27°C. The deep *L. ochroleuca* adult population (Az) was thermally inhibited by the highest sMHW temperatures but able to recover indicating photoinhibition that was not observed in the F1 juveniles (Me). F1 juvenile sporophytes from the North population were unable to fully recover photosynthetically (photodamage) from all sMHWs. This intraspecific variation may potentially be associated with reduced thermal tolerance in cooler northern regions.

Keywords: Kelp forests, marine heatwave, intraspecific variation, thermal stress, warm distributional edge

Resumo

Compreender como as espécies estruturantes em ecossistemas, incluindo savanas e pradarias, florestas terrestres, recifes de corais e florestas de kelp, se adaptam e persistem em toda a sua área de distribuição às mudanças nas condições ambientais é fundamental para prever as respostas dos ecossistemas face ao aumento da intensidade, frequência e duração das anomalias de aquecimento do ambiente e mudanças de longo prazo nos regimes térmicos. Uma destas anomalias de aquecimento são os ondas de calor marinhas (MHWs), eventos anómalos discretos de aumento da temperatura da água do mar que excedem os registos históricos e que causaram mudanças massivas de espécies e perda de biodiversidade em todo o mundo. As consequências podem ser particularmente graves para espécies estruturantes e engenheiros de ecossistemas, como pradarias de ervas marinhas, recifes de coral, mangais e florestas de kelp, onde os efeitos em cascata do seu declínio e/ou desaparecimento têm consequências profundas em todo o ecossistema. As florestas de kelp, formadas por grandes macroalgas castanhas são ecossistemas altamente produtivos e diversificados, atuando como viveiros, alimento e abrigo para uma variedade de organismos marinhos que podem ser encontrada em áreas costeiras relativamente baixas em todo o mundo, fornecendo importantes recursos socioeconômicos diretamente através da produção de alimentos, e extração de alginato/hidrocolóide, e indiretamente por espécies de interesse associadas (por exemplo peixes, moluscos, crustáceos). No entanto, eventos climáticos extremos, incluindo MHW, empurraram florestas de kelp inteiras para além dos limites ecofisiológicos com consequências graves, incluindo a perda maciça de biomassa de algas, o desaparecimento total das florestas e alterações nos ecossistemas. A variação intraespecífica entre populações de todo o limite de distribuição provavelmente inclui contribuições de adaptação local (mudanças adaptativas nas frequências alélicas em direção aos ótimos locais) e de plasticidade fenotípica (a capacidade de um genótipo de expressar diferentes fenótipos em resposta a diferentes condições ambientais). Populações antigas no limite de distribuição mais quente contemporâneo normalmente exibem uma diversidade genética rica e única em comparação com as populações mais recentes do

norte devido à dispersão relativamente baixa de propágulos, efeitos fundadores e "genetic surf". Foi sugerida resiliência ao stresse térmico devido à aclimatação, adaptação e plasticidade fenotípica em populações no limite quente de distribuição para algumas espécies de kelp.

O objetivo desta tese foi abordar uma grande lacuna de conhecimento na pesquisa de espécies marinhas: avaliar a variação intraespecífica em nível populacional (ou seja, plasticidade fenotípica e/ou adaptação local) em espécies de kelp formadoras de florestas. Para isso, testamos duas espécies de algas pertencentes a grupos filogenéticos irmãos com diferentes afinidades térmicas; *Laminaria hyperborea* (grupo temperado frio) e *L. ochroleuca* (grupo temperado quente). Para cada espécie, adultos de campo foram amostradas e (para *L. ochroleuca*) estabelecidas culturas de gametófitos ao longo do gradiente latitudinal das respetivas regiões norte, central e sul de suas distribuições no Atlântico Nordeste. Regimes térmicos locais e métricas de MHW de longo prazo foram obtidos e analisados para caracterizar o histórico de exposição térmica de cada população e integrar a temperatura no desenho experimental. Para a *L. ochroleuca*, também fomos capazes de investigar experimentalmente duas populações profundas (-50 m) juntamente com as populações costeiras mais rasas (-4 m) do gradiente latitudinal. Realizamos ondas de calor simuladas em laboratório (sMHWs) específicas para cada espécie, *L. hyperborea* (19, 21, 23 ºC) usando apenas adultos amostrados em campo e *L. ochroleuca* (21, 23, 25 ºC) usando adultos amostrados em campo, gametófitos cultivados originados desses adultos, e em esporófitos juvenis da geração F1 cultivados in vitro (removendo assim a "memória" de exposição ao campo parental) derivados de cruzamentos de gametófitos masculinos e femininos. Também fomos capazes de preencher uma lacuna de conhecimento para *L. hyperborea*, ao realizarmos a primeira (até quanto sabemos) análise da estrutura genética em toda a distribuição continental. A análise genética destaca padrões semelhantes de diversidade nas duas espécies de Laminaria ao longo do gradiente latitudinal, em ambos os casos as populações mais quentes do limite Sul exibindo uma diversidade genética rica e única em comparação ás correspondentes regiões Centro e Norte. No entanto, quando avaliamos as respostas ecofisiológicas dos esporófitos adultos as sMHWs, a similaridade nos seus padrões de diversidade genética não se traduziu em respostas semelhantes ao stresse térmico entre as espécies. A população do grupo temperado frio *L. hyperborea* no limite Sul teve 100% de mortalidade no sMHW mais elevada (23 ºC) no final do período de recuperação, enquanto as regiões Centro e Norte conseguiram recuperar. Por outro lado, o desempenho fotossintético das populações do grupo quente L. ochroleuca do limite Sul não diferiu das populações Centro e Norte. Mostramos que o enriquecimento com nutrientes teve um efeito positivo nos parâmetros ecofisiológicos da fotossíntese (Fv/Fm,

rETRmax) e crescimento em resposta as sMHWs nos esporófitos adultos e juvenis F1 de *L. ochroleuca*. Gametófitos mostraram variação intraespecífica na sobrevivência sendo a população do Norte a mais sensível termicamente, com mortalidade a começar a 23°C, enquanto a mortalidade nas restantes populações só foi aparente a 27°C. As populações também variaram no sucesso reprodutivo, com Espanha e Marrocos exibindo um sucesso reprodutivo muito baixo no final da recuperação de 23°C e 25°C, enquanto após a recuperação de 27°C ambas as populações ultrapassaram a França e a Itália no desenvolvimento reprodutivo e produção de esporófitos. Isto pode indicar uma seleção potencial para uma estimulação da produção reprodutiva quando confrontados com stresse térmico extremo. Populações profundas de esporófitos adultos de *L. ochroleuca* destacaram a sua suscetibilidade as sMHWs, com valores mais baixos de ambos os parâmetros fotossintéticos (F_v/Fm, $rETR_{max}$) em comparação com as populações costeiras de pouca profundidade. Isto pode indicar alguma combinação de foto dano ou foto inibição durante a sMHW a 25°C. Isto pode ser uma indicação de adaptação local das populações profundas à baixa disponibilidade de luz e à estabilidade térmica no seu ambiente natural, uma vez que a penetração da luz em profundidade é rapidamente atenuada mesmo em águas límpidas e as oscilações térmicas são muito baixas (0,9°C), portanto a seleção de genótipos mais adequados para crescer e se reproduzir nessas condições podem estar em andamento. Comparações regionais de esporófitos juvenis F1 destacam a fraca capacidade geral de recuperação da população do Norte no desempenho fotossintético (especialmente $rETR_{max}$) em ambos os tratamentos com nutrientes e em todas as temperaturas das sMHWs (21, 23, 25°C), indicativo de foto dano (necrose do tecido e/ou danos ao aparelho fotossintético). Abordamos ainda futuras linhas de pesquisa e medições para proteger e manter as antigas e únicas populações de profundidade e do Sul.

Palavras-chave: Florestas de kelp, variação intraespecífica, stresse térmico, limites de distribuição quentes

TABLE OF CONTENTS

LIST OF ABBREVIATIONS AND ACRONYMS

MHWs - marine heatwaves

UST - upper survival temperatures

MST - maximum mean seawater temperatures

sMHW - simulated marine heatwave

AR - allelic richness

HE - expected heterozygosity

PA - private alleles

RGR - relative growth rate

SST – sea surface temperature

D_{mean} - mean MHW duration

D_{max} - maximum MHW duration

I_{avrmax} - average of the highest temperatures during MHWs

I_{max} - single highest temperature value during MHW

I_{cum} - and the cumulative intensity

PAM fluorometer - pulse amplified modulated fluorometer

RLC - rapid light curve

PSII - photosystem II

F_m - maximum fluorescence level elicited by a saturating light pulse that closes all PSII reaction centers

F_0 - minimum fluorescence level measured with a very low intensity modulated measuring light under which PSII reaction centres remain open

F_v/F_m - maximum quantum yield of PSII

ETRmax - maximum electron transport rate

rETRmax - relative maximum electron transport rate

ETR_{mPot} - maximum potential light-saturated electron transport rate

a - alpha, the initial slope of the RLC

β - photoinhibition parameter

PES - Provasoli Enriched Seawater

RC - recovery

SW – seawater

IT – Italy

Mo – Morocco

SP – Spain

FR – France

F1 – First filial generation

Me – Messina deep population

Az – Azores deep population

SWT – sea water temperature

Chapter 1

General introduction

1.1 Kelp forests

Kelp forests formed by large brown macroalgae (Class Phaeophyceae; Order Laminariales *sensu stricto*) are among the most productive marine ecosystems on the planet (Duarte et al., 2022; Pessarrodona et al., 2022). The high biomass canopies that extend into the water column (D. C. Reed et al., 2008; Bartsch et al., 2008) result in three-dimensional habitats that modify the surrounding physical environment by reducing wave and current energy (Rosman et al., 2007), attenuating light levels (Wernberg et al., 2005; Desmond et al., 2015), and changing sedimentation composition (Alsuwaiyan et al., 2021). Kelp forests cover ca. 25% of the world rocky shores across temperate and subpolar regions (Steneck et al., 2002; Teagle et al., 2017), with a world-wide distribution including all continents except Antarctica (Fig. 1.1) (Wernberg, Krumhansl, Filbee-Dexter, & Pedersen, 2019).

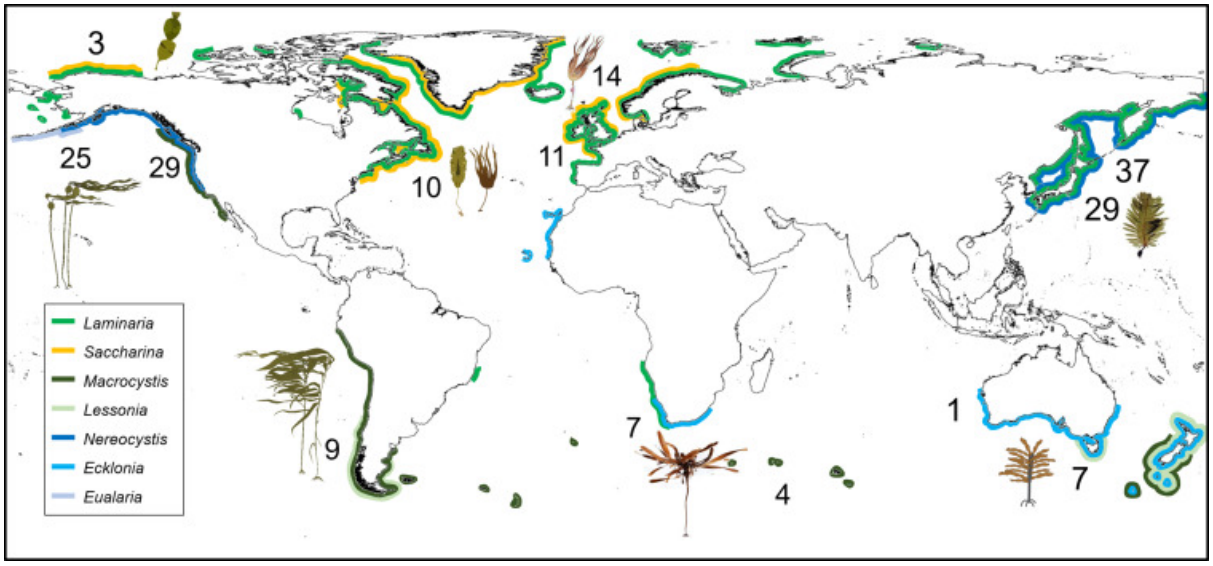

Figure 1.1: Kelp forests distribution worldwide. Colored lines indicate the distribution of kelp genera and numbers correspond to number of kelp species. From Wernberg et al., 2019.

The high productivity and diversity of kelp forest ecosystems provide nursery grounds, food and shelter for a variety of marine life (Steneck et al., 2002; Teagle et al, 2017; Wernberg et al., 2019; C. M. Duarte et al., 2022). As kelp forests and their associated community can be found in relatively shallow coastal areas world-wide (Wernberg et al., 2019), their extraction and cultivation has a long association with coastal human societies worldwide (Erlandson et al., 2005) and potentially facilitated human dispersal from Asia to the Americas (Erlandson et al., 2015). This prolific ecosystem thus provides important socio-economic resources directly

through food production, and alginate/hydrocolloid extraction (Bartsch et al., 2008), and indirectly through the shelter and nutrition of associated species of interest (*e.g.*, fish, molluscs, crustaceans; Beaumont et al., 2008; Bertocci et al., 2015; Wernberg et al., 2019). Additional important ecosystem services of increasing relevance include nutrient sequestration (Kim et al., 2015) and carbon storage (Krause-Jensen & Duarte, 2016). The estimated value of kelp forests per hectare range from $38.8 in the South-eastern Pacific to $280.6 in the North-western Pacific, with a global annual production estimated at $500 billion and a 20 year global estimated value of 7.4 trillion dollars internationally (Eger et al., 2023).

1.2 Life cycle and knowledge gaps

Kelps have a haploid-diploid heteromorphic life cycle (Fig. 2) in which sex is expressed in the haploid (N) microscopic gametophyte phase. External fertilization of the female egg by the male sperm, which are attracted by a pheromone produced by the former (Muller et al., 1979). After syngamy, the resulting zygotes develop to produce the diploid (2N) macroscopic sporophyte which grow, develop and eventually produce reproductive tissue (sorus) containing haploid flagellated spores (N) by meiosis (*i.e.,* meiospores) that are released into the water column. The negatively phototactic spores swim to the benthos and attach, subsequently generating by mitosis a male or female gametophyte (N) and completing the life cycle (Bartsch et al., 2008; Schiel & Foster, 2015; Veenhof et al., 2022) (Fig. 1.2).

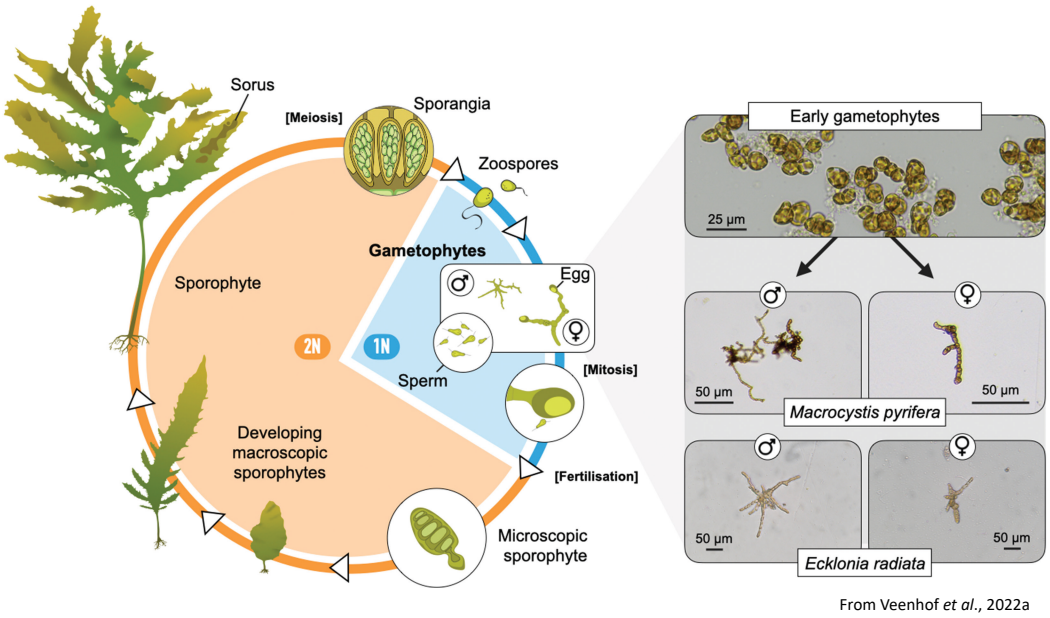

Figure 1.2: Laminariales life cycle: Diploid (2N) reproductive sporophyte produces haploid spores (N) by meiosis from which male and female gametophytes (N) develop. After gametes are form, female egg is fertilized by male sperm forming a microscopic sporophyte (2N) that develops. From Veenhof et al., 2022a.

The physiological requirements of the alternating life stages of Laminariales (*sensu stricto)* are regulated by abiotic and endogenous factors. Gametophyte sexual reproduction – gametogenesis - is induced by blue light and Fe ions (Lüning & Dring, 1972; Motomura & Sakai, 1984) at (depending on the species) optimum temperatures between 5 to 18°C and between 4 to 90 µmol m^{-2} s^{-1}. Sporophyte reproduction (sporogenesis) is regulated by photoperiodic induction and occurs at optimal temperatures between 1 to 18°C and 5 to 200 µmol m^{-2} s^{-1} (see Bartsch et al., 2008 [p.18] and references therein for factors governing the different stages of Laminariales life cycle). Growth of sporophytes is controlled by both circadian and circannual cycles with light saturation between the 20 to 100 µmol m^{-2} s^{-1}, optimum temperatures between 5 to 15°C and nutrient dependency (Bartsch et al., 2008 and references within). Gametophytes are sometimes considered analogous to terrestrial plant seed banks (Chapman, 1986) that persist as dormant or semi-dormant microscopic stages in the benthic substrata, or potentially as endophytes (Garbary et al., 1999; Bringloe et al., 2018) able to withstand periods of unfavourable environmental conditions such as marine heatwaves (MHWs). Indeed, gametophyte upper survival temperatures (UST) range from 1 to 7°C above those of sporophytes (tom Dieck, 1993), and may contribute to their capacity to persist until favourable conditions for microscopic gametophyte reproduction and sporophyte growth are present. Nevertheless, several studies have reported the failure of kelp forests to recover after the total loss of sporophytes following a MHW event (Smale & Wernberg, 2013; Filbee-Dexter

et al., 2016; Arafeh-Dalmau et al., 2019; but see also Ladah et al., 1999) suggesting either that the gametophyte UST was exceeded or that life history transitions such as gametogenesis or sporophyte recruitment were impaired (Veenhof et al., 2022a).

An increase in research focused on kelp microscopic life stages over the last years has begun to shed some light on how complex and dynamic these stages are with, for example, the development of metabarcoding by next-generation sequencing to identify gametophytes in natural seed bank (Robuchon et al., 2014; Akita et al., 2019), the role of herbivory in the seed bank as both consumers and dispersal agents by expelling gametophytes in faecal matter (Veenhof et al., 2022b), or the identification of gametophytes as endophytes in several red algae that may serve as a grazing avoidance mechanism (Garbary et al., 1999; Hubbard et al., 2004; Bringloe et al., 2018). Nevertheless, there are still major knowledge gaps and questions to address, related to the intrinsic difficulty of studying microscopic life stages in the field (Veenhof et al., 2022a; Edwards, 2022): For how long can gametophytes be dormant in the seed bank and what are the effects of multiple stressors such as MHWs, sedimentation or pollution on dormancy time? What is the impact of such stressors (especially in combination) on life history progression (gametogenesis and microscopic sporophyte recruitment) as these processes are specifically connected to environmental cues such as light intensity, temperature, and circadian rhythms (Bartsch et al., 2008)?

The macroscopic sporophytes (the kelp forests) also have a variety of constraints on their study such as the limitations on sampling in wave exposed and strongly tidal systems where most kelps are found (Birkett et al., 1998), the seasonality of their reproduction or growth (Sjøtun et al., 2010) and the depth and inaccessibility of some populations (*e.g.* deep populations in very clear seawater [page 18 table 4 in Bartsch et al., 2008]). Several knowledge gaps have started to be addressed but require further investigation such as detailed research on ecophysiology and population biology (biomass, density, age structure and fertility) for a range of Laminariales species and between different populations over latitudinal and depth gradients and across seasons (Bartsch et al., 2008; Smale et al., 2013), the role of the microbiome in response to external abiotic and biotic stressors (e.g., temperature [Minich et al., 2018], grazing [Tan et al., 2020], or competition), the effects of pathogens on growth and reproduction in species and populations (King et al., 2023), and the assessment of competitive abilities of Laminariales with sympatric or alien species under changing environmental conditions scenarios (García-Sánchez et al., 2016).

1.3 Kelp evolution and biogeography of the genus *Laminaria*

The origin (crown age) of the kelps dates back to approximately 73 million years (Ma), but the major burst of diversification that form modern kelp diversity (Laminariales) with 137 species occurred during the Eocene-Oligocene boundary, approximately 31.5 Ma in the Northeast Pacific (Starko et al., 2019; Bringloe et al., 2020). It has been suggested that the accelerated rate of marine speciation inferred during the Eocene-Oligocene boundary was due to a previous marine mass extinction event associated with a decrease in seawater temperature (Ivany et al., 2000) ideal for kelp expansion into new habitats that were putatively less biodiverse and resilient (Erwin, 1998; Starko et al., 2019). From the Northeast Pacific, kelps dispersed across continents and oceans, crossing the equator and entering the Arctic in several iterations and speciation rates increased 6-fold in the past 15 million years (Starko et al., 2019). Two morphological characteristics that appear to have evolved independently multiple times were upright growth and branching associated with complex 3-dimensional kelp forest habitats, supporting the hypothesis that adaptive radiation (rapid increase in the number of species from a common ancestor, characterized by high ecological and morphological diversity [Neige, 2015]) drove kelp diversification (Starko et al., 2019).

The genus *Laminaria* originated in the Northwest Pacific around 25 Ma with subsequent dispersal to the eastern Pacific (Fig. 1.3). According to the phylogenetic evidence

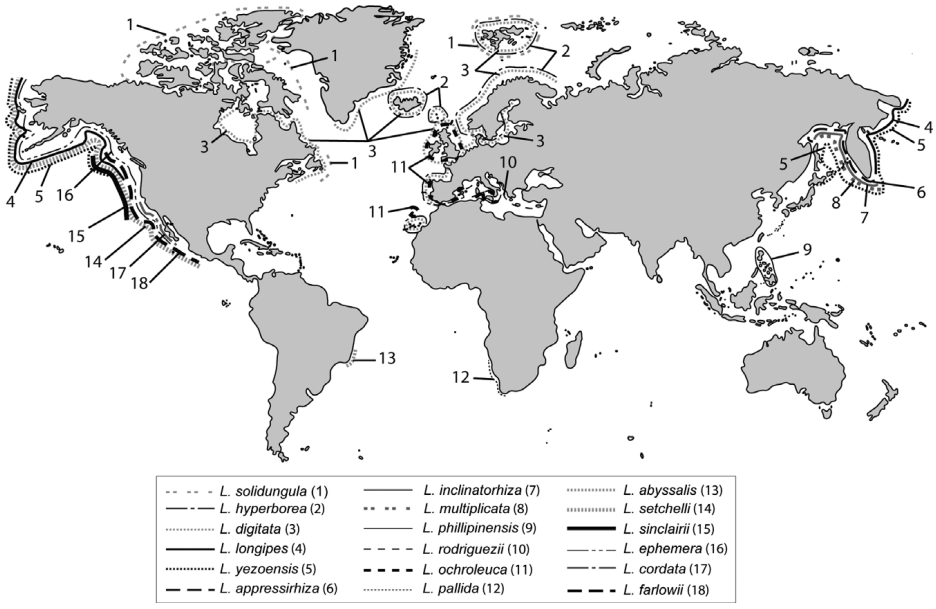

Figure 1.3: Laminaria species global distribution. Adapted from Rothman et al., 2017.

Presented in Rothman et al. (2017), *Laminaria* then crossed through the Arctic to the Atlantic at least twice after the opening of the Bering Strait ~ 5.3 Ma, once giving rise to *L. solidungula* and a second event resulting in the other Atlantic species (Rothman et al. 2017). The second event was followed by dispersal south towards North Atlantic American and European coasts, the Mediterranean, North Africa. Finally, *Laminaria* crossed the equator twice to the South Atlantic coasts of Africa and America (Rothman et al., 2017; Starko et al., 2019) resulting in a contemporary total of 18 *Laminaria* species globally (Fig. 3; Rothman et al., 2017). In the Arctic/Atlantic and Mediterranean there are currently 7 recognized *Laminaria* species: *L. solidungula, L. hyperborea, L. digitata, L. rodriguezii, L. ochroleuca, L. pallida* and *L. abyssalis* (Fig. 3). These 7 species form 3 phylogenetic clades (Rothman et al., 2017) that also correspond to thermal clades based on the UST of the sporophyte (tom Dieck, 1992): an Arctic clade with the solitary species *L. solidungula* that only occurs in the Arctic circle, a cold-temperate clade containing *L digitata* and *L. hyperborea,* and a warm-temperate clade containing *L. ochroleuca, L. pallida, L. abyssalis* and *L. rodriguezii*. The divergence of the cold- and warm-temperate clades is estimated to have occurred relatively recently, ~ 3.5 Ma (Rothman et al., 2017).

1.4 Study models: *L. hyperborea* and *L. ochroleuca*

We used two species model, one each from the cold- and warm temperate clades, *Laminaria hyperborea* and *Laminaria ochroleuca*, respectively. *Laminaria hyperborea* is distributed across the Northeast Atlantic Ocean from the North of Portugal (current southern limit of distribution) to North of Norway in mainland Europe (Kain, 1967; Rothman et al., 2017) (Fig. 1.4), and as far north as the Arctic Ocean (Svalbard; (Hop et al., 2012)).

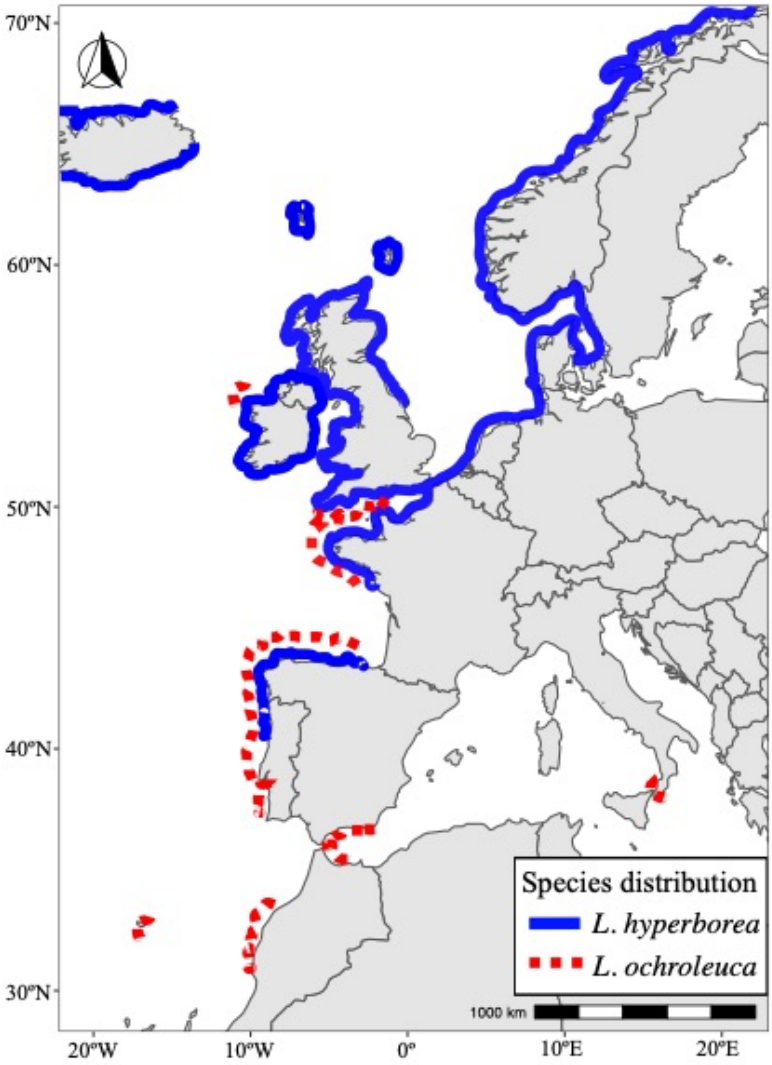

Figure 1.4: Distribution of *L. hyperborea* (blue line) and *L. ochroleuca* (red dotted line) across the Northeast Atlantic and Mediterranean.

L. hyperborea forms monospecific perennial kelp forests producing high biomass stands and providing shelter to a diverse associated fauna and flora (Sjøtun et al.,1995; Leclerc et al., 2015; Fig. 1.5).

Figure 1.5: Monospecific *L. hyperborea* forest with adult and juvenile under canopy forming a complex 3d habitat. By George-Stoyle

L. hyperborea characterized by a upright growth (rigid stipe) and branching of the blade (Starko et al., 2019), with a high biomass and richness of epiphytes in both the haptera and the stipe (Mikhaylova & Shtrik, 2007) due to the longevity of this species (estimated maximum age 18 years; Sjortun & Fredriksen, 1995). It inhabits relatively shallow rocky subtidal habitats (max depth 32 m; Bartsch et al., 2008 and references within) with semi to strong wave exposure (Rinde & Sjøtun, 2005; Pedersen et al., 2012). Growth occurs mainly during winter and beginning of spring (Luning, 1979) with the shedding of the old blade material. Reproduction (sporulation) also occurs in winter. Laboratory assessed UST for *L. hyperborea* was 20ºC for juvenile sporophytes and 21ºC for gametophytes (J. J. Bolton & Lüning, 1982). The Southern edge of distribution is in the North of Portugal with an alarming rate of population disappearance in the NW Iberian Peninsula region (Fernández, 2011; Casado-Amezúa et al., 2019). *L. hyperborea* is the main kelp species being harvested in Europe, mainly in Norway (Vea & Ask, 2011; Barbier et al., 2019) with a steady annual harvest of 130,000–180,000 t wet weight (Vea & Ask, 2011) which corresponds only to 1% of the estimated global algae production industry (Barbier et al., 2019).

The golden kelp, *L. ochroleuca*, the representative warm-temperate clade species, is distributed not only on shallow coastal rocky bottoms but also occurs as deep populations in habitats > 90m depth, particularly on open ocean seamounts and in the Mediterranean Sea (Assis et al., 2018; Schoenrock et al., 2019; Strasser et al., 2022) (Fig. 1.6).

Figure 1.6: Monospecific deep *L. ochroleuca* forest. By OCEANA / Juan Carlos Calvín

L. ochroleuca forms perennial subtidal forests, sometimes intermixed with *L. hyperborea* and *Saccorhiza polyschides* were species distributions overlap. It is also characterized by a upright growth (rigid stipe) and branching of the blade (Starko et al., 2019), with a high biomass production together with a rich suite of gastropod grazers (Smale et al., 2015). Laboratory experimental UST was 21ºC for juvenile sporophytes (tom Dieck, 1992) and ranged between 24-25ºC for both male and female gametophytes (Franco et al., 2018; tom Dieck, 1992). Range contractions have been observed for *L. ochroleuca* in the Iberian Peninsula (Fernández, 2011; Tuya et al., 2012; Voerman et al., 2013) and poleward distributional shifts are reported into the English Channel (UK, Smale et al., 2015) and more recently into Ireland (Schoenrock et al., 2019).

1.5 Intraspecific variation

In the Northern Hemisphere, interglacial periods correspond to a poleward recolonization by species as temperatures rise and/or ice cover retreats (Hewitt, 1996; Stewart et al., 2010; Bringloe et al., 2020). For such species, the long-term centre of distribution corresponds to areas where populations have continuously persisted across glacial – interglacial periods near the contemporary warmer southern distributional edges (Bennett & Provan, 2008;

Stewart et al., 2010; Assis et al., 2018). Intraspecific variation among populations from the entire distributional range likely includes contributions from **local adaptation** (adaptive changes in allele frequencies towards local optima; King et al., 2018), and **phenotypic plasticity** (the ability of a genotype to express different phenotypes in response to different environmental conditions; Becker et al., 2015). Ancient populations at the contemporary warmest distributional edge typically display rich and unique genetic diversity compared to more recent northern populations due to relatively low propagule dispersal (King et al., 2018), founder effects (Barton & Charlesworth 2003) and genetic surfing (Hallatschek & Nelson 2008; Neiva et al., 2010). Resilience to thermal stress due to acclimation, adaptation and phenotypic plasticity in low latitude edge populations has been suggested for some kelp species (Atkins & Travis, 2010; Wernberg et al., 2018; King et al., 2019; Liesner et al., 2020). However, decadal-scale ocean warming and the increasing frequency and intensity of MHWs threaten to outpace adaptative capacities under rapidly deteriorating environmental conditions, and the potential extirpation of unique gene pools in some species (Wernberg et al., 2018; Filbee-Dexter et al., 2020). Despite accumulating evidence for the role of local adaptation and phenotypic plasticity in responses to environmental change (Valladares et al., 2014; Liesner et al., 2020; Strasser et al., 2022), studies focused on detecting intraspecific variation in response to MHWs remain scarce (King et al., 2018; Liesner et al., 2020; Strasser et al., 2022). Models that aim to predict future species distribution often assume a uniform species response (Reed et al., 2011 ;Holt & Gomulkiewicz, 2004), potentially compromising the effectiveness of kelp conservation, restoration and farming actions taken by decision-makers.

1.6 Threats to kelp forests, the case of MHWS

Understanding how foundation species such as kelps adapt and persist across their distribution range under (rapidly) changing environmental conditions is fundamental to predict ecosystem responses in the face of increasing intensity, frequency and duration of warming anomalies and long term shifts in thermal regimes (Pecl et al., 2017; Schirpke et al., 2017; Frade et al., 2018; Smale et al., 2019). Temperature is the major factor constraining the distribution of marine species at latitudinal scales, and biogeographical ranges are often defined by the species tolerance to winter minimum and summer maximum mean seawater temperatures (MST; Edgar et al., 2017; Stuart-Smith et al 2017). The gradual increase of MST (0.6°C on average NOA, 2021) observed over the past century has already caused shifts in

species distribution (Parmesan & Yohe, 2003) and phenology (e.g., reproduction; Hu et al., 2022; Hoppit & Schmidt, 2022). Moreover, the last 3 decades have seen abrupt high seawater temperature anomalies increase in frequency and duration (Oliver et al., 2018; Holbrook et al., 2019). Indeed, marine heatwaves (MHWs – discrete anomalous events of seawater temperature increase exceeding historical records; Hobday et al., 2016) have caused massive species shifts and biodiversity loss worldwide (Jones et al., 2018; Smale et al., 2019; Cheung et al., 2021; Garrabou et al., 2022). In recent years, extreme climate events including MHWs have pushed entire forests beyond ecophysiological thresholds, causing severe impacts including massive kelp biomass loss (Filbee-Dexter et al., 2016; Krumhansl et al., 2016; Arafeh-Dalmau et al., 2019), reductions in survival and growth (Bennett et al., 2015; Filbee-Dexter et al., 2020), and in some cases ecosystem shifts from kelp forests to much less productive and diverse turf algae-dominated systems (Filbee-Dexter et al., 2016; Karen Filbee-Dexter & Wernberg, 2018). Due to their rapid development as well as their increasing magnitude and duration, MHWs are particularly dangerous for sedentary organisms that are unable to evade warm water masses (Perez, Garrabou et al., 2000; Smale et al., 2017). The consequences may be particularly severe for foundation species and ecosystem engineers such as seagrass meadows, coral reefs, mangroves and kelp forests (Hays et al., 2021), where the cascading effects of their decline and/or disappearance have profound consequences on the entire ecosystem (Coleman & Williams, 2002; Thomson et al 2014 ; Smale et al., 2019). The disruption due to MHWs of ecosystem services provided by foundation species worldwide (*e.g.*, nursery areas, food supply, shelter, fisheries, coastal erosion protection; Wernberg et al., 2012; Smale et al., 2019 ; Garrabou et al., 2022) may amount to socio-economic losses of billions of dollars (Beaumont et al., 2008; Vassallo et al., 2013; Vásquez et al., 2014; Bennett et al., 2016; Blamey & Bolton, 2017; Himes-Cornell et al., 2018). Indirect socio-economic costs of a single MHW has been accounted above $3.1 billion with the loss of carbon storage and ecosystem services provided by a seagrass meadow in Sharkbay, Australia (Arias-Ortiz et al., 2018).

1.7 Aims and objectives

There is a large consensus on the need to fill severe knowledge gaps for kelp forests (Bartsch et al., 2008; Smale et al., 2013; Starko et al., 2019) as these prolific, rich and diverse ecosystems are currently under extreme global declines in the face of oceanic warming conditions

(Krumhansl et al., 2016b; Pessarrodona et al., 2019; Smale et al., 2019) Nimbs et al., 2023). Nonetheless, the number of research studies focused on kelp forests is the low than that for the other main marine foundation groups (corals, mangroves and seagrasses) and just a very small fraction of the overall number of studies in marine science overall (Elliott Smith & Fox, 2022) (Fig.7).

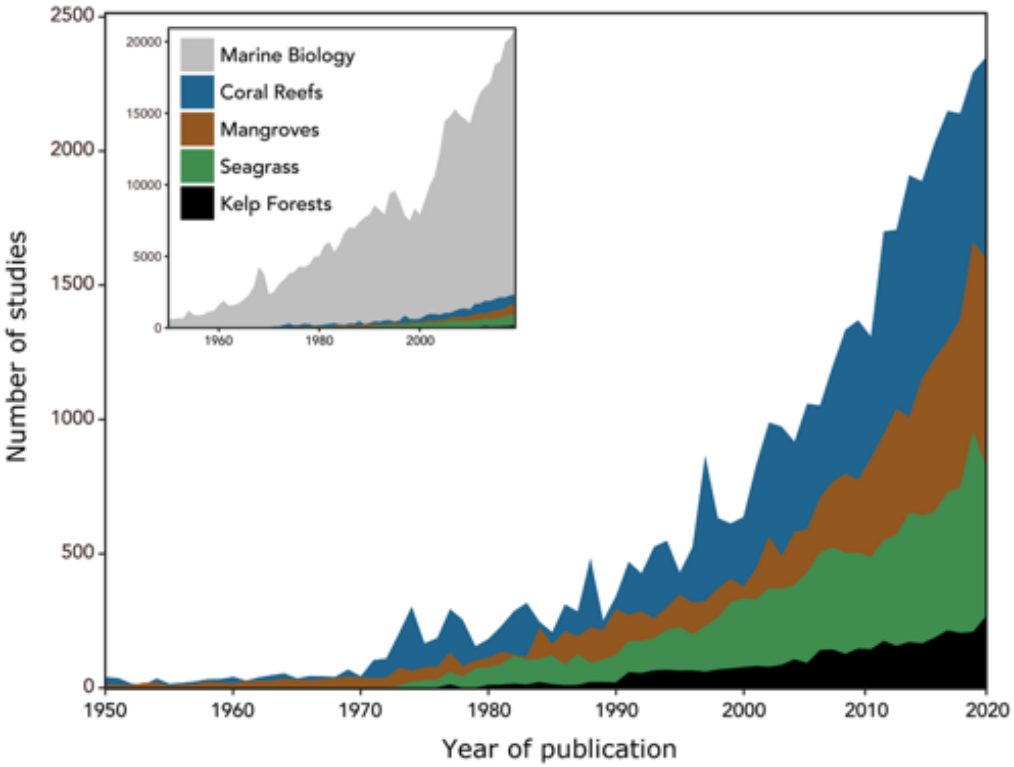

Figure 1.7: Number of studies for for kelp forests (black), seagrass systems (green), mangrove habitats (brown) and coral reefs (blue) and overall marine biology sciences (grey). From (Elliott Smith & Fox, 2022)

Although global drivers such as increasing mean sea water temperature and frequency of storms might be affecting kelps forest at multiple levels, research shows that local stressors and regional variation are the main factors in the decline and loss of kelp systems (Krumhansl et al., 2016; Perkins-Kirkpatrick & Lewis, 2020). As such, in this study we proposed to analyse a major knowledge gap in kelp forest research, intraspecific (population level) variation of two phylogenetically and thermally distinct clades of the *Laminaria* genus, a cold-temperate clade member *L. hyperborea,* and a warm-temperate clade member *L. ochroleuca*:

L. hyperborea: Our aim was to analyse the currently undescribed genetic structure and phenotypic variability of this species, in which populations from the southern (warm edge) distribution have declined and/or disappeared over the last 3 decades (Casado-Amezúa et al., 2019). We additionally analysed the thermal regime and long-term MHW metrics from 3

geographically distinct regions covering the contemporary distribution of the species. Available field survey data were used to characterize density, size and structure of *L. hyperborea* beds in each region. We investigated intraspecific (population level) variation in ecophysiological responses (photosynthesis, growth and survival) to simulated heat waves in the laboratory (sMHW, including the interacting effects of temperature and nutrient availability) in field-collected adult individuals from each region. Genetic diversity and differentiation among populations was assessed using a broader sample of 12 populations.

L. ochroleuca: Our aim was to analyse intraspecific (population level) variation across 1) a latitudinal gradient of the species distribution (North, Centre and South) but also 2) between shallow (-4m) and deep (-50m) populations. For this we used different ontogenetic stages: field-collected adult sporophytes, cultured gametophytes, and *in vitro* generated (F1s) sporophytes cultured under common garden conditions, to account for environmental history of acclimation/exposure. We assessed ecophysiological responses (photosynthesis and growth) to different simulated marine heatwave (sMHW) scenarios with interacting effects of temperature and nutrient availability. We additionally analysed the thermal regime and long-term MHW metrics from 5 geographically distinct regions covering the contemporary distribution of the species.

Chapter 2

Marine heatwave susceptibility at the trailing edge of the foundational kelp, *Laminaria hyperborea* (Phaeophyceae, Laminariales)

In preparation for publishing:

Barreto LM, Serrão EA, Martins N, Neiva J, Bartsch I, Valero M, Franco JN, Juterbock A, Assis J, Fragkopoulou E, Engelen A, Rinde E, Hartvig C, Bárbara I, de Clerck O, Pearson GA (2024). Marine heatwave susceptibility at the trailing edge of the foundational kelp, *Laminaria hyperborea* (Phaeophyceae, Laminariales)

2.1 Abstract

To understand why the decline and disappearance of warm distributional edge populations of a cold-temperate marine foundation kelp *Laminaria hyperborea* over the last 3 decades, we analysed intraspecific variation (population level) across a latitudinal gradient. Thermal regimes and long-term MHW metrics from 3 geographically distinct regions covering the contemporary continental distribution of the species in the northeast Atlantic were analysed to provide a benchmark and for integration with experimental simulated marine heatwave (sMHW) experimental design and results. Available field survey data were obtained to characterize density, size and structure of *L. hyperborea* beds in each region. Ecophysiological responses (photosynthesis, growth and survival) were investigated in response to sMHW, with interacting effects of temperature and nutrient availability. The previously undescribed genetic structure, diversity and phenotypic variability of this species were analysed with 13 microsatellite markers and a broader sample of 12 populations (n = 3 per region). The results show that the South warm edge population completely lacked resilience to the highest sMHW (23°C) resulting in 100% mortality before the recovery, in contrast to those from the present-day central or northern range. Concordantly, higher genetic diversity (allelic richness [AR] and expected heterozygosity [H_E]) and uniqueness (private alleles [PA]) of the South edge population did not confer higher resilience to thermal stress. Our results revealed novel genetic structure and characterization across the entire species distribution gradient and added to the already compelling evidence that the warm South edge populations are at great risk of extirpation. Loss of these ancient populations would result in the loss of the unique, rich and diverse gene pool of *L. hyperborea*.

2.2 Introduction

Understanding how foundation species in ecosystems including grasslands, terrestrial forests, coral reefs, and kelp forests adapt and persist across their distribution range to changing environmental conditions is fundamental to predict ecosystem responses in the face of increasing intensity, frequency and duration of warming anomalies and long term shifts in thermal regimes (Pecl et al., 2017; Schirpke et al., 2017; Frade et al., 2018; Smale et al., 2019). Species are typically exposed to different environmental conditions across their latitudinal and/or biogeographical distribution. The responses of populations (e.g., reproductive output,

growth or survival) to local environmental conditions may therefore vary due to some combination of plasticity and locally adaptive variation (i.e., phenotypic and genotypic variation within and among populations; Reed et al., 2011; Valladares et al., 2014). It is therefore paramount to understand whether, across the environmental gradient of foundation species, locally adapted populations are better able to withstand and survive these challenges (Wernberg et al., 2018; Liesner et al., 2020). Studies focused on intraspecific variation in marine foundation species remain scarce (King et al., 2018; Liesner et al., 2020; Strasser et al., 2022). Consequently, species-level responses to environmental stressors or predictions from species distribution modelling (SDM) are often constrained in assuming homogenous responses across the entire distribution range. The result is the potential misestimation of species vulnerability, compromising conservation and management strategies across entire ecosystems (Vargas et al., 2017; Des Roches et al., 2021; Hays et al., 2021).

Temperature is the major factor constraining the distribution of marine species at latitudinal scales, and biogeographical ranges are often defined by the species tolerance to winter minimum and summer maximum mean seawater temperatures (MST; Edgar et al., 2017; Stuart-Smith et al 2017). The gradual increase of MST (0.6°C on average NOA, 2021) observed over the past century has already caused shifts in species distribution (Parmesan & Yohe, 2003) and phenology (e.g., reproduction; Hu et al., 2022; Hoppit & Schmidt, 2022). Moreover, the last 3 decades have seen abrupt high seawater temperature anomalies increase in frequency and duration (Oliver et al., 2018; Holbrook et al., 2019). Indeed, marine heatwaves (MHWs - discrete anomalous events of seawater temperature increase exceeding historical records; Hobday et al., 2016) have caused massive species shifts and biodiversity loss worldwide (Jones et al., 2018; Smale et al., 2019; Cheung et al., 2021; Garrabou et al., 2022).

Due to their rapid development as well as their increasing magnitude and duration, MHWs are particularly dangerous for sedentary organisms that are unable to evade warm water masses (Perez, Garrabou et al., 2000; Smale et al., 2017). The consequences may be particularly severe for foundation species and ecosystem engineers such as seagrass meadows, coral reefs, mangroves and kelp forests (Hays et al., 2021), where the cascading effects of their decline and/or disappearance have profound consequences on the entire ecosystem (Coleman & Williams, 2002; Thomson et al 2014 ; Smale et al., 2019). The disruption due to MHWs of ecosystem services provided by foundation species worldwide (*e.g.*, nursery areas, food supply, shelter, fisheries, coastal erosion protection; Wernberg et al., 2012; Smale et al., 2019 ; Garrabou et al., 2022) may amount to socio-economic losses of billions of $ (Beaumont et al.,

2008; Vassallo et al., 2013; Vásquez et al., 2014; Bennett et al., 2016; Blamey & Bolton, 2017; Himes-Cornell et al., 2018).

Kelp forests formed by large brown macroalgae (Phaeophyceae; Laminariales *sensu stricto*, but also including fucoids and others) produce a high biomass canopy in the water column (Reed et al., 2008; Bartsch et al., 2008) resulting in a three-dimensional habitat that modifies the surrounding physical environment (*i.e.,* wave and current energy [Rosman et al., 2007], light levels [Wernberg et al., 2005; Desmond et al., 2015] and sedimentation composition (Alsuwaiyan et al., 2021). These ecosystems are productive and highly diverse, providing nursery grounds, food and shelter for a variety of marine life (Steneck et al., 2002; Teagle et al, 2017; Wernberg et al., 2019; C. M. Duarte et al., 2022). As kelp forests and their associated community can be found in relatively shallow coastal areas world-wide (Wernberg et al., 2019), their extraction and cultivation has a long association with coastal human societies worldwide (Erlandson et al., 2005; Erlandson et al., 2015). This prolific ecosystem provides important socio-economic resources directly through food production, and alginate/hydrocolloid extraction (Bartsch et al., 2008), and indirectly by associated species of interest (*e.g.*, fish, molluscs, crustaceans; Beaumont et al., 2008; Bertocci et al., 2015; Wernberg et al., 2019). However, extreme climate events including MHWs have pushed entire forests beyond ecophysiological thresholds, causing severe impacts including massive kelp biomass loss (Arafeh-Dalmau et al., 2019; Filbee-Dexter et al., 2016; Krumhansl et al., 2016), reductions in survival and growth (Bennett et al., 2015; Filbee-Dexter et al., 2020), and in some cases ecosystem shifts from kelp forests to much less productive and diverse turf algae-dominated systems (Filbee-Dexter et al., 2016; Karen Filbee-Dexter & Wernberg, 2018).

In the Northern Hemisphere, interglacial periods correspond to a poleward recolonization by species as temperatures rise and/or ice cover retreats (Hewitt, 1996; Stewart et al., 2010; Bringloe et al., 2020). For such species, the long-term centre of distribution corresponds to areas where populations have continuously persisted across glacial – interglacial periods near the contemporary warmer southern distributional edges (Bennett, K. D. & Provan, J. 2008; Stewart et al., 2010; Assis et al., 2018). Intraspecific variation among populations from the entire distribution range likely includes contributions from local adaptation (adaptive changes in allele frequencies towards local optima; King et al., 2018), and phenotypic plasticity (the ability of a genotype to express different phenotypes in response to different environmental conditions; Becker et al., 2015). Ancient populations at the contemporary warmest

distributional edge typically display rich and unique genetic diversity compared to more recent northern populations due to relatively low propagule dispersal (King et al., 2018), founder effects (Barton & Charlesworth 2003) and genetic surfing (Hallatschek & Nelson 2008; Neiva et al., 2010). Resilience to thermal stress due to acclimation, adaptation and phenotypic plasticity in low latitude edge populations has been suggested for some kelp species (Atkins & Travis, 2010; Wernberg et al., 2018; King et al., 2019; Liesner et al., 2020). However, decadal-scale ocean warming and the increasing frequency and intensity of MHWs threaten to outpace adaptative capacities under rapidly deteriorating environmental conditions, and the potential extirpation of unique gene pools in some species (Wernberg et al., 2018; Filbee-Dexter et al., 2020). Despite accumulating evidence for the role of local adaptation and phenotypic plasticity in responses to environmental change (Valladares et al., 2014; Liesner et al., 2020; Strasser et al., 2022), studies focused on detecting intraspecific variation in response to MHWs remain scarce (King et al., 2018). Models that aim to predict future species distribution often assume a uniform species response (Reed et al., 2011 ;Holt & Gomulkiewicz, 2004), potentially compromising the effectiveness of kelp conservation, restoration and farming actions taken by decision-makers.

In this study, we used *Laminaria hyperborea* as a model cold-temperate kelp species with a broad distribution range in the Northeast Atlantic Ocean (Kain, 1967; Rothman et al., 2017). Our aim was to analyse the currently undescribed genetic structure and phenotypic variability of this species, in which populations from the southern (warm edge) distribution have declined and/or disappeared over the last 3 decades (Casado-Amezúa et al., 2019). We additionally analysed the thermal regime and long-term MHW metrics from 3 geographically distinct regions covering the contemporary distribution of the species. Available field survey data were used to characterize density, size and structure of *L. hyperborea* beds in each region. We investigated intraspecific (population level) variation in ecophysiological responses (photosynthesis, growth and survival) to simulated marine heat waves in the laboratory (sMHW, with interacting effects of temperature and nutrient availability) in field-collected adult individuals from each region. Genetic diversity and differentiation among populations was assessed using a broader sample of 12 populations.

2.3 Methods

2.3.1 Sampling area

In this study, we used 3 regions along the distribution of *Laminaria hyperborea* in the eastern Atlantic: North (Norway), Centre (English Channel), and South (Northwest Iberian Peninsula) to assess population differentiation across the entire species distribution (Fig. 2.1).

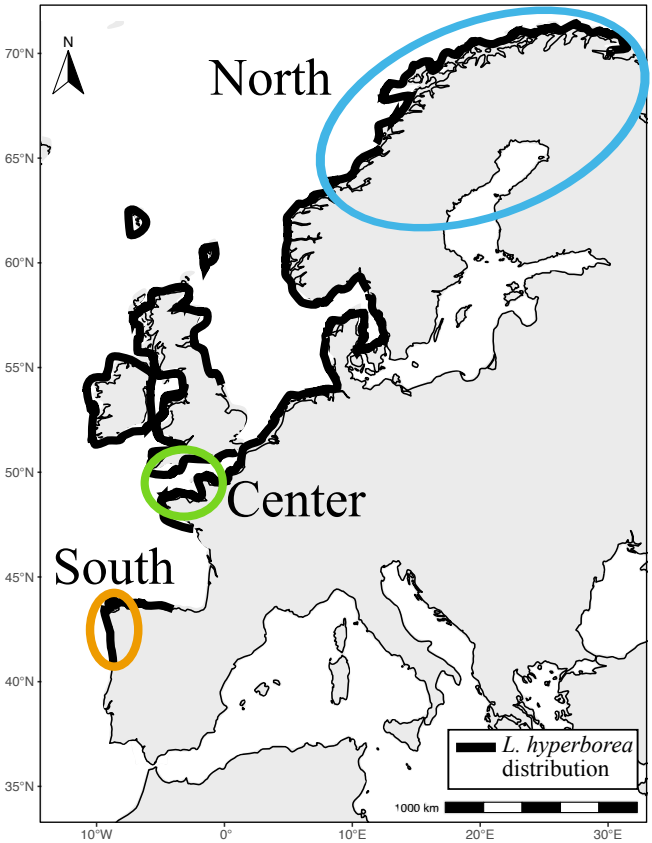

Figure 2.1 – *Laminaria hyperborea* distribution across the Northeast Atlantic and studied regions: North in Norway, Centre in the English Channel (France and England) and South, in the Northwest Iberian Peninsula (Spain and Portugal).

For each experiment or analysis, 1 or 3 populations from each region were used (see Table S2.2 for specific population locations).

2.3.2 Regional thermal regimes and MHW metrics

In order to characterize local oceanographic thermal regimes, we calculated the minimum, mean and maximum sea surface temperature (SST, °C) for each region, using Bio-Oracle (Assis et al., 2017; see Table S2.1 for layers used). We used the Global Ocean Physics Reanalysis gridded dataset (Global Monitoring and Forecasting Centre, 2018) generated by the E.U. Copernicus Marine Service (CMEMS) (https://www.copernicus.eu/en) to calculate MHW for each site of interest. This dataset is the product of a 3D model (NEMOVAR) with a bias correction scheme, that combines satellite and in-situ measurements for a resolution of 0.083-degree covering the period from 01/01/1994-31/12/2019.

Following the definition of Hobday *et al.*, (2016), we described a MHW as a discrete prolonged anomalously warm water event of at least 5-day duration, during which daily temperatures exceeded the seasonally varying 90th percentile threshold of the historical baseline climatology. If two events took place less than 3 days apart, they were considered as a single event. The historical baseline climatology for a given day was calculated using an 11-day window centred on that date across all years of the climatology period, while an additional 31-day moving average was applied to smooth the climatology (Hobday et al., 2016). A seasonally varying threshold was preferred to an absolute fixed value, as it allowed the identification of MHW events throughout the year, rather than during the warmest seasons only. Climatologies were produced and MHWs were calculated for each site of interest. Each MHW event was characterised by a set of metrics (Hobday et al., 2016), mean and maximum duration (D_{mean} and D_{max}, days), mean, maximum and cumulative intensity (I_{avrmax}, I_{max} and I_{cum} ,°C days). MHW frequency was measured as the total number of events occurring during the modelled period (1993-2019).

2.3.3 Adult field surveys

Field surveys on *Laminaria hyperborea* beds were performed by scuba diving in coastal rocky subtidal areas between depths of 3 – 20 m to assess density and stipe length using quadrats on 3 locations per region (see Table S2.2 for coordinates). South and Centre region surveys were performed during 06/2019 and 07/2017, respectively, and during August-September 1985 in the North region (from Rinde & Sjøtun, 2005). Individuals with stipe length < 6 cm were considered juveniles. Density across the 3 regions was standardized to sporophytes / 0.5 m^2.

2.3.4 Experimental ecophysiological (photosynthetic and growth) performance

Laminaria hyperborea adults were sampled by snorkeling or scuba in rocky subtidal areas between 2 and 10 m depth with at least 2 m distance between individuals at Mjeldevika, Norway (September 2019), Roscoff, France (November 2018) and Esposende, Portugal (May 2020) encompassing the majority of the species distribution range in the NE Atlantic (see Table S2.2 for coordinates). Sampling and data processing were conducted complying with local Portuguese, French and Norwegian legislation and the Nagoya protocol on the Access to Genetic Resources and Benefit-Sharing Clearing-House.

Adult sporophytes were sampled by cutting the stipe junction to the meristem. To avoid impacting the low-density southern edge *L. hyperborea* beds (South – Esposende) 30 individual sporophytes were sampled, while 40 were sampled from the Centre (Roscoff) and North (Mjeldevika). Sporophytes were immediately processed in indoor facilities. Tissue was cleaned of epiphytes with moist paper and 6 discs (2 cm Ø) were cut from the meristematic region and wrapped (per individual) in seawater-moistened paper rolls and placed in independent zip lock bags. Discs were stored between 5 - 8°C and transported in cool boxes within 48h to the experimental facilities at Centro de Ciências do Mar do Algarve (CCMAR), Portugal.

Discs from the same individual were placed in a 1 L beaker with 900 mL artificial sea water (ASW; Tropic Marin® Classic and Elix H_2O) at 32 ppm salinity, with 10 mL/L modified Provasoli enrichment (PES; Provasoli, 1968, modifications: HEPES buffer instead of TRIS, double concentration of Na_2-glycerophosphate). The medium was circulated with aeration (AIR Pump DB-120, Esoair) at 6°C, a 16:8 light:dark cycle and irradiance of 12 µmol m^2 s^{-1} (AquaBeam 1500 MW Marine 24 White, Tropical Marine Centre) to allow wound healing. The medium was renewed every 3 days. Temperature and light were gradually increased every other day over 18 days at 1°C and 2 µmol m^2 s^{-1} steps, until the target temperature of 15°C and irradiance of 30 µmol m^2 s^{-1} were reached.

The factorial experimental design consisted of simulated dynamic gradient heat waves with 4 temperatures selected based on the MHW data modelled from each site (see MHW section below and Results): 15°C (control, ≈ mean SST in the South region), 19°C , 21°C (≈maximum SSTs for Centre and South regions) and 23°C (3°C above the reported sporophyte upper survival temperature for a 14 day exposure with no thermal ramp [Wiencke et al., 1994]).

For the South region, only 15°C and 23°C thermal treatments were used due to the low number of individuals available during sampling. As anomalously high sea water temperature events are highly correlated with nutrient depletion (Carr & Kearns, 2003; Hayashida et al., 2020), two nutrient treatments were used: PES-enriched and non-enriched ASW with 5 replicates per treatment. A replicate consisted of a 1 L beaker with 6 discs from the same individual. After 18 days of wound healing, there followed a further 5-day acclimation phase to the nutrient-enriched and non-enriched conditions (day -5 in Fig. 2.2).

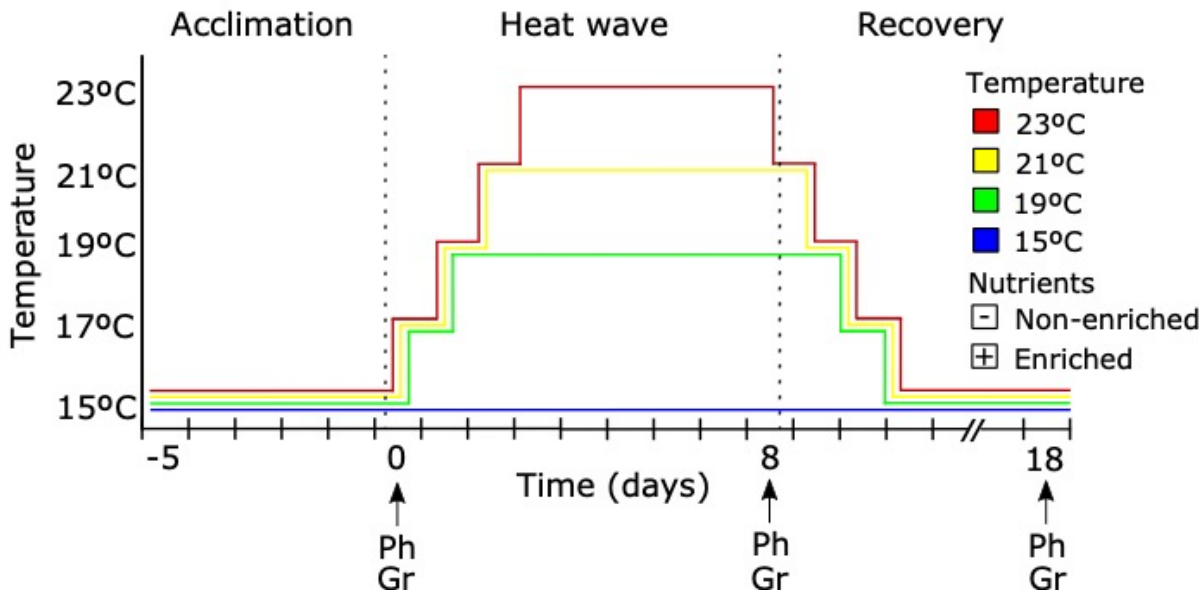

Figure 2.2: Experimental design of simulated marine heat waves (sMHW) applied in *Laminaria hyperborea* adult sporophytes. Dotted vertical lines define the experimental stages: "Acclimation" from day -5 to 0, dynamic "Heat wave" from day 0 to 8 and "Recovery" from day 8 to 18. Experimental temperatures were 15°C (control), 19°C, 21°C and 23°C. Nutrient treatments corresponded to Provasoli enriched (+) and non-enriched (-) medium. ↑ indicates sampling for photosynthetic performance (Ph) and growth (Gr) taken on days 0 (control), 8 (end of heat wave) and 18 (end of recovery).

At day 0, the sMHW phase started with 2°C daily increments until the targeted maximum temperature for each thermal treatment was reached, followed by 7 days at 19°C, 6 days at 21°C and 5 days at 23°C. At day 8, the recovery phase started, consisting of a 2°C daily reduction until 15°C was reached by all treatments, followed by an additional 7 days under control conditions and lasting a total of 10 days. Each temperature treatment consisted of an independent thermally controlled water bath (Huber Variostat Pilot One, Offenburg, Germany) with a temperature stability of 0.02K. Measurements for photosynthesis performance and growth were taken at day 0 (control), day 8 (end of sMHW) and day 18 (end of recovery).

One random sporophyte meristem disc per replicate (n=5) was dark acclimated for 5 min. Maximum photochemical efficiency of photosystem II (F_v/F_m) followed by rapid light curve (RLC) with 8 irradiance steps between 4 and 420 µmol photons m^{-2} s^{-1}, were measured on day 0 (control), day 8 (end of sMHW) and day 18 (end of recovery) using a pulse amplitude modulated fluorometer (Diving PAM, Walz GmbH, Germany) and parameters were calculated using Wincontrol-3 software (Walz GmbH, Germany). The use of fluorometry as a proxy for thermal stress response is reliable (*i.e.* has a significant linear relationship to O_2 production) under sub-saturating irradiances (Duarte et al, 2013; Beer et al., 2014). Sampling always started after discs were exposed to at least 6 hours of light. F_v/F_m corresponds to the maximum quantum yield of photochemistry of photosystem II and was calculated as:

$$\frac{F_v}{F_m} = \frac{(F_m - F_0)}{F_m}$$

Where F_m corresponds to the maximum fluorescence level elicited by a saturating light pulse that closes all PSII reaction centres, and F_0 correspond to the minimum fluorescence level measured with a very low intensity modulated measuring light under which PSII reaction centres remain open.

From the RLCs, the maximum relative electron transport rate ($rETR_{max}$) as µmol electrons m^{-2} s^{-1} was calculated as:

$$rETR_{max} = ETR_{mPot}\left(\frac{\alpha}{a+\beta}\right)\left(\frac{\beta}{a+\beta}\right)^{\beta/\alpha}$$

Where ETR_{mPot} corresponds to the maximum potential light-saturated electron transport rate, a is the initial slope of the RLC corresponding to the quantum efficiency of photosynthesis and β corresponds to the photoinhibition parameter (Platt et al., 1980).

Meristem disc fresh weight (g) was measured on day 0 (control), day 8 (end of sMHW) and day 18 (end of recovery) from a randomly selected disc per replicate (n = 5). Relative growth rate (RGR) was estimated as:

$$RGR\ (g\ day^{-1}) = \left(\frac{ln(sMHW\ or\ RC\ weight(g)) - \ln\ (control\ weight(g))}{Time\ (days)}\right)$$

Where sMHW corresponds to the end of the simulated marine heatwave (day 8), RC to the end of the recovery (day 18) and Time corresponds to the culture period (days).

2.3.5 Genetic analysis

Genetic data were assessed from individuals sampled during previous field campaigns (see Table S2.2). For each of our sampling sites (Fig. 2.1), the 3 nearest available populations were used to allow replication of populations in regional comparisons. Between 11 and 24 sporophytes per population were used for genetic analysis (Table S2). Genomic DNA was extracted from silica-dried blade tissue using the Nucleospin 96 Plant II kit (Macherey-Nagel, Germany). Microsatellites were amplified and manually scored for 9 polymorphic loci (Table S2.3) according to Neiva et al. (2020).

2.3.5.1 Population structure

To analyse population structure, a Bayesian model-based genetic admixture analysis with all individuals combined and with no prior population assignment was performed in STRUCTURE 2.3 (Pritchard Lab, Stanford University; http://pritchardlab.stanford.edu/structure.html). Each number of assumed populations (K, set sequentially from 1 to 10) was repeated ten times using a burn-in of 500,000 iterations and a run-length of 1,000,000 iterations. Harvester web v0.6.94 (Earl & vonHoldt, 2012) was used to summarize assignment results across independent runs. The ΔK criterion (Evanno et al., 2005) was used to assess the likely number of clusters (K). Population genetic affinity was further assessed by a Factorial Correspondence Analysis (FCA), using Genetix 4.05 (Laboratoire Génome, Populations, Interactions, Université de Montpellier II; http://kimura. univ-montp2.fr/genetix), based on spatial clustering of individual multi-locus genotypes.

2.3.5.2 Genetic diversity

For each region (North, Centre and South) and population (see Table S2.2) genetic diversity was estimated as allelic richness (AR), expected heterozygosity (HE), observed heterozygosity (HO), and multi-locus inbreeding coefficient (FIS) using GENETIX 4.05). Private alleles (PA) were assessed using CONVERT (Glaubitz, 2004). An index of regional differentiation (Jost´s D) was calculated using GENODIVE 3.0 (Meirmans, 2020) and plotted using the R package ComplexHeatmap (Gu et al., 2016).

2.3.6 Statistical analysis

Field surveys: Density (adults and juveniles) and adult stipe length data were analysed using the PERMANOVA+ module (Anderson et al., 2008) within PRIMER 7 (Clarke et al., 2014). A single-factor design with Region (North, Centre and South) as fixed factor, was used for each variable.

Experimental ecophysiological performance: Photosynthetic performance (F_v/F_m and $rETR_{max}$) and relative growth rates (RGR, g day^{-1}) were analysed using the PERMANOVA+ module within PRIMER 7. A 4-factor design with temperature (15°C and 23°C), nutrients (enriched and non-enriched), time (end of the simulated marine heat wave [day 8] and end of the recovery [day 18]) and region (North, Centre and South) as fixed factors, was used for each variable. As all individuals from the South region at 23°C died before the end of the recovery (day 18), we performed 2 separate analyses: 1) For the 3 regions at the end of sMHW (day 8), and 2) for both sMHW (day 8) and recovery (day 18) between North-Centre populations.

All Permanova analyses were performed using Euclidian distances, 9999 permutations and Monte Carlo *P*-value was used when unique permutations were < 100. Whenever a significant main effect or interaction was found ($p < 0.05$), post-hoc pair-wise t-tests were performed to identify differences among treatments levels. PERMDISP analysis were used to test the homogeneity of multivariate dispersions among *a priori* groups.

2.4 Results

2.4.1 Regional thermal regimes and Marine Heat-wave metrics

The long-term MHW metrics highlighted regional differences across the Northeast Atlantic (Fig. 2.3A, B), with the region at the southern distributional edge being exposed to the highest MHW intensities (temperature anomaly above the climatology; Fig. 2.3B, C).

A)

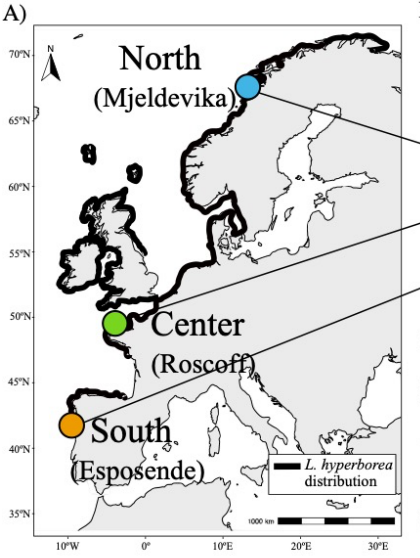

B)

Region	SST (°C) Min	Mean	Max	MHW events metrics (1994-2020) D_{mean} (days)	D_{max} (days)	I_{avrmax} (°C)	I_{max} (°C)	I_{cum} (°C days)
North	2.3	7.8	17.2	13.377	73	2.093	4.719	1307
Center	8.7	13.0	20.5	13.274	66	1.524	2.600	1115
South	12.1	15.7	21.5	13.079	68	2.496	4.895	1863

C)

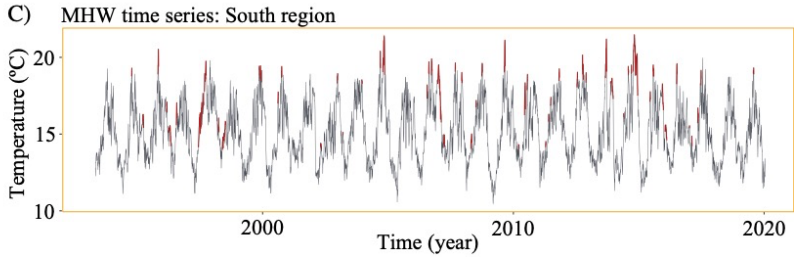

Figure 2.3: (A) Sampling locations of field individuals used in ecophysiology experiments: North (Mjeldevika, Norway), Centre (Roscoff, France) and South (Esposende, Portugal). (B) Minimum, mean and maximum sea surface temperature (SST, °C) for each location calculated using Bio-Oracle (Assis et al., 2017; see Table S2.6). Long-term (1994-2020) marine heatwaves (MHWs) metrics for each location: mean duration (D_{mean}, days), maximum duration (D_{max}, days), average maximum intensity (I_{avrmax}, °C), maximum intensity (I_{avrmax}, °C) and cumulative intensity (I_{cum}, °C). (C) MHW time series from the South region, red lines correspond to MHW periods.

The average of the highest temperatures during MHWs (I_{avrmax}), the single highest temperature value during MHW (I_{max}) and the cumulative intensity (I_{cum}) were all higher in the South region (2.50°C, 4.90°C and 1863 °C days, respectively) followed by the North and finally the Centre regions (Fig. 2.3B). The mean MHW duration (D_{mean}) and maximum duration (D_{max}) were similar across the entire study area (≈ 13 days and between 66 and 73 days, respectively). MHW time series for the South region (Fig. 2.3C) highlight that MHWs have been occurring in this region for at least the past 25 years, with periods of strong events (1995-97, 2004, 2009-10 and 2013-14).

2.4.2 Field surveys

Field surveys in *L. hyperborea* beds highlighted regional differences, with the North region displaying longer adult individuals (Fig. 2.4A) but in lower density (Fig. 2.4B) and lower juvenile recruitment (Fig. 2.4C).

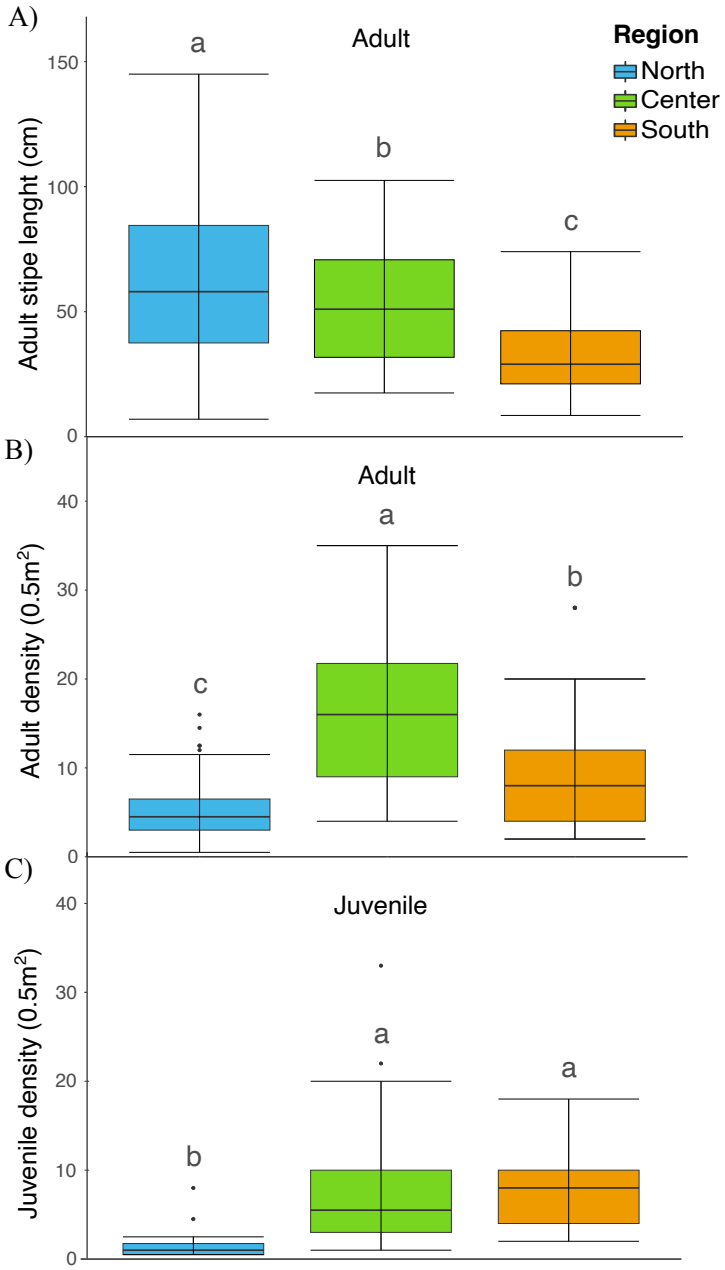

Figure 2.4: *Laminaria hyperborea* field (A) adult median stipe length (cm), (B) adult density (0.5m^2) and (C) juvenile (*i.e.* individuals with stipe length < 6 cm) density (0.5m^2) for each region: North (Norway), Centre (Roscoff, France) and South (from Esposende, Portugal to Coruña, Spain) with 3 population per region (see table S2.2 for locations). Small letters (above bars) correspond to significant differences between regions using permutation *P*-value ($p < 0.05$).

North region adult stipe length (average 64.9 cm) was 18.6% and 34.4% longer compared to the Centre (average 52.9 cm) and South (average 32.7 cm) regions, respectively (*P*-values < 0.001) (Fig. 2.4A). Centre region stipe length was 38.1% longer than the South region (*P*-values < 0.001). Adult density per 0.5 m^2 (Fig. 2.4B) in the Centre (average 16.5) was 68.9% higher than the North (average 5.1) and 47.4% higher compared to the South (average 8.6) regions, respectively (*P*-values < 0.001). South region had 40.8% higher adult density compared to the North *P*-values < 0.001). Juvenile density per 0.5 m^2 (*i.e.*, individuals with

stipe length < 6 cm) (Fig. 2.4C) in the North region (average 1.3) was 5.8 and 6.1-fold lower compared to the Centre (average 7.4) and South (average 7.8), respectively (*P*-values < 0.001), but did not differ between Centre and South regions (*P*-value = 0.684). In any case, differences found can be due to differences in means and or variance (Permdisp *P*-values < 0.001).

2.4.3 Experimental ecophysiological (photosynthetic and growth) performance

Photosynthetic responses (F_v/F_m and $rETR_{max}$) and growth rate (RGR) are presented in Figs 5-7 at the end of the simulated marine heatwave (sMHW) (day 8) and end of the recovery (day 18). The values presented are proportional to the control (day 5) to facilitate comparisons between regions and time points. Our results showed a lack of resilience in Southern edge *Laminaria hyperborea* under the highest thermal stress (23°C) with 100% mortality at the end of the recovery (Fig. 2.5). Therefore, statistical comparisons presented in the figures (letters and numbers) were only performed for the end of the sMHW (day 8) for all regions as no data were available for the South region at 23°C due to mortality by day 18. Statistical comparisons between North and Centre regions were performed for both time points, end of the simulated marine heatwave (sMHW) (day 8) and end of the recovery (day 18) and are presented in the text.

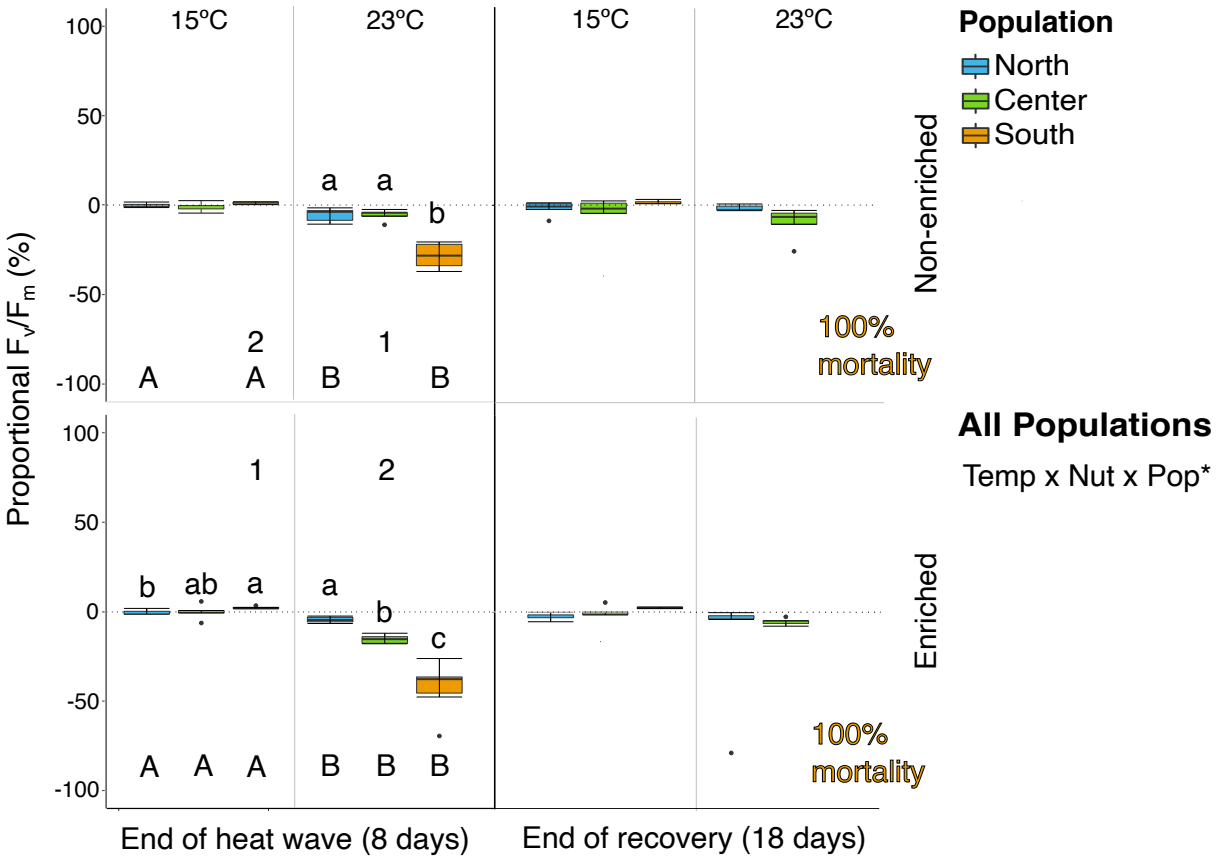

Figure 2.5: Maximum quantum yield of photosystem II (F_v/F_m) at the end of the simulated marine heatwave (sMHW) (day 8) and recovery (day 18) proportional to day 0 represented by the dotted line at 0 for the North (Mjeldevika), Centre (Roscoff) and South (Esposende) regions (see table s2.2) at 15°C (control) and 23°C (maximum temperature). Top panels correspond to non-nutrient enriched (Non-enriched) and bottom panels correspond to nutrient enriched (Enriched) treatments. Boxplot with median, 25th and 75th percentiles corresponding to the upper and lower boxes hinges respectively, whiskers corresponding to values no further than the inter-quartile range × 1.5 and outliers as black dots (n=5). Statistical comparisons were only performed for the end of the heatwave (day 8) as no data for the South at 23°C at the end of the recovery (day 18) was available: Small letters (above bars) correspond to significant differences between regions within the same temperature and nutrient at the end of the heat wave (day 8) using permutation *P*-value ($p < 0.05$). Capital letters (bellow bars) correspond to significant differences between temperatures within the same region and nutrient at the end of the heat wave (day 8) using permutation *P*-value ($p < 0.05$). Numbers correspond to significant differences between nutrient treatments (non-enriched and enriched) within the same temperature and region at the end of the heat wave (day 8) using permutation *P*-value ($p < 0.05$) (see table S2.4).

At the end of the sMHW, the South individuals exposed to 23°C showed a significant reduction in F_v/F_m compared to the North and Centre region (Fig. 2.5, lower case letters, see table S2.4) in both the non-enriched (5.1-fold and 5.0-fold respectively) and enriched treatments (10.3-fold and 2.8-fold respectively). Differences among regions in other thermal treatments were only observed at 15°C with nutrient enrichment, with the North individuals showing lower F_v/F_m values compared to the South at the end of the sMHW (33.5-fold). Nutrient enrichment (Fig. 2.5, numbers; Table S2.4), had only a positive effect on F_v/F_m values, compared to the non-enriched treatments, at 15 °C in the South individuals, at both the end of the sMHW (2.5-fold) and at 23°C in the Centre individuals at the end of the sMHW (2.6-fold). The highest thermal treatment (23°C) had a negative effect on F_v/F_m for all regions at the end

of the sMHW (Fig. 2.5, capital letters) compared to the 15°C control temperature, except for the Centre region non-enriched treatment. Interactions between North - Centre regions only, including both time points [end of the sMHW (day 8) and end of the recovery (day 18)] were marginally significant for Nutrients x Region (*P*-value: 0.046) and Temperature x Nutrients (*P*-value: 0.040) (Table S2.5). Post-hoc analysis showed significant differences only for the Temperature x Nutrients interaction with F_v/F_m values at 15°C > 23°C in both non-enriched (*P*-value: 0.012) and enriched (*P*-value: 0.005) treatments.

Maximum relative electron transport rate ($rETR_{max}$) was lower in the South individuals exposed to 23°C at the end of the sMHW (day 8) compared to the North and Centre regions (7.4-fold and 9.0-fold, respectively) and no differences found between North and Centre regions (Fig. 2.6, small letters, Table S2.6).

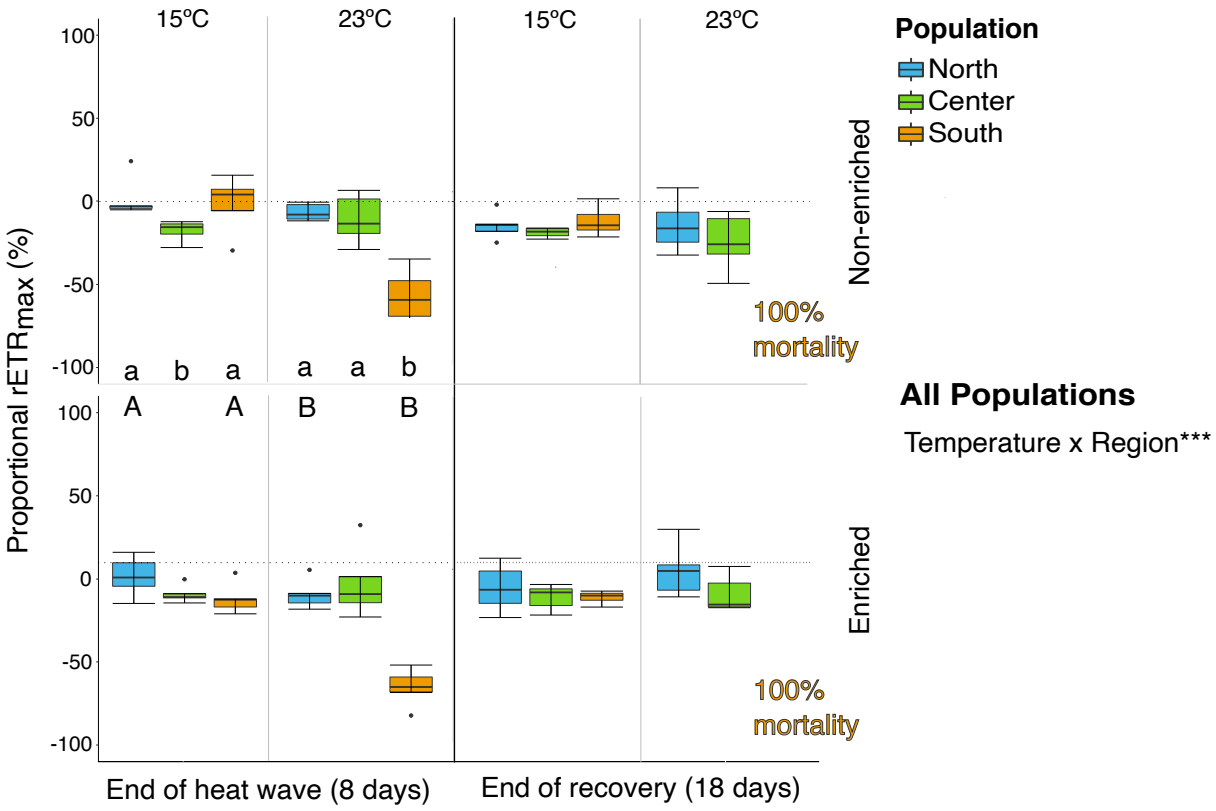

Figure 2.6: Maximum relative electron transport rate ($rETR_{max}$) at the end of the simulated marine heatwave (sMHW) (day 8) and recovery (day 18) proportional to day 0 represented by the dotted line at 0 for the North (Mjeldevika), Centre (Roscoff) and South (Esposende) regions (see table s2.2) at 15°C (control) and 23°C (maximum temperature). Top panels correspond to non-nutrient enriched (Non-enriched) and bottom panels correspond to nutrient enriched (Enriched) treatments. Boxplot with median, 25th and 75th percentiles corresponding to the upper and lower boxes hinges respectively, whiskers corresponding to values no further than the inter-quartile range × 1.5 and outliers as black dots (n=5). Statistical comparisons were only performed for the end of the heatwave (day 8) as no data for the South at 23°C at the end of the recovery (day 18) was available: Small letters correspond to significant differences between regions within the same temperature at the end of the heat wave (day 8) using permutation *P*-value ($p < 0.05$). Capital letters correspond to significant differences between temperatures within the same region at the end of the heat wave (day 8) using permutation *P*-value ($p < 0.05$) (see table S2.6).

Differences among regions were also observed at 15°C at the end of the sMHW, with the population from the Centre region showing lower $rETR_{max}$ compared to those from the North (8.4-fold) and South (1.9-fold) regions. The highest temperature (23°C) (Fig. 2.6, capital letters) had a negative effect in the North (5.3-fold) and specially in the South region individuals (8.9-fold) at the end of the sMHW (day 8) compared to the control (15°C). The effects of thermal stress (23°C) were maximum at the end of the recovery (day 18) for the South individuals (100% mortality); mortality precluded statistical comparisons between the South and the other two regions. No significant effect or interactions of nutrient-enriched culture media on $rETR_{max}$ were found (Table S2.6). Interactions between North - Centre regions only, including both time points [end of the sMHW (day 8) and end of the recovery (day 18)] were non-significant (Table S2.7).

Relative growth rate (g day^{-1}) was higher in the South region under control conditions (15°C) at the end of the sMHW (day 8) compared to the North (4.1-fold) and Centre regions (18.2-fold) (Fig. 2.7, Table S2.8).

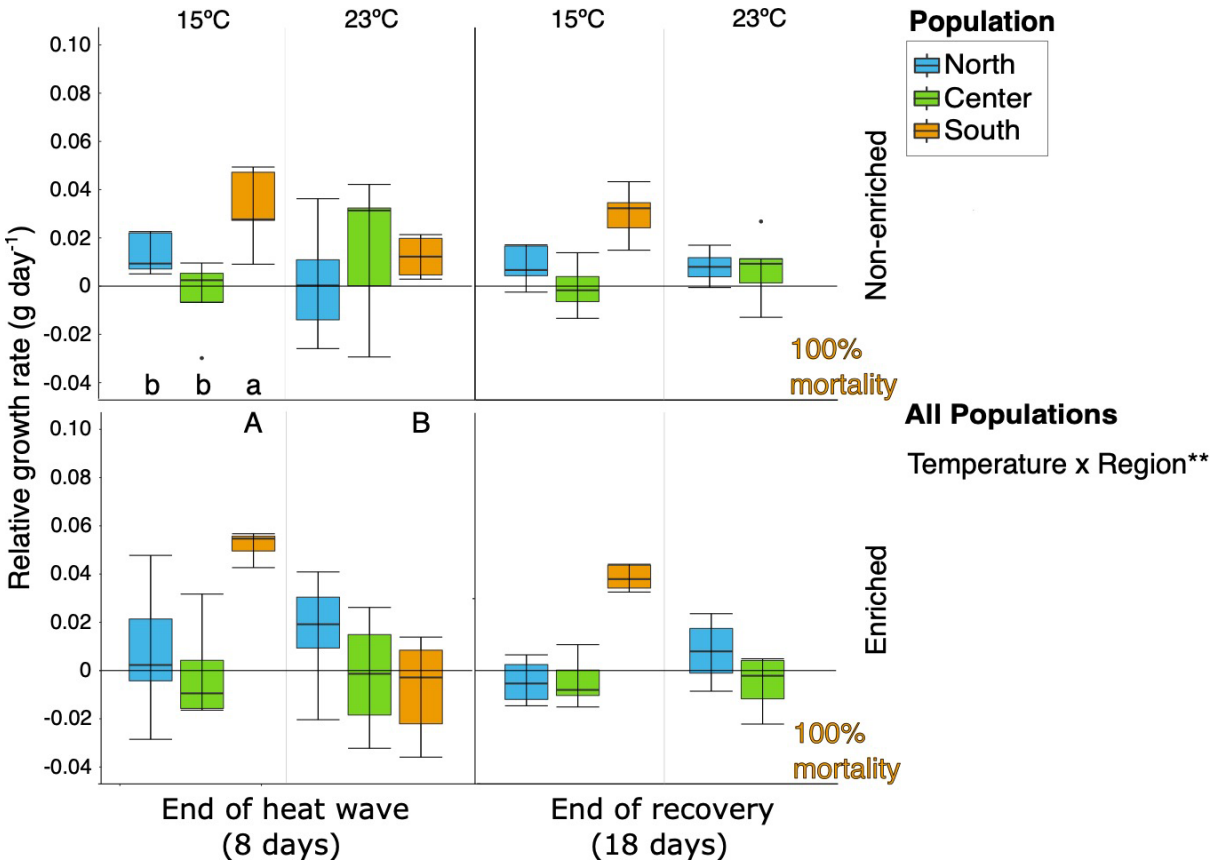

Figure 2.7: Relative growth rate (g day^{-1}) at the end of the simulated marine heatwave (sMHW) (day 8) and recovery (day 18) proportional to day 0 represented by the dotted line at 0 for the North (Mjeldevika), Centre (Roscoff) and South (Esposende) regions (see table s2.2) at 15°C (control) and 23°C (maximum temperature). Top panels correspond to non-nutrient enriched (Non-enriched) and bottom panels correspond to nutrient enriched (Enriched) treatments. Boxplot with median, 25th and 75th percentiles corresponding to the upper and lower boxes hinges respectively, whiskers corresponding to values no further than the inter-quartile range × 1.5 and outliers as black dots (n=5). Statistical comparisons were only performed for the end of the heatwave (day 8) as no data for the South at 23°C at the end of the recovery (day 18) was available: Small letters correspond to significant differences between regions within the same temperature at the end of the heat wave (day 8) using permutation *P*-value ($p < 0.05$). Capital letters correspond to significant differences between temperatures within the same region at the end of the heat wave (day 8) using permutation *P*-value ($p < 0.05$) (see table S2.8).

Also, at 15°C but at the end of the recovery (day 18), South region had significant higher RGR compared to North (*P*-value < 0.001) and Centre (*P*-value < 0.001) and did not differ significantly between North and Centre regions (*P*-value: 0.302).

At the highest thermal treatment (23°C), no differences were found between the South and the other regions except the 100% mortality at the end of the recovery (day 18). At 23°C, South region individuals growth was reduced 17.5-fold at the end of the sMHW when compared to the control (15°C). We found no significant effect or interactions of the nutrient enrichment of the culture media on relative growth rate (Table S2.8). Interactions between North - Centre regions only, including both time points [end of the sMHW (day 8) and end of the recovery (day 18)] were non-significant (Table S2.9).

2.4.4 Genetic analysis

Two major population clusters in *L. hyperborea* were apparent in the STRUCTURE analysis based on the ΔK criterion, with populations in the South region clustering independently from those in the North and Centre (Fig. 2.8A, B).

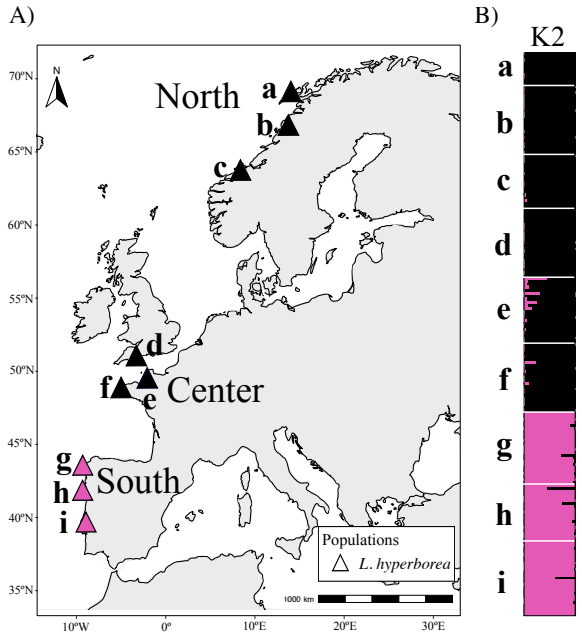

D)

	AR	PA	H_E	H_O	F_{IS}
North	**6.33**	**8**	**0.596**		
a (LOF)	3.22	2	0.467	0.459	0.058
b (SKJ)	3.89	0	0.461	0.466	0.012
c (TIT)	4.67	5	0.452	0.471	-0.015
Center	**8.44**	**8**	**0.661**		
d (HCO)	5.00	2	0.472	0.440	0.089*
e (GUE)	6.78	2	0.676	0.639	0.077*
f (ROS)	5.56	2	0.637	0.620	0.047
South	**14.33**	**66**	**0.792**		
g (COR)	9.33	8	0.754	0.667	0.137*
h (VHC)	10.22	14	0.750	0.706	0.083*
j (LPA)	9.33	10	0.773	0.745	0.058*

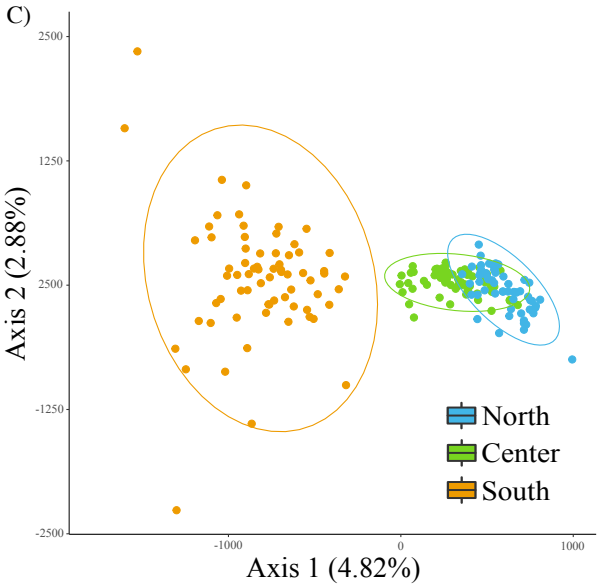

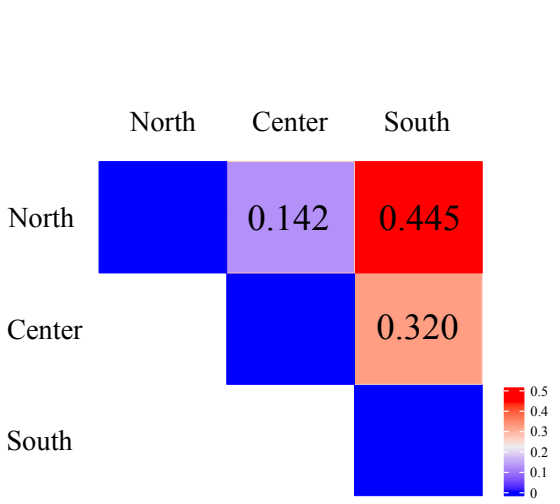

Figure 2.8: (A) *Laminaria hyperborea* population locations used for genetic analysis (see table S2.2). (B) Hierarchical genetic structure assuming subdivision with 2 groups (K=2). (C) Factorial correspondence analysis (FCA) plot based on individual multilocus genotypes. (D) Genetic diversity for each region (North, Centre and South) and population as mean allelic richness (AR), private alleles (PA), expected heterozygosity (H_E), observed heterozygosity (H_O) and multi-locus inbreeding coefficient (F_{IS}; * if significant). (D) Pairwise genetic differentiation (Jost´s D) between regions.

The FCA plot (Fig. 2.8C) confirms the separation between the South and the other two regions with the South region individuals distanced from the North and Centre region individuals while the last two overlapped their clusters. Genetic diversity (AR and H_E) was highest in the South region (14.33 and 0.792, respectively) compared to the North (6.33 and 0.596, respectively) and the Centre regions (8.44 and 0.661, respectively) (Fig. 2.8D). The number of private alleles (PA) occurring in the South region was 8.25-fold higher than the other regions. F_{IS} values were significantly positive in all South region populations (COR, VCH and LPA) and significantly positive in two populations of the Centre region (GUE and HCO) indicating a significant heterozygote deficiency (mates are more closely related than expected in equilibrium). On the North region, no population registered significant F_{IS} values. Genetic differentiation among regions (JOST´s D, Fig. 2.8E) was significant between all comparisons (p-value < 0.001) with higher differentiation between South - North (0.445) and South - Centre (0.320) followed by North – Centre (0.142).

2.5 Discussion

In this study we combined data describing field surveys, ecophysiological responses to sMHWs and genetic differentiation to show that *L. hyperborea* individuals from the South edge distribution were unable to survive the maximum sMHW temperature of 23°C (100% mortality), in contrast to those from the present-day central or northern range. The hypothesis that individuals from the South area would be more resilient to MHW events due to either field preacclimation to higher temperatures in their local environment, or to the presence of locally adapted genotypes was not supported. Instead, individuals near the southern distributional edge were more susceptible to our sMHW conditions. Concordantly, higher genetic diversity (allelic richness [AR] and expected heterozygosity [H_E]) and uniqueness (private alleles [PA]) of the South edge population did not confer higher resilience to thermal stress contradicting previous studies on other kelp (Wernberg et al., 2018) and seagrass (Ehlers et al., 2008) species, where populations with higher genetic diversity were associated to improved resilience to thermal stress.

Another assumption based on previous studies on kelp species was that nutrient enrichment could improve photosynthetic performance and growth rate in response to a thermal

stress. For example, on the sister species *Laminaria ochroleuca*, nutrient enrichment was found to increase growth rate at all temperatures including sub-lethal temperatures of 22°C and 24°C compared to non-enriched treatments (Franco et al., 2018). On another kelp species, *Undaria pinnatifida*, nutrient enrichment increased both survival and relative growth rate (%/day) in response to temperature treatments up to 24°C (Gao et al., 2013). On our experiment, when comparing all populations at the end of the heatwave (8 days), nutrient enrichment only improved the photosynthetic yield (F_v/F_m) of the Centre population. No differences between nutrient treatments were found for $rETR_{max}$ or growth rate (RGR) including on the South population individuals which were already showing significant lower ecophysiological responses at 23°C compared to the control 15°C. Although unexpected, this result might be a consequence of a rapid heat wave event, where the physiological capacity of the algae to use the available nutrients in the water might be impaired by the heat stress by less effective photosynthesis process and/or direct tissue degradation. Thus, we did not observe a positive effect of nutrient enrichment in the ecophysiological response of *L. hyperborea*, from these populations to a 23°C MHW event but caution must be taken interpreting this results as field adults from the North and Centre regions were collected during September and November, respectively, corresponding to the beginning of the winter dormancy period of this species sporophytes in which growth stops and uptake of nutrients is greatly reduced (Luning, 1979; Schaffelke & Luning, 1994).

In our experiment we want to highlight and discuss two constrains found: 1) Due to the low number of field individuals present in the South population we collected only enough individuals for 2 thermal treatments (15°C and 23°C) as we wanted to reduce, as much as possible, impacting the already sparse and small population. It would be optimal if we were able to assess at least the 21°C treatment, in order to observe the South population individual's response. Such temperature is just below the maximum SST registered for the region (21.5°C) and given the 100% mortality at 23°C it would be optimal to have the potential sub lethal response. 2) Individuals from the North and Centre populations were collected during the dormancy period of the species (September and November, respectively) while South population individuals were sampled during the growth period (May) (Lüning, 1969) due to the rough oceanographic conditions on the NW Iberian that precluded Winter sampling. Although such constraints might pose difficulties interpreting growth rates among populations across the experiment (*i.e.* South population individuals at the control 15°C grew while the other populations did not), the concern that the lack of resilience to the highest thermal

treatment of the South edge individuals was caused or facilitated by the growth phase is not supported by a previous study on another *Laminaria* species, *L. digitata*, where individuals were actually found to be more resilient to simulated MHW stress during growth period than during dormancy (Hereward et al., 2020, growth and dormancy periods acording to Kain, 1979).

We consider that the South population individuals 100% mortality at 23°C was a result of smaller and especially thinner individuals, possibly with low reserves that were not able to sustain the thermal stress. The field conditions highlighted by the long-term MHW metrics also indicate a degradation of suitable habitat on the South edge distribution with the average maximum intensity (I_{avrmax}), maximum intensity (I_{max}) and specially the cumulative intensity (I_{cum}) higher at this region compared to the other regions. The I_{cum}, which corresponds to the sum of daily thermal intensity anomalies (integral of intensity over the duration of the event), highlights the increase in MHW days and °C observed on the South region with 1863 (°C days) vs the 1307 (°C days) and 1115 (°C days) of the North and Centre regions, respectively. The maximum SST observed on the South (21.5°C) and Centre (20.5°C) regions are already above the upper thermal limit known for the species juveniles of 20°C (Wiencke et al., 1994) and already 3°C higher than the 18°C limit from which gametophyte growth and fecundity are extremely impaired (Lüning, 1980). The continuous habitat degradation, specially evidenced on the warm South distribution edge, shifted a perennial kelp forest system with large adults to a sparse and patchy distribution of young individuals that are small and thin compared to their northerner populations. Such demographic differences are highlighted by the field surveys results where South region individuals are 57% smaller than the North region but also by previous studies (Pereira et al., 2017). A cascading deteriorating effect occurs on low density kelp forests, where patchy kelp beds are worse at facilitate conspecific recruitment and development (Layton et al., 2019) and are less resilient to other stressors such as herbivory (Sjøtun, Christie, & Fosså, 2006; Franco et al., 2017). Dense monospecific *L. hyperborea* are very resilient to storms while sparce or mixed kelp canopy reduce storm resilience (Smale & Vance, 2015). Another putative outcome of continuous habitat degradation and reduction of population size is the reduction of allelic richness and heterozygosity, already observed for other foundation species such as seagrass meadows (Manent et al., 2020).

This outcome was not confirmed when we compare the genetic results of the warm South to the other regions as genetic diversity (allelic richness [AR] and expected

heterozygosity [H_E]) and uniqueness (private alleles [PA]) of the South population were the highest. This pattern of high genetic diversity and uniqueness on the warm distribution end corresponding to the long term (millennia) persistent refugia of species has been reported for other kelp species such as *Laminaria ochroleuca* (Assis et al 2018), *Macrocystis pyrifera* (Johansson et al., 2015), *Saccharina latissima* (Neiva et al, 2018) and other brown algae such as *Bifurcaria bifurcata* (Neiva et al 2015). Significant positive multi-locus inbreeding coefficient (F_{IS}) was observed in all 3 South region populations and in 2 Central populations. A significant positive F_{IS} value indicates a deficit in heterozygotes, meaning that mates are more closely related than expected in Hardy-Weinberg equilibrium. Although, selfing in kelps (*i.e.* fertilization between male and female gametophytes produced by the same adult sporophyte) might theoretically result in inbreeding depression (Raimondi et al 2004), on some kelp species the heterozygosity reduction resultant from selfing did not affect significantly individual fitness (growth, reproduction and survival) (*Postelsia palmaeformis*; Barner et al 2011) nor the capability for dispersal and survival in a newly colonized area from a low number of individuals (*Undaria pinnatifida*; Guzinski et al 2018). Thus, the significant F_{IS} values might be a result of more patchy populations but not deleterious in terms of genetic diversity and private alleles if you consider the South region values compared to the other regions, although a continuous deleterious process might be ongoing within the South region over the last decades which can only be assessed by future genetic analysis on the same populations. On the other hand, the lack of significant positive F_{IS} value in the 3 North region populations might be related to the potential older age structure of this population: individuals size (stipe length) in the North region was 30.9% and 57.0% larger compared to the Centre and South regions, respectively and generational turnover (juvenile density at North region = 1 juvenile $0.5m^{-2}$) was 7.5 and 7.9 fold lower compared to the Centre and South regions, respectively. As individuals in the North region grow over many years and number of recruits is low, the probability of two individuals being close related decreases resulting in a proximity to Hardy-Weinberg equilibrium ($F_{IS} = 0$). Another clear result from our genetic analysis was that South region populations are clearly differentiated and distanced from their Northerner counterparts (FCA and Jost´s D plots). The division and distance between the South and the other regions might be old (several ice ages) and the recolonization of the north in past post-glacial periods might have been performed only by Northerner refugia populations (SW Ireland, W English Channel, Faroe Islands and S Iceland have been suggested by predictive models [Assis et al., 2016]) as Centre and North regions overlap in the FCA plot. As so, the differences in responses (and morphology) of the South populations might be a phenotypic adaptation to the

environment, passing from a perennial, long living population with large individuals characteristic of the more northerner populations to a short living small specimens with fragmented populations that invest possibly in reproduction in the first season.

Over the last decades, the South edge distribution of *L. hyperborea* that used to go all across the North Spanish coast, has been shrinking to the North-west tip of the Iberian Peninsula, where upwelling regimes are still strong (Fernández, 2011) (Casado-Amezúa et al., 2019). This pattern was also observed on the west Iberian coast with a range contraction of 260 km since 1970 from praia do Magoito at the centre of Portugal (38.86143, -9.45060) (Ardré, 1970) to the current known South edge limit of praia da Aguda (41.04554, -8.65282) (Monteiro et al., 2022). Predictive models on future distribution of *L. hyperborea* for this region have also indicated the possible disappearance of all populations on the South range (NW Iberia) in all RCP scenarios (Assis, Lucas, et al., 2016). The extirpation of this ancient structuring kelp populations with a unique, rich and diverse gene pool will greatly reduce the species future genetic potential and impacting local economies reducing not only direct human harvestable stocks but also biodiversity and other services provided by perennial kelp forests (Bertocci et al., 2015; Smale et al., 2013; Vásquez et al., 2014). In order to understand the impacts of marine heatwaves in the entire life cycle of *L. hyperborea* we suggest the replication of this ecophysiological experiment with gametophytes and next generation F1 juveniles under sMHW. The creation of seed banks from this populations is crucial to preserve this unique and rich gene pool for future generation. Reforestation programs with local gene pool in areas where kelp forest used to occur and known factors of reduction or disappearance such as human harvest or sedimentation have been removed or greatly reduced, should be implemented to increase the number of populations resulting in higher connectivity and resilience for the entire region.

Chapter 3

Population level variation in reproductive development and output in the golden kelp Laminaria ochroleuca under marine heat wave scenarios

Chapter published in:

Strasser FE†, Barreto LM†, Kaidi S, Sabour B, Serrão EA, Pearson GA and Martins N (2022). Population level variation in reproductive development and output in the golden kelp Laminaria ochroleuca under marine heat wave scenarios. Front. Mar. Sci. 9:943511. doi: 10.3389/fmars.2022.943511

†*These authors share first authorship*

3.1 Abstract

Thermal tolerance is often interpreted as a species-wide thermal niche disregarding the adaptive potential of populations to exhibit differential thermal tolerance. Thus, considering intraspecific thermal plasticity and/or local adaptation between populations along distributional gradients when interpreting and predicting species responses to warming is imperative. Removing the effect of environmental histories by raising kelp gametophyte generations *in vitro* under common garden conditions allows unbiased comparison between population-specific adaptive variation under different environmental conditions. Following this approach, this study aims to detect (potentially) adaptive differentiation in microscopic life-stages (gametophytes) between populations of a temperate forest forming kelp, *Laminaria ochroleuca* from locations with distinct thermal conditions. Gametophytes from four geographically distinct populations were subjected to different temperature treatments (17, MHWs of 23, 25 and 27ºC) and gametophyte survival during thermal stress as well as reproductive success and photosynthetic responses during recovery were investigated. Intraspecific variation in resilience and reproductive output to thermal stress was found in *L. ochroleuca*; gametophytes from the most northern population (Brittany, France) were the most thermally sensitive, with mortality onset at 23ºC, whereas mortality in the remaining populations was only apparent at 27ºC. Gametophytes from northern Spain and Morocco exhibited very low reproductive success during recovery from 23 and 25ºC. However, when recovering from the highest thermal treatment (27ºC) the reproductive development and sporophyte output was higher than in the gametophytes from France and Italy (Mediterranean). The population-specific responses of gametophyte resilience and reproductive success to temperature stress suggest genotypic differentiation in response to variation in local thermal regimes.

3.2 Introduction

Species with extensive geographical ranges are not homogeneous units, but rather a collection of conspecific populations inhabiting distinct environmental regimes (Linhart & Grant, 1996). Over evolutionary periods, populations may exhibit intraspecific variation driven by local thermal conditions (King et al., 2018; Valladares et al., 2014) resulting in locally adapted populations, with specific fitness advantages (e.g. thermal resilience, growth rate, etc.) that may surpass the species average response (Denny, 2017). Among the consequences of climate change, sudden and anomalous warm thermal events such as marine heatwaves

(MHWs) have drastically affected entire ecosystems (Garrabou et al., 2009; Wernberg et al., 2012; Duarte et al., 2020) particularly in warming hotspots, which may lead to population-specific responses. Nonetheless, most studies investigating responses of marine species to environmental stressors or models aiming to predict geographical distributions under future climate conditions, assume that tolerances are reflected solely on a species-level which can ultimately lead to the over- or under-estimated impacts of climate changing conditions on biodiversity and ecosystems (Bellard et al., 2012; Applebaum et al., 2014).

Kelp forests are predominantly composed of brown algae of the order Laminariales (Dayton, 1985), dominating rocky shores of the world's temperate and cold-water marine ecosystems (Steneck et al., 2002; Smale et al., 2019). These forests provide a variety of ecosystem goods and services, either directly as a source of food or medicinal products, or indirectly as biogenic habitats for a variety of economically and ecologically important marine species (R. S. Steneck et al., 2002; Teagle et al., 2017). As the distribution and survival of habitat-forming algae is generally determined by species thermal limits and seawater temperatures (King et al., 2019b), many kelp populations are severely threatened by global warming and large-scale declines in their abundance and range shifts have been reported worldwide (A. B. Anderson et al., 2021; McPherson et al., 2021; Wernberg, 2021). Habitat-forming algae such as kelps are good models to study intraspecific variability due to their high dependence on ocean temperatures, limited dispersal, strong spatial structuring (King et al., 2018; Miller et al., 2020) as well as reduced connectivity and relative isolation which is facilitated by ocean currents and upwelling regions acting as thermal refugia for local genetic diversity (e.g. Coleman, 2013; Pereyra et al., 2013; Buonomo et al., 2016; Lourenço et al., 2016, 2017). Additionally, historical depth range shifts in *Laminariales* were found to preserve and isolate ancient gene pools during warming periods enabling long-term persistence and facilitating local adaption (Assis, Coelho, et al., 2016; Graham, Vasquez, & Buschmann, 2007; Santelices, 2007).

Laminariales have a heteromorphic life cycle, alternating between a microscopic haploid gametophyte and a macroscopic diploid sporophyte life stage (Colin et al., 2003; Lane, Mayes, Druehl, & Saunders, 2006). Although microscopic gametophytes show higher thermal tolerance for growth and survival than the macroscopic sporophytes, a lower and narrower temperature window is required for successful reproduction between sexually mature gametophytes (tom Dieck, 1992; Bartsch et al., 2013; Martins et al., 2017). Therefore,

temperature increases may delay reproductive development (Martins et al., 2020), with negative effects on kelp recruitment (Martins et al., 2017; Silva et al., 2022). Microscopic gametophytes may remain vegetative under unfavorable environmental conditions, acting as a "seed bank" (tom Dieck, 1993; Carney & Edwards, 2010; Martins et al., 2017; Silva et al., 2022) allowing the persistence of kelp populations following significant sporophyte mortality, e.g., due to extreme climatic events (Ladah & Zertuche-Gonzalez, 2007; Barradas et al., 2011).

The genus *Laminaria* presents one of the most diverse distribution ranges among kelp (John J. Bolton, 2010; Rothman et al., 2017) which is assumed to have led to higher speciation rates compared to other genera and includes species that exhibit some of the highest temperature tolerances among kelp (tom Dieck, 1992). *Laminaria ochroleuca*, the golden kelp, is a warm temperate kelp species that can be found in the north-eastern Atlantic. Its distribution ranges from the southern UK to Morocco but also forms deeper populations in the Azores and Mediterranean Sea (Assis et al., 2009; Birkett, Maggs, Dring, & Boaden, 1998; Flores-Moya, 2012; Ramos et al., 2016). Locally isolated biodiversity hotspots of *L. ochroleuca* were discovered at lower latitudes, exhibiting reduced connectivity as well as higher and unique genetic diversity (Assis et al., 2018). However, the level of population variability in thermal tolerance remains poorly understood for *L. ochroleuca* (but see Pereira et al., 2015). Thus, this species with a distributional range covering different thermal gradients provides an excellent model to investigate intraspecific adaptive variation. Investigating intraspecific adaptive variation to warming events is crucial in predicting the persistence of foundation species along their distributional ranges (Pearman, D'Amen, Graham, Thuiller, & Zimmermann, 2010) and therefore the fate of coastal communities and ecosystems. However, distinguishing genetic variation among populations from phenotypic short-term acclimation in species is difficult. By removing the influence of environmental history, common garden conditions allow us to investigate whether a generation of individuals from distinct populations raised in the same conditions exhibits different ecophysiological responses to environmental stress, and therefore the existence of adaptive differentiation rather than phenotypic plasticity.

This study aims to detect potential intraspecific adaptive differentiation to extreme thermal conditions in the habitat-forming kelp species *L. ochroleuca*. Using four populations spanning distinct thermal regimes and broadly representing the species distributional range in the NE Atlantic (NW France, NW Spain, Morocco) and Mediterranean (Italy), we compared the resilience and recovery capacity of gametophytes to simulated MHWs. Gametophyte survival

during thermal stress as well as reproductive success and photosynthetic responses during recovery were investigated. The gametophytes were raised *in vitro* under common garden conditions from spores to remove the effect of environmental histories (although epigenetic inheritance cannot be discounted entirely, e.g., see Gauci et al., 2022), allowing comparison between population-specific adaptive variation under different environmental conditions. Inter-population variation in response to simulated MHW focused on detecting adaptive variation delivers fundamental insights into local marine coastal ecology and evolution, which can potentially be incorporated into models anticipating future vulnerability and geographic range shifts of this foundation species under climate change scenarios.

3.3 Materials and Methods

3.3.1 Algal material

Mature specimens of *Laminaria ochroleuca* were collected in Roscoff, France (FR, November 2018), the Strait of Messina, Italy (IT, November 2019), Galicia, NW Spain (SP, May 2019) and El Jadida, Morocco (MO, August 2019) by SCUBA diving or snorkelling (see Table 3.1 for detailed sampling information, Fig. 3.1).

Table 3.1: Locations of *Laminaria ochroleuca* sampling sites (country, sampling date, geographical coordinates of each site, depth). Minimum, mean and maximum sea surface temperature (SST), except for the deep (-50m) population from Italy in which sea bottom temperature is presented, were obtained from Bio-Oracle (http://www.bio-oracle; supplementary material 2).

Population	Sampling date	Site	Coordinates	Depth (m)	Sea water temperature (ºC)		
					Min.	Mean	Max.
France (FR) Roscoff	14/11/2018	An Nehou	48°41’35.90”N 03°56’28.53”W	4	8.84	12.97	16.35
Italy (IT) Messina	16/11/2019	Messina Strait	38°15'27.97"N 15°37'40.04"E	50	13.79	14.15	14.65
Spain (SP) Muxia	03/05/2019	Playa Lago	43°06'17.01"N 09°10'10.04"W	4	12.36	15.81	18.59

Morocco (MO) El Jadida	03/08/2019	El Jadida	33°14'48.46"N 08°32'38.87"W	1	15.48	19.44	23.19

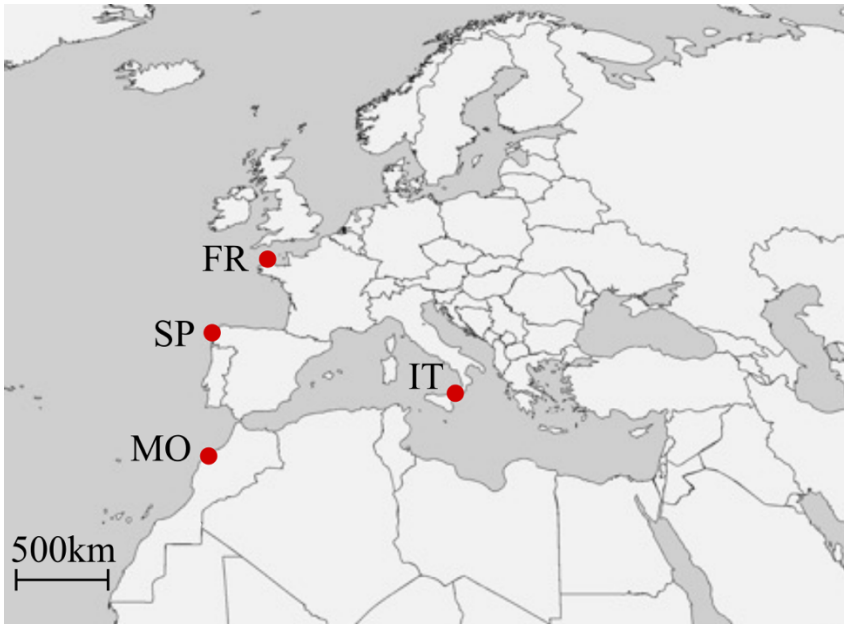

Figure 3.1: Sampling locations of Laminaria ochroleuca populations (red circles): France (FR), Italy (IT), Spain (SP) and Morocco (MO).

These four populations of *L. ochroleuca* originate from different latitudes and local habitat type (variable shallow coastal [FR, SP, MO] versus deeper stable [IT] habitat) with distinct local *in situ* temperatures (Table 1). The northernmost population (FR) is locally exposed to maximum sea surface temperature (SST) of 16.35°C while the southernmost (MO) is exposed to maximum SST of 23.19°C (Table 1, temperatures were obtained from Bio-Oracle (http://www.bio-oracle; Assis et al., 2017; supplementary material 2).

Two disks (2 cm Ø) were excised from reproductive tissue (sorus) of each mature adult sporophyte and cleaned with dry paper towel. The disks were placed into a Falcon tube with sterile seawater and two glass slides and left overnight in darkness to induce meiospore release. The seawater and the slides were then transferred to Petri dishes and left to germinate. The male and female gametophytes obtained from multiple *L. ochroleuca* sporophytes per population (IT: 6 individuals; FR, SP, MO: 5 individuals) were maintained together in a vegetative state in sterile half-strength Provasoli enriched seawater (PES; Provasoli 1968,

modifications: HEPES buffer instead of TRIS, double concentration of Na_2-glycerophosphate). The cultures were maintained in climate-controlled chambers (Fitoclima, S600, Aralab, Lisboa, Portugal) at 13°C under 3-6 µmol photons m^{-2} s^{-1} of fluorescent red light to prevent gametogenesis under a 16:8 h light:dark photoperiod (controlled via Fitolog400R software). The culture medium was changed monthly, until the start of the experiment (ca. 1-2 y). Sterile artificial seawater (Tropic Marin Sea Salt, Dr. Biener, GmbH, Wartenberg, Germany) with 30-32 ppm salinity (hand refractometer ATAGO Co., Ltd) was used for culture maintenance and all experiments.

3.3.2 Experimental setup

The gametophyte cultures were acclimated for two days at 15°C before the start of the experiment for a gradual temperature increase. The same amount of gametophyte vegetative tissue derived from multiple *L. ochroleuca* individuals were combined per population, gently fragmented with a pestle and mortar, sieved (stainless stell sieve with 100 µm mesh), and diluted in sterile 10% PES to produce four stock solutions of gametophytes with lengths of ≤ 100 µm. The density of each stock solution was determined using an inverted microscope (100× magnification, Zeiss Axio Observer D1, Carl Zeiss MicroImaging GmbH, Göttingen, Germany) and the respective volume needed to obtain ~500-600 gametophytes cm^{-2} was added to glass beakers (5.5 cm diameter, 5.5 cm height) filled with 80 ml of 10% PES. Four replicate beakers were used per population and thermal treatment (4 populations × 4 temperatures × 4 replicates = 64 beakers in total). The gametophytes were allowed to settle and recover from the mechanical stress induced by fragmentation at 17°C under 3-6 µmol photons m^{-2} s^{-1} of red light for 5 days.

After this period, the gametophytes were transferred to each heatwave (sMHW) treatment (with a maximum temperature of 23ºC, 25ºC and 27ºC) for 11 experimental days or left under control conditions at 17ºC. To avoid gametophyte thermal shock and to mimic natural temperature changes the temperature was gradually increased in the sMHW treatments from 17ºC to each maximum temperature at a warming rate of 2-3°C day^{-1}. The maximum temperatures of 25ºC and 27ºC were kept for 5 days (following Hobday et al., 2016), while 23ºC was kept over a period of 7 days. After this sMHW peak, the temperatures were gradually decreased back to 17°C again at a cooling rate of 2-3°C day^{-1}, initiating a recovery phase for the subsequent 29 days (see Fig. 3.2 for detailed experimental design). Experiments were conducted in temperature-controlled waterbaths (Huber Variostat with Pilot ONE, Offenburg,

Germany), provided with 20 µmol photons m^{-2} s^{-1} white LED light in a 16:8 h light:dark photoperiod. Culture medium (10% PES, 30-32 ppm) was 50% changed per beaker after 12 and 29 days.

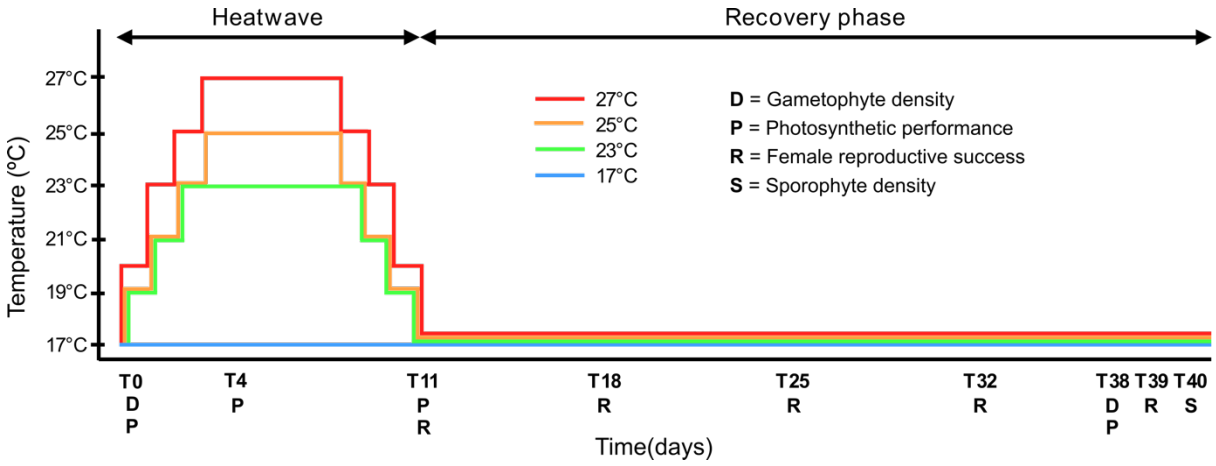

Figure 3.2: Design of the simulated MHW and recovery experiment. Laminaria ochroleuca gametophytes from four populations were exposed to different thermal treatments (17°C, 23°C, 25°C, 27°C) for 11 days and subsequently transferred to 17°C (recovery phase) for 29 days. Gametophyte density, photosynthetic performance, female reproductive success and sporophyte density were evaluated in different time periods.

The irradiance of 20 µmol photons m^{-2} s^{-1} and the control temperature of 17ºC chosen were reported as optimal conditions for *L. ochroleuca* gametogenesis (Izquierdo et al., 2002). Whereas the sub-lethal and lethal temperatures of 23ºC, 25ºC and 27ºC for *L. ochroleuca* gametophytes (tom Dieck, 1992) were used to test for physiological and ontological differences between populations.

3.3.3 Gametophyte density

To assess the survival capacity of gametophytes after sMHW, the density of combined male and female gametophytes (gametophytes cm^{-2}) was determined at day 0 and 38 (11 days of heat treatment + 27 days of recovery). The number of gametophytes was quantified in a minimum of 70 fields of view per replicate using an inverted microscope (100× magnification).

3.3.4 Photosynthetic performance

To assess the physiological status of gametophytes during sMHW and subsequent recovery, maximum quantum yield of PSII (F_v/F_m) was estimated (AquaPen-P AP 110-P fluorometer; Photon Systems Instruments, Drásov, Czech Republic). Gametophytes were dark-acclimated for five minutes before the measurements. Measurements were taken throughout the course of

the experiment (day 0, 4, 11 and 38) to allow continuous assessment of gametophyte performance.

3.3.5 Female reproductive success

During the recovery phase, gametogenesis development was quantified every seven days (day 11, 18, 25, 32 and 39) by assessing the relative occurrence of three ontogenetic stages of female gametophytes (vegetative state, egg released state and gametophytes with sporophytes attached). A minimum of 100 fields of view were examined per replicate using an inverted microscope (100× magnification). For each female gametophyte, the most advanced reproductive state was recorded. Female gametophytes were identified as being in the sporophyte stage as soon as the first cell division was visible in the zygote. The percentages of gametophytes with eggs and sporophytes were summed to obtain the proportion of reproductive female gametophytes.

Reproductive success was also evaluated as the absolute numbers of sexually-derived and putatively asexual sporophytes (i.e., possible partheno-sporophytes with irregular morphology *sensu* tom Dieck 1992) per female gametophyte (sporophyte density) at the end of the recovery phase (day 40). Sporophytes with normal morphology (clear polar differentiation into the basal rhizoid and proximal elongated blade) and attached to the respective female oogonium are considered fertilized diploid sporophytes, whereas sporophytes with malformed shapes, normally missing rhizoids and unattached to the female gametophyte were considered to derive from parthenogenesis (tom Dieck, 1992). Most partheno-sporophytes in *Laminaria* are generally unable to complete development and thus represent unsuccessful recruits (tom Dieck, 1992). The absolute number of normal and parthenogenetic sporophytes was counted in a minimum of 100 fields of view (Zeiss Observer D1 inverted microscope; 100× magnification) per replicate. Final female gametophyte density was determined on day 39.

3.3.6 Statistics

Gametophyte density was analysed by 2-way ANOVA with population and temperature as fixed factors using SPSS (version 27.0, IBM Corp, 2017). The proportion of reproductive females and sporophyte density of each population were expressed relative to the respective controls at 17°C to account for significant variation between populations, allowing comparisons amongst them. Normality of the data (Shapiro-Wilk test) and homogeneity of variances (Levene's test) were tested before the statistical analyses. Estimated marginal means

pairwise comparisons (Bonferroni-corrected) were performed to determine differences between treatments when a significant interaction was found. Differences were considered significant at $p < 0.05$. Three-way repeated measures ANOVA was performed using SPSS to test for differences in the percentage of female reproductive gametophytes and F_v/F_m over time between populations and temperatures. Data were tested with the Mauchly test for sphericity and Greenhouse Geisser or Huynh-Feldt corrections were used if sphericity could not be assumed.

The sporophyte density data did not fulfil Levene's assumption of homogeneity of variance even after transformation. Therefore, data were analysed with the PERMANOVA module within PRIMER 7 software (Anderson, 2001; McArdle & Anderson, 2001) under a two-factor design with population and temperature as fixed factors. PERMDISP tests were performed for homogeneity of multivariate dispersion, which was verified without transformation. Pair-wise t-test comparisons were performed to identify differences between treatments when significant interactions were found. Data analysis was performed with Euclidian distances and 9999 permutations.

3.4 Results

3.4.1 Gametophyte survival

The final gametophyte density differed significantly due to the interaction of population × temperature (Table 3.2, Fig. 3.3; F = 14.539, $p < 0.001$).

Table 3.2. Two-way ANOVA for the effects of population and temperature on the gametophyte density of *Laminaria ochroleuca* after 38 days. The post-hoc results are presented in Fig. 3.3.

Factors	SS	df	MS	F	*p*
Population	0.216	3	0.072	5.528	**0.002**
Temperature	2.957	3	0.986	75.681	**<0.001**
Population × Temperature	1.704	9	0.189	14.539	**<0.001**
Error	0.625	48	0.013		

Significant ($p < 0.05$) interactions or main effects are highlighted in bold. SS: sum of squares; df: degrees of freedom; MS: mean sum of squares; F: F-statistic

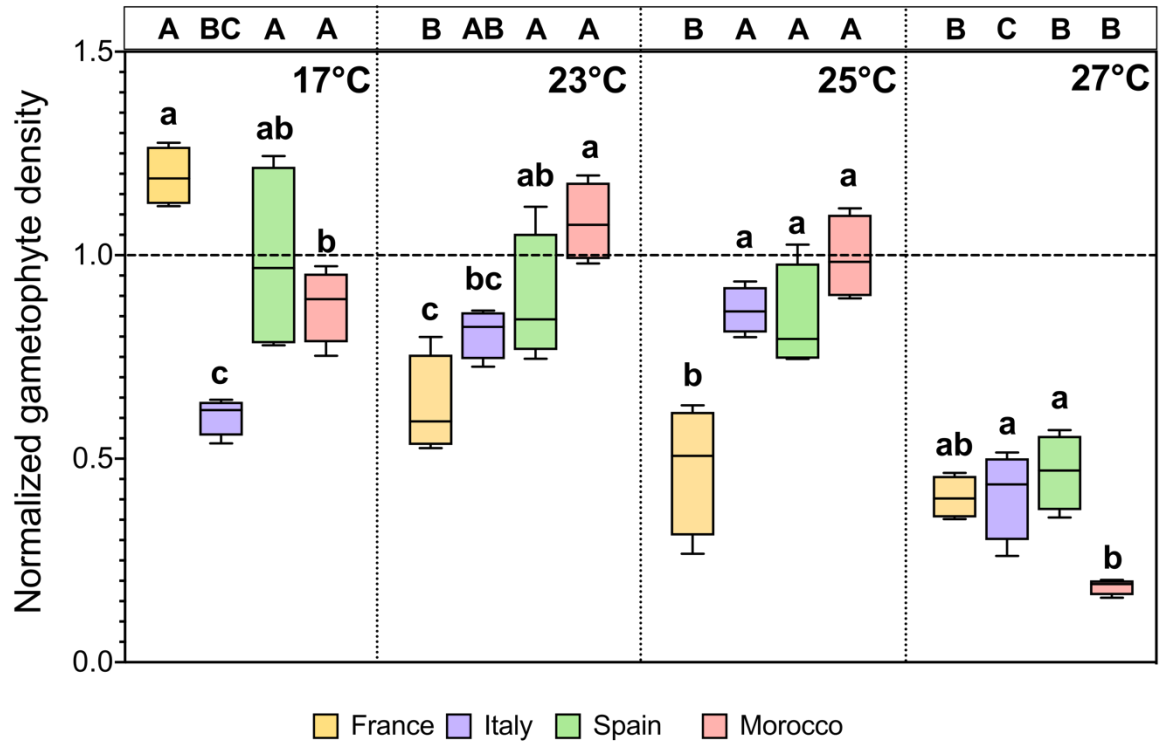

Figure 3.3: Gametophyte density from different populations (FR, IT, SP, MO) of Laminaria ochroleuca after recovery (day 38) at 17°C from different thermal treatments (17°C, 23°C, 25°C and 27°C). Note that density values were normalized to the respective initial value for each population (dotted line). Box plots with median, boxes for 25th and 75th percentiles and whiskers indicating min and max values (n = 4). For each temperature, different lowercase letters above boxplot bars indicate significant differences between populations. For each population, different uppercase letters indicate differences between temperatures ($p < 0.05$). See Table 2 for statistical analysis.

The most striking effect in all populations was the significant decline in gametophyte density at the highest temperature (27°C) compared to the control temperature. Gametophytes from the FR population showed the greatest thermal sensitivity, with density reduction apparent at all temperatures between 23°C and 27°C compared to controls at 17ºC. In contrast, gametophyte densities of the other Atlantic populations from SP and MO were only affected following the highest sMHW temperature (27ºC). The Mediterranean population (IT) showed a slightly different trend of increasing density following sMHW at intermediate temperatures (significantly so at 25ºC), before declining at 27ºC to a level not significantly different from the control, which also showed reduced density over time (Fig. 3.3).

3.4.2 Photosynthetic efficiency during heat stress and recovery

The maximum quantum yield of photosystem II (F_v/F_m) showed significant time × population × temperature interactions (Table 3.3; $F = 5.984$, $p < 0.001$).

Table 3.3 - Three-way repeated measures ANOVA for the effects of population, temperature, and time on the maximum quantum yield of photosystem II (F_v/F_m) of *Laminaria ochroleuca* gametophytes. The post-hoc results are presented in Fig. 3.4.

Factors	**SS**	**df**	**MS**	**F**	***p***
Time	1.602	3	0.534	522.686	**<0.001**
Population	0.042	3	0.014	9.640	**<0.001**
Temperature	0.606	3	0.202	138.440	**<0.001**
Time × Population	0.195	9	0.022	21.248	**<0.001**
Time × Temperature	2.180	9	0.242	237.115	**<0.001**
Population × Temperature	0.058	9	0.006	4.436	**<0.001**
Time × Population × Temperature	0.165	27	0.006	5.984	**<0.001**
Error	0.147	144	0.001		

Significant ($p < 0.05$) interactions or main effects are highlighted in bold. SS: sum of squares; df: degrees of freedom; MS: mean sum of squares; F: F-statistic

Overall, during the 11th day simulated sMHW F_v/F_m progressively decreased over time and with increasing sMHW temperature (Fig. 3.4), clearly indicating reduced maximum PS2 efficiency resulting from photoinhibition and/or photodamage.

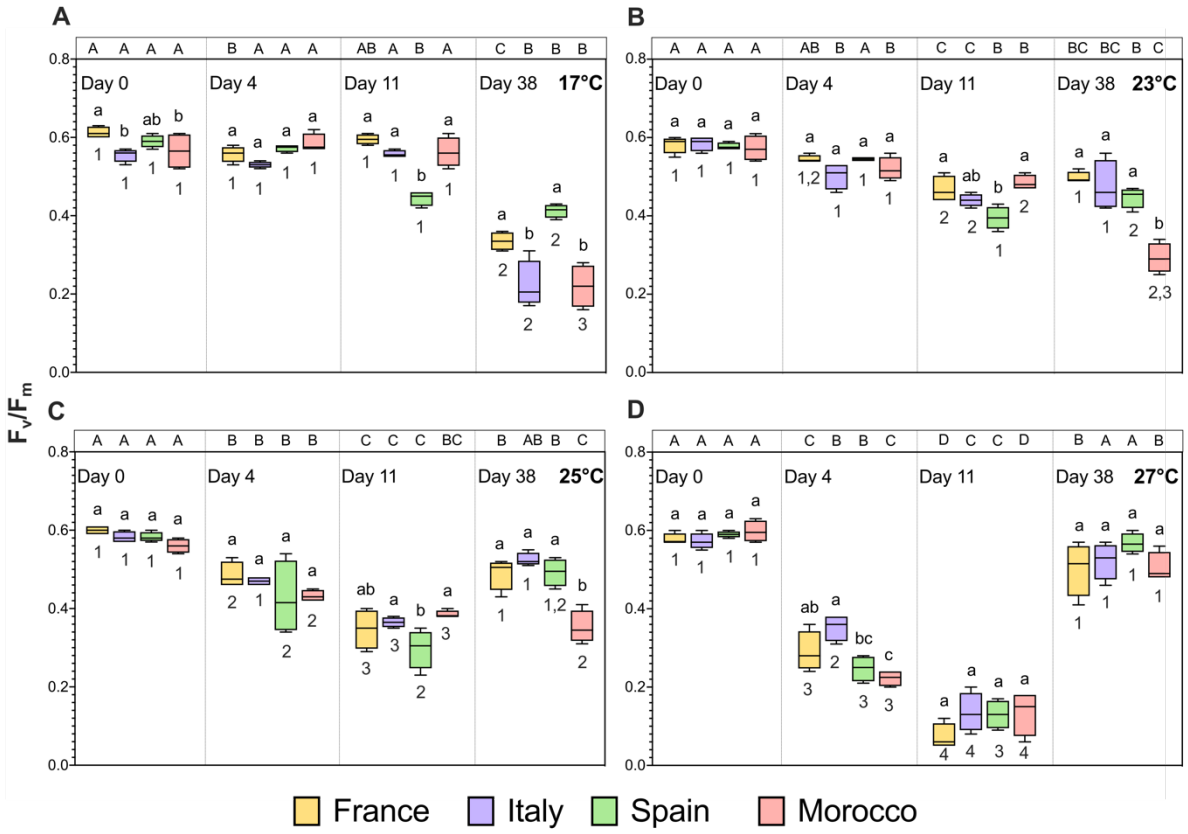

Figure 3.4: Maximum quantum yield of photosystem II (Fv/Fm) of Laminaria ochroleuca gametophytes from different populations (FR, IT, SP, MO) exposed to thermal treatments of 17°C (A), 23°C (B), 25°C (C) and 27°C (D) over time (heat wave: days 0, 4, 11 and recovery: day 38). Box plots with median, boxes for 25th and 75th percentiles and whiskers indicating min and max values (n = 4). For each temperature and time period, different lowercase letters above boxplot bars indicate significant differences between populations. For each population and temperature, different uppercase letters indicate differences between time periods. For each population and time period, different numbers indicate differences between temperatures ($p < 0.05$). See Table 3 for statistical analysis.

At the end of recovery period (day 38), we observed some surprising effects with respect to the thermal history of the gametophytes: F_v/F_m in controls declined relative to initial values in all populations, suggesting the cumulative experimental irradiance (20 µmol m^{-2} s^{-1} PAR) induced progressive photoinhibition and/or photodamage, since temperature was a constant 17ºC over this period (Fig. 3.4A). Across all populations, F_v/F_m decreased (mean value of 0.298) in the gametophytes exposed to 17°C at the end of recovery compared to the initial 11 days (mean value of 0.561). Following intermediate sMHW of 23 and 25ºC, a trend for recovery of F_v/F_m after 38 d was observed, particularly in FR and IT populations, and less evident in MO (Fig. 3.4B,C), while after the most severe sMHW (27ºC) all populations recovered to values not significantly different from initial F_v/F_m prior to the thermal stress (Fig. 3.4D). Overall, although the mechanisms remain unclear, our results suggest that sMHW of increasing intensity have positive effects on the resilience of PS2 functioning at the population level, either through a positive interaction between irradiance and high temperature, selective effects of

thermal stress favouring survival of the most resilient cells, or a shifting balance between mortality and production of new cells with increased resilience.

3.4.3 Gametophyte reproductive success during recovery from heat stress

The normalized female gametophyte reproductive success during the recovery phase showed significant time × population × temperature interactions (Table 3.4; F = 4.886, $p < 0.001$).

Table 3.4: Three-way repeated measures ANOVA for the effects of population, temperature, and time on the relative reproductive potential of female gametophytes of *Laminaria ochroleuca*. The post-hoc results are presented in Fig. 3.5.

Factors	**SS**	**df**	**MS**	**F**	***p***
Time	27.183	1.262_{GG}	21.538	47.382	**<0.001**
Population	1.307	3	0.436	1.072	0.373
Temperature	9.881	2	4.940	12.154	**<0.001**
Time × Population	4.015	3.786_{GG}	1.060	2.333	0.073
Time × Temperature	22.204	2.524_{GG}	8.797	19.352	**<0.001**
Population × Temperature	24.399	6	4.066	10.004	**<0.001**
Time × Population × Temperature	16.818	7.572_{GG}	2.221	4.886	**<0.001**
Error	20.653	45.435_{GG}	0.455		

Significant ($p < 0.05$) interactions or main effects are highlighted in bold. SS: sum of squares; df: degrees of freedom (df_{GG} denotes adjustment following Greenhouse-Geisser F-test as sphericity was not met); MS: mean sum of squares; F: F-statistic

On the first day of recovery (day 11), no reproduction was observed in the female gametophytes pre-exposed to all the sMHW treatments (23°C, 25°C and 27ºC), indicating that the heat treatments delayed the onset of gametogenesis (Fig. 3.5).

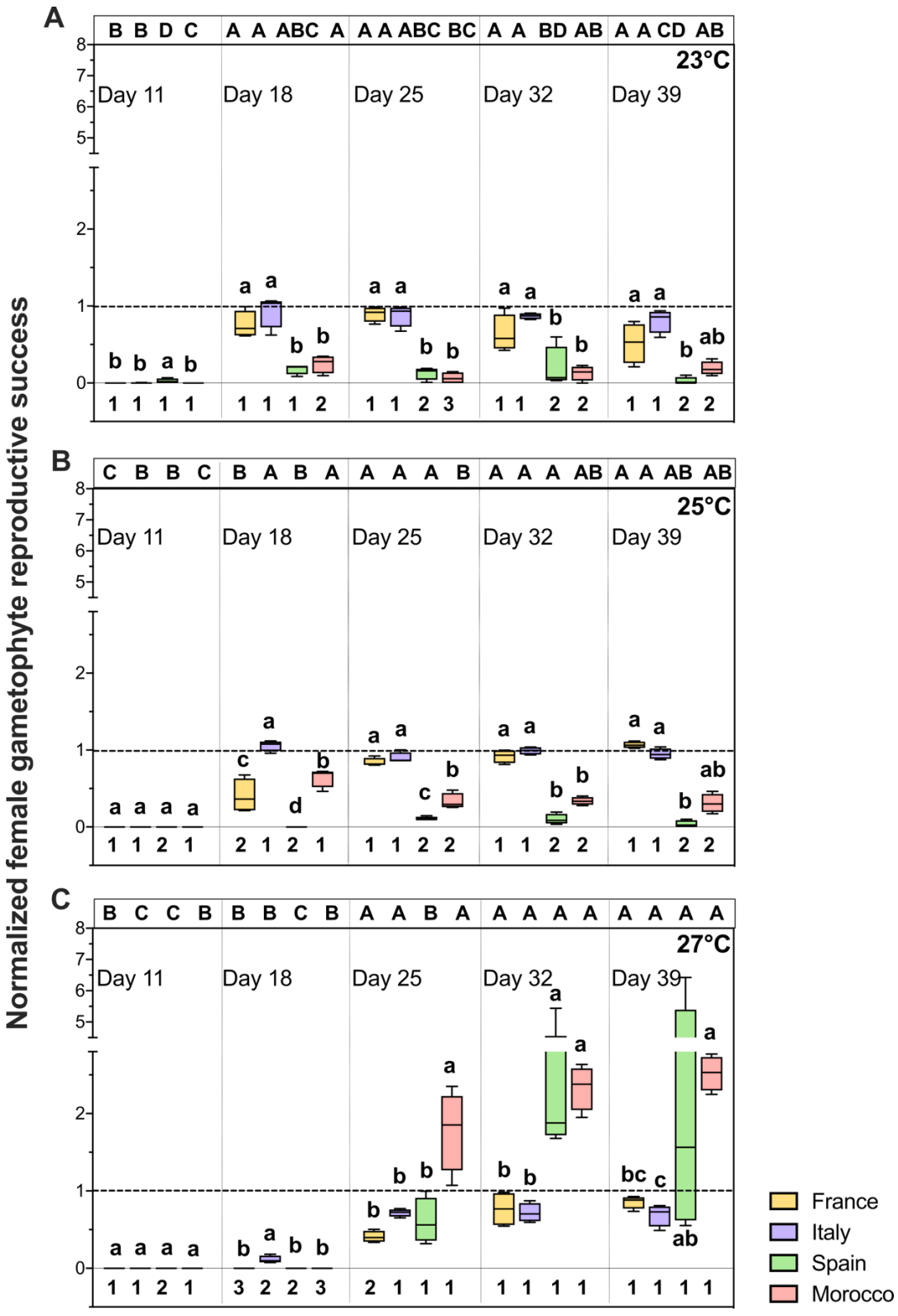

Figure 3.5: Female gametophyte reproductive success (proportion of female gametophytes with eggs and sporophytes) of different populations of Laminaria ochroleuca over recovery (day 39) at 17°C from sMHW treatments of 23°C (A), 25°C (B) and 27°C (C). Note that the female reproductive values were normalized to the control treatment (17°C) value for each population (dotted line). Box plots with median, boxes for 25th and 75th percentiles and whiskers indicating min and max values (n = 4). For each temperature and time period, different lowercase letters above boxplot bars indicate significant differences between populations. For each population and temperature, different uppercase letters indicate differences between time periods. For each population and time period, different numbers indicate differences between temperatures ($p < 0.05$). See Table 4 for statistical analysis.

From day 18 onwards, reproductive success significantly increased in the female gametophytes from FR and IT recovering from 23°C and 25ºC, and from day 25 for those recovering from 27ºC. In contrast, the SP (sMHW of 23 and 25ºC) and MO (sMHW of 23ºC) gametophytes remained mostly vegetative during the recovery phase (Fig. 3.5A,B). In all four populations, the gametophytes pre-exposed to 27°C remained vegetative during the first two time periods (day 11 and 18), however the female reproduction significantly increased from day 25 onwards (Fig. 3.5C). Notably, the SP and MO gametophytes pre-exposed to the sMHW of 27°C exhibited the highest reproductive success from day 25 onwards (normalised reproduction ≥ 1), and exceeded levels of reproductive success observed in their respective controls and in both FR and IT gametophyte populations (Fig. 3.5C).

The normalized sporophyte density after 40 days showed significant population × temperature interactions (Table 5; pseudo-F = 2.2834; $p = 0.011$) and exhibits an overall similar pattern as the proportion of reproductive females (Fig. 3.5 and 3.6).

Table 3.5: PERMANOVA for the effects of population and temperature on the number of sporophytes per female gametophytes after 40 days in *Laminaria ochroleuca*. The post-hoc results are presented in Fig. 3.6.

Factors	**SS**	**df**	**MS**	**Pseudo-F**	***p* (perm)**
Population	1.7562	3	0.58541	0.37332	0.8655
Temperature	20.294	2	10.147	6.4707	**<0.001**
Population × Temperature	21.484	6	3.5807	2.2834	**0.011**
Error (time)	56.453	36	1.5681		

Significant interactions or main effects are highlighted in bold. * PERMDISP, $p > 0.05$. SS, sum of squares; df, degrees of freedom; MS, mean sum of squares; Pseudo-F, F value by permutation.

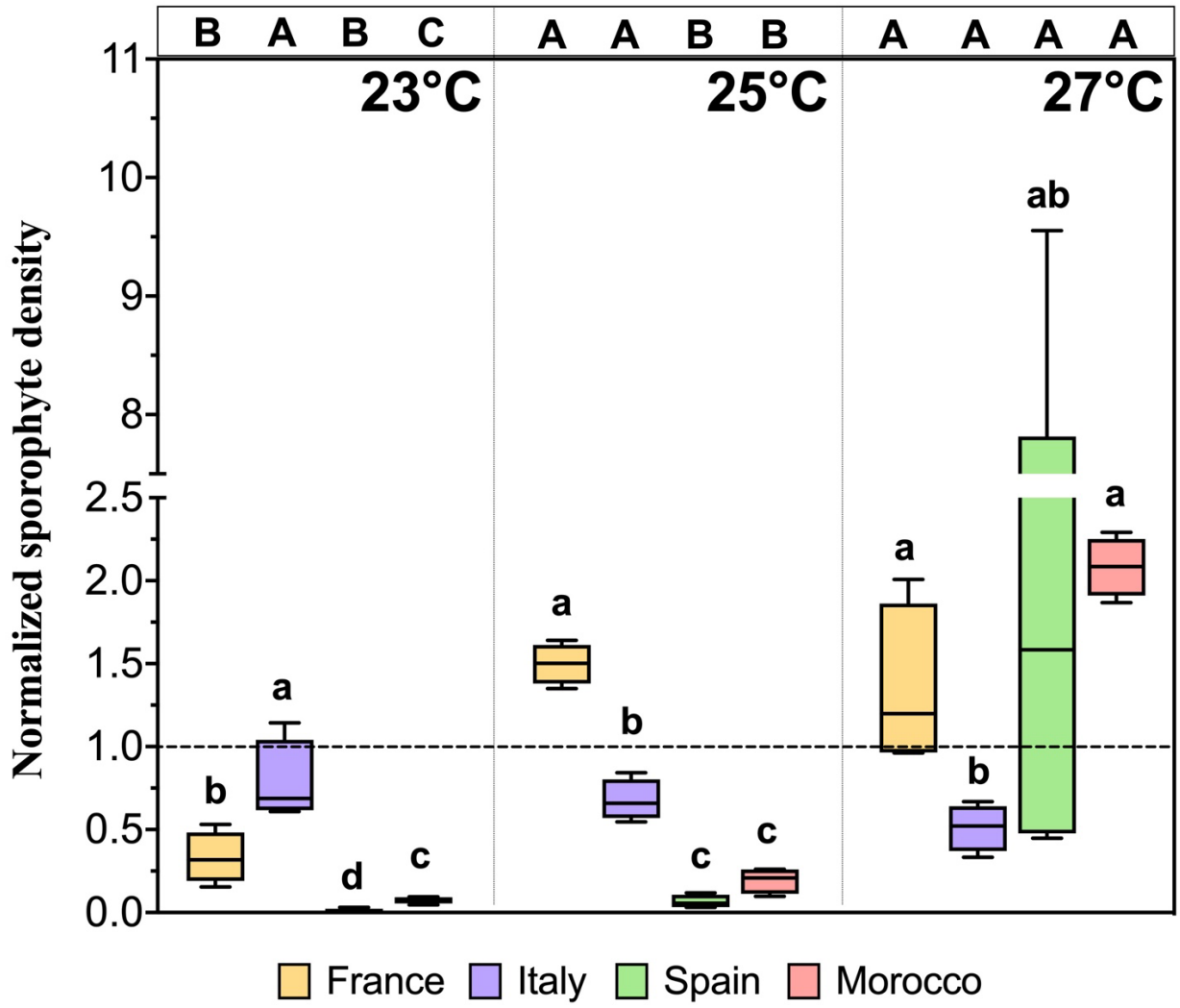

Figure 3.6: Absolute number of sporophytes per female gametophytes of different populations of Laminaria ochroleuca after recovery (day 40) from different sMHW treatments. Note that the sporophyte density values were normalized to the mean control treatment value (17°C) for the respective population (dotted line). Box plots with median, boxes for 25th and 75th percentiles and whiskers indicating min and max values (n =4). For each temperature, different lowercase letters above boxplot bars indicate significant differences between populations. For each population, different uppercase letters indicate differences between temperatures ($p<0.05$). See Table 3.5 for statistical analysis.

Overall, extremely low normalised sporophyte densities (close to zero) were observed in the SP and MO gametophytes recovering from 23°C and 25°C compared to the FR and IT gametophytes (Fig. 3.6), suggesting that intermediate heat stress negatively affects the subsequent reproductive success in these two populations. On the other hand, when pre-exposed to 27ºC a high number of sporophytes developed (normalised density ≥ 1) in the gametophytes from the FR, SP and MO populations, indicating that a short pre-exposure to a critical high temperature enhanced subsequent sporophyte formation. In contrast to the Atlantic populations, sporophyte production in the Mediterranean IT population was temperature independent following simulated sMHW exposure, and always lower than controls at 17ºC. In

the FR, SP and MO populations the gametophytes pre-exposed to 27ºC had the highest sporophyte densities compared to 23ºC.

Interestingly, a considerable number of sporophytes with irregular morphology (i.e. likely partheno-sporophytes) developed after 40 days only in the FR gametophytes pre-exposed to 17°C (324 sporophytes cm^{-2}), 23°C (1271 sporophytes cm^{-2}), and 25°C (628 sporophytes cm^{-2}) compared to sexually formed sporophytes (Fig. S3.1).

3.5 Discussion

This study revealed inter-population variability in the resilience, recovery, and subsequent reproductive success of microscopic gametophytes to thermal stress along the distribution range of *L. ochroleuca*, which potentially reflect evolutionary adaptations in response to local thermal regimes. The gametophytes from France (the most northern and cool-water population) were the most sensitive to thermal stress with mortality onset at 23ºC compared to 27ºC in the remaining populations. During recovery gametophytes from Spain and Morocco exhibited very low reproductive success after exposure to simulated sMHWs of 23 and 25ºC. However, when recovering from the highest thermal treatment (sMHW of 27ºC) the reproductive development and sporophyte output exceeded the levels obtained under control conditions (17ºC). In contrast, the gametophytes from France and Italy (Mediterranean) pre-exposed to sMHWs of 23ºC, 25ºC and 27ºC were able to resume reproduction at levels similar to those of controls by the end of the recovery period. This highlights the need for fine scale regional data to accurately predict species response to future climate changes.

Gametophytes are the most thermally tolerant life cycle stage in kelps, withstanding higher temperatures than sporophytes (tom Dieck, 1992, 1993; tom Dieck & Oliveira, 1993). The upper survival temperature of *L. ochroleuca* gametophytes was previously reported to be 25ºC (tom Dieck 1993). In our study, exposure to a simulated heat wave of 27ºC negatively affected *L. ochroleuca* gametophyte density (more than 50% of mortality) in all four populations. However, the gametophytes from the most northern population, France, exhibited greater thermal sensitivity, with loss of gametophyte density (i.e., balance between growth and mortality) already apparent at 23ºC. This intraspecific variation in gametophyte thermal tolerance suggests (potentially) adaptive divergence between populations of *L. ochroleuca* as all gametophytes were developed from meiospores under common garden conditions to remove the influence of previous thermal histories (although carry over effects cannot be discounted

entirely, e.g., see Gauci et al., 2022). Inter-population variability (both adaptive and mal-adaptive) in the resistance to heat stress has been reported for other laminarian and fucoid macrophytes (Pearson et al., 2009; Saada et al., 2016; King et al., 2018). Locally adapted ecotypes were demonstrated for *L. digitata*, where trailing edge populations had a stronger heat shock response to thermal stress than range centre populations (King et al., 2019). In addition, gametophytes of *L. digitata* from the Arctic exhibited lower growth rates and reduced sporophyte recruitment after heat stress compared to Atlantic gametophytes (Martins, Pearson, Bernard, Serrão, & Bartsch, 2020). Evidence for adaptive variation was recently shown for the intertidal seaweed *Hormosira banksii*, as high temperatures (21°C) led to increased mortality in individuals from cooler locations, while individuals from warmer niches were relatively unaffected (Miller et al., 2020). Intraspecific variation in thermal tolerance was also found for *Fucus vesiculosus*, with southern individuals showing higher resilience to heat stress than northern ones (Saada et al., 2016).

It was recently shown that the northern populations (English Channel) of *L. ochroleuca* exhibit much lower genetic diversity and endemism compared to southern populations such as western Morocco (Assis et al., 2018). This skewed pattern of genetic diversity was found to be driven by past climate changes and oceanographic barriers (Assis et al., 2018; Lourenço et al., 2016b). Genetic diversity can have substantial effects on the adaptive capacity of kelp populations to respond to environmental changes (Reed & Frankham, 2003; Coleman & Wernberg, 2020, 2021, Vranken et al., 2021) as higher genetic diversity provides a greater range of functional responses (i.e., adaptive potential) and may increase the capacity to endure a stressor (Reusch et al., 2005, Wernberg et al., 2018). We may hypothesise that the lower resilience to heat stress of the gametophytes from the most northern population (France) might be associated with reduced genetic diversity. The effects of marine heat waves on kelps appears related with the level of genetic diversity of populations affected (Wernberg et al., 2018): *Eklonia radiata* adults from low diversity populations were extirpated by heatwaves in Western Australia (Wernberg et al., 2012). Similarly, trailing edge populations of the intertidal fucoid *Fucus serratus* showing reduced genetic diversity were also less tolerant to heat shock than central populations (Pearson et al., 2009). In the seagrass *Zostera marina*, genetically diverse populations show enhanced heat stress resilience (Ehlers et al., 2008). Thus, the conservation of genetic diversity may be crucial for evolutionary adaptation of macrophytes to global climate change.

Thermal stress causes photoinhibition in kelps (Bruhn & Gerard, 1996) and F_v/F_m is frequently used as an indicator of stress affecting photosystem II (PSII, Beer et al., 2014). The progressive decrease in F_v/F_m we observed in gametophytes with increasing temperature and exposure time during simulated sMHWs in all populations of *L. ochroleuca* indicates dynamic downregulation (e.g., Pereira et al., 2015), or impaired function of PSII reaction centres in response to thermal stress (particularly at 27°C), potentially imposing individual fitness costs. Overall, gametophytes failed to fully recover F_v/F_m following simulated sMHWs by the end of recovery period. Counterintuitively however, we observed an increasing trend for recovery of F_v/F_m with greater sMHW temperature, notably including controls at 17ºC, which were quite severely affected after 38 d. Indeed, full recovery to initial F_v/F_m values were only observed after moderate to severe sMHW in gametophytes from Italy (25 and 27ºC) and Spain (27ºC).

Several factors may have contributed to these patterns. First, optimal thermal conditions for gametogenesis in the controls (tom Dieck, 1992; Izquierdo et al., 2002) and the earlier diversion of resources to reproduction may result in a trade-off between physiological performance and ontogeny, and/or competition for nutrients, space or light between gametophytes and microscopic sporophytes (Edwards & Connell, 2012). The inhibition of reproduction imposed by simulated sMHWs may serve to delay this process, and partially explain higher F_v/F_m after the recovery period. In addition, the 27ºC sMHW reduced mean gametophyte density between > 50% (FR, SP, IT) to ca. 80% (MO), potentially alleviating sources of limitation. Microscopic sporophytes are an actively growing early life stage, requiring nutrient levels that can exceed those of mature thalli (Thomas et al., 1985). Therefore, despite the medium being renewed twice through the experiment, the nutrient consumption by both life cycle stages (particularly by the actively growing sporophytes) might have created a nutrient deficit affecting physiological status. Negative effects of nutrient limitation on sporophyte photosynthesis have been described in several kelp species (*Saccharina japonica*: Gao et al., 2017; Liu et al., 2021; *Macrocystis pyrifera*: Fernández et al., 2020). Furthermore, potentially suboptimal or limiting irradiance for gametophytes developing beneath the growing sporophytes might have also contributed to the observed decrease in maximum photosynthetic efficiency of PSII.

The optimal reproductive development of *L. ochroleuca* gametophytes occurs between 11–18°C (tom Dieck, 1992; Izquierdo et al., 2002). However, studies investigating the influence of warming on the reproductive success of *L. ochroleuca* gametophytes are scarce

(but see Pereira et al., 2011). In our study, simulated sMHWs (23ºC, 25ºC and 27ºC) prevented the onset of gametogenesis in all populations of *L. ochroleuca*, with gametophytes remaining in the vegetative state. Gametophytes can delay the formation of sexual cells and thus sporophyte production when exposed to unfavourable environmental conditions (tom Dieck, 1993; Carney & Edwards, 2010; Silva et al., 2022) such as extreme climatic events (Martins et al., 2020), but are able to resume their reproductive capacity as soon as conditions improve (Carney & Edwards, 2010; Martins et al., 2020). This may provide an advantage for populations living in habitats subjected to severe climatic events, which usually lead to drastic sporophyte mortality (Ladah et al., 1999; Barradas et al., 2011). However, the capacity of gametophytes to recover and reproduce after limiting conditions seems to be species-specific (Silva, Pearson, Serrão, Bartsch, & Martins, 2022).

We found that the gametophyte potential to reproduce when recovering from heat stress varies among populations of *L. ochroleuca*. Overall, female gametophytes from Spain and Morocco showed very low ability to successfully reproduce and form sporophytes after exposure to simulated sMHW of 23ºC and 25ºC. In contrast, the gametophytes from France and Italy pre-exposed to simulated sMHW of 23ºC, 25ºC and 27ºC were able to resume reproduction at levels similar to their respective controls by the end of the recovery period. Although, the gametophyte generation from each population were raised under common garden conditions from meiospores, intrinsic differences in reproductive investment after a heat stress were seen, which might suggest genetically based thermal responses (or strong carry-over effects) linked to their regional origin. Similarly, *L. digitata* gametophytes from the Atlantic produced a greater number of sporophytes during recovery from heat stress than those from the Arctic, suggesting differential thermal adaptation (Martins et al., 2020). Variations across populations in the reproductive response to temperature have previously been observed in the giant kelp (*Macrocystis pyrifera*) along its distributional range, indicating local adaption to thermal gradients (Hollarsmith et al., 2020).

Surprisingly, the gametophytes from Spain and Morocco exhibited the highest levels of reproductive success after the simulated sMHW of 27°C, exceeding the reproductive levels obtained under control conditions (17ºC). This extreme thermal treatment might have promoted the subsequent gametogenesis via an ultimate stress-induced survival mechanism, similar to heat-stimulated bolting and flowering observed in plants (*Arabidopsis thaliana*, Balasubramanian et al., 2006; Tonsor et al., 2008) and seagrasses (Blok et al., 2018; Marín-

Guirao et al., 2019; Ruiz et al., 2018). Alternatively, thermal stress may have resulted in selective survival of extreme thermotolerant genotypes, a particularly interesting hypothesis for the core, high genetic diversity population from MO (Assis et al., 2018). While it is tempting to search for population-specific reproductive responses that might be associated with regional thermal regimes, such conclusions are difficult to draw. For example, although reproductive success in the relatively cool and stenothermal IT population was poor after exposure to sMHW > 23ºC, the cool-water Atlantic population from FR was relatively successful after moderate to high sMHW exposure. Similarly, gametophytes from the warmest thermal niches (SP and MO) successfully reproduced after a 27ºC sMHW, but were very unsuccessful at 23 and 25ºC. Moreover, reproduction at 27ºC may be a non-adaptive stress-induced response, since local seawater temperatures in Spain and Morocco do not naturally reach 27°C.

Species of the order Laminariales can develop sporophytes via parthenogenesis from unfertilized eggs (tom Dieck, 1992; Oppliger et al., 2007; Martins et al., 2019). Most parthenogenetic sporophytes have an irregular morphology and show high mortality rates (Ar Gall et al., 1996), however in some species adult fertile partheno-sporophytes with normal morphology develop (Shan et al., 2013). In the most northern population of *L. ochroleuca* (France) that displays less genetic diversity, partheno-sporophytes sensu tom Dieck (1992) developed in controls at 17ºC. Subsequent exposure to sMHWs of 23ºC and 25ºC further increased the number of partheno-sporophytes. Species adaptation to marginal habitats has often been associated with parthenogenetic reproduction (Kawecki, 2008). It would be interesting to understand whether the geographical parthenogenesis found in *L. ochroleuca* (i.e., partheno-sporophytes developing near the northern distributional edge) plays an adaptive role in a marginal ecological niche, contributing to the geographic distribution of the species over evolutionary time. Similarly, a southern-limit population of *L. digitata* showed a high propensity for producing unreduced spores, a consequence of the life in a marginal habitat (Oppliger et al., 2014).

The *in-vitro* experimental setup using gametophytes raised under common garden conditions has shown to be efficient in revealing *L. ochroleuca* population differences in thermal traits while excluding the influence of environmental histories. The study highlights the need for species distribution and climate niche models to incorporate intraspecific variation to generate more reliable predictions of species responses to future climates. Deciphering intraspecific

variation may also provide valuable insight for future management of wild and farmed kelp populations, incorporating evolutionary potential for “climate-proofing” marine ecosystems.

Chapter 4

Ancient deep populations show susceptibility to marine heatwaves in the golden kelp *Laminaria ochroleuca*

In preparation for publishing:

Barreto LM, Serrão EA, Bartsch I, Martins N, Valero M, Assis J, Fragkopoulou E, Kaidi S, Sabour B, Milla D, Afonso P, Pearson GA (2024). Ancient deep populations show susceptibility to marine heatwaves in the golden kelp *Laminaria ochroleuca*

4.1 Abstract

To understand the putative interspecific variation (*i.e.* phenotypic plasticity and/or local adaptation) among populations across the biogeographic distribution of the warm-temperate forest-forming kelp species *L. ochroleuca*, we analysed the responses to simulated marine heatwave (sMHWs) in field-collected adult sporophytes, and *in vitro* cultured common garden grown F1 juvenile sporophytes (to account for genotype-environment interactions). We analysed the thermal regime and long-term MHW metrics from 5 geographically distinct regions to support and integrate into the experimental sMHW design. We additionally assessed intraspecific variation across the latitudinal gradient of the species distribution according to known genetic structure (North, Centre and South), and between shallow (-4 m depth) and deep (-50m depth) populations, by analysing ecophysiological responses (photosynthesis [F_v/F_m and $rETR_{max}$] and growth) to different simulated marine heatwave (sMHW) scenarios with interacting effects of temperature and nutrient availability. Nutrient enrichment had a positive effect across all treatments and populations on the resilience of both field adult and F1 juvenile sporophytes to the highest sMHWs. The deep adult population (Az) was photoinhibited at 23 and 25°C at the end of the sMHW while the other shallower regions were unaffected. However, the deep population was able to recover, indicating that photoinhibition might have occurred due long-term acclimation or local adaptation to thermally stable conditions (± 0.9°C) and low PAR light availability conditions of deep habitats. The hypothesised higher resilience to sMHWs of South warm edge adults and F1s juvenile sporophytes (either due to acclimation, local adaptation and/or higher and unique genetic diversity) was observed in $rETR_{max}$ but was detected in growth rates under these experimental conditions. We further discuss future research lines and measurements to protect and maintain the ancient and unique deep populations.

4.2 Introduction

Understanding how foundation species in ecosystems including grasslands, terrestrial forests, coral reefs, and kelp forests adapt and persist across their distribution range to changing environmental conditions is fundamental to predict ecosystem responses in the face of increasing intensity, frequency and duration of warming anomalies and long term shifts in thermal regimes (Pecl et al., 2017; Schirpke et al., 2017; Frade et al., 2018; Smale et al., 2019).

Species are typically exposed to different environmental conditions across their latitudinal and/or biogeographical distribution. The responses of populations (e.g., reproductive output, growth or survival) to local environmental conditions may therefore vary due to some combination of plasticity and locally adaptive variation (i.e., phenotypic and genotypic variation within and among populations; Reed et al., 2011; Valladares et al., 2014). It is therefore paramount to understand whether, across the environmental gradient of foundation species, locally adapted populations are better able to withstand and survive these challenges (Wernberg et al., 2018; Liesner et al., 2020). Studies focused on intraspecific variation in marine foundation species remain scarce (King et al., 2018; Liesner et al., 2020; Strasser et al., 2022). Consequently, species-level responses to environmental stressors or predictions from species distribution modelling (SDM) are often constrained in assuming homogenous responses across the entire distribution range. The result is the potential misestimation of species vulnerability, compromising conservation and management strategies across entire ecosystems (Vargas et al., 2017; Des Roches et al., 2021; Hays et al., 2021).

Temperature is the major factor constraining the distribution of marine species at latitudinal scales, and biogeographical ranges are often defined by the species tolerance to winter minimum and summer maximum mean seawater temperatures (MST; Edgar et al., 2017; Stuart-Smith et al 2017). The gradual increase of MST (0.6°C on average NOA, 2021) observed over the past century has already caused shifts in species distributions (Parmesan & Yohe, 2003) and phenology (e.g., reproduction; Hu et al., 2022; Hoppit & Schmidt, 2022). Moreover, the last 3 decades have seen abrupt increases in the frequency and duration of high seawater temperature anomalies (Oliver et al., 2018; Holbrook et al., 2019). Indeed, marine heatwaves (MHWs - discrete anomalous events of seawater temperature increase exceeding historical records; Hobday et al., 2016) have caused massive species shifts and biodiversity loss worldwide (Jones et al., 2018; Smale et al., 2019; Cheung et al., 2021; Garrabou et al., 2022).

Due to their rapid development as well as their increasing magnitude and duration, MHWs are particularly dangerous for sedentary organisms that are unable to evade warm water masses (Perez, Garrabou et al., 2000; Smale et al., 2017). The consequences may be particularly severe for foundation species and ecosystem engineers such as seagrass meadows, coral reefs, mangroves and kelp forests (Hays et al., 2021), where the cascading effects of their decline and/or disappearance have profound consequences on the entire ecosystem (Coleman & Williams, 2002; Thomson et al 2014 ; Smale et al., 2019). The disruption due to MHWs of

ecosystem services provided by foundation species worldwide (*e.g.*, nursery areas, food supply, shelter, fisheries, coastal erosion protection; Wernberg et al., 2012; Smale et al., 2019 ; Garrabou et al., 2022) may amount to socio-economic losses of billions of dollars (Beaumont et al., 2008; Vassallo et al., 2013; Vásquez et al., 2014; Bennett et al., 2016; Blamey & Bolton, 2017; Himes-Cornell et al., 2018).

Kelp forests of large brown macroalgae (Phaeophyceae; Laminariales *sensu stricto*, but also including fucoids and others) produce a high biomass canopy in the water column (D. C. Reed et al., 2008; Bartsch et al., 2008) resulting in a three-dimensional habitat that modifies the surrounding physical environment (*i.e.,* wave and current energy [Rosman et al., 2007], light levels [Wernberg et al., 2005; Desmond et al., 2015] and sedimentation composition (Alsuwaiyan et al., 2021). These ecosystems are productive and highly diverse, providing nursery grounds, food and shelter for a variety of marine life (Steneck et al., 2002; Teagle et al, 2017; Wernberg et al., 2019; C. M. Duarte et al., 2022). As kelp forests and their associated community can be found in relatively shallow coastal areas world-wide (Wernberg et al., 2019), their extraction and cultivation has a long association with coastal human societies worldwide (Erlandson et al., 2005; Erlandson et al., 2015). This prolific ecosystem provides important socio-economic resources directly through food production, and alginate/hydrocolloid extraction (Bartsch et al., 2008), and indirectly by associated species of interest (*e.g.*, fish, molluscs, crustaceans; Beaumont et al., 2008; Bertocci et al., 2015; Wernberg et al., 2019). However, extreme climate events including MHWs have pushed entire forests beyond ecophysiological thresholds, causing severe impacts including massive kelp biomass loss (Arafeh-Dalmau et al., 2019; Filbee-Dexter et al., 2016; Krumhansl et al., 2016), reductions in survival and growth (Bennett et al., 2015; Filbee-Dexter et al., 2020), and in some cases ecosystem shifts from kelp forests to much less productive and diverse turf algae-dominated systems (Filbee-Dexter et al., 2016; Karen Filbee-Dexter & Wernberg, 2018).

In the Northern Hemisphere, interglacial periods correspond to a poleward recolonization by species as temperatures rise and/or ice cover retreats (Hewitt, 1996; Stewart et al., 2010; Bringloe et al., 2020). For such species, the long-term centre of distribution corresponds to areas where populations have continuously persisted across glacial – interglacial periods near the contemporary warmer southern distributional edges (Bennett, K. D. & Provan, J. 2008; Stewart et al., 2010; Assis et al., 2018). Intraspecific variation among populations from the entire distribution range likely includes contributions from local adaptation (adaptive

changes in allele frequencies towards local optima; King et al., 2018), and phenotypic plasticity (the ability of a genotype to express different phenotypes in response to different environmental conditions; Becker et al., 2015). Ancient populations at the contemporary warmest distributional edge typically display rich and unique genetic diversity compared to more recent northern populations due to relatively low propagule dispersal (King et al., 2018), founder effects (Barton & Charlesworth 2003) and genetic surfing (Hallatschek & Nelson 2008; Neiva et al., 2010). Resilience to thermal stress due to acclimation, adaptation and phenotypic plasticity in low latitude edge populations has been suggested for some kelp species (Atkins & Travis, 2010; Wernberg et al., 2018; King et al., 2019; Liesner et al., 2020). However, decadal-scale ocean warming and the increasing frequency and intensity of MHWs threaten to outpace adaptative capacities under rapidly deteriorating environmental conditions, and the potential extirpation of unique gene pools in some species (Wernberg et al., 2018; Filbee-Dexter et al., 2020). Despite accumulating evidence for the role of local adaptation and phenotypic plasticity in responses to environmental change (Valladares et al., 2014; Liesner et al., 2020; Strasser et al., 2022), studies focused on detecting intraspecific variation in response to MHWs remain scarce (King et al., 2018). Models that aim to predict future species distribution often assume a uniform species response (Reed et al., 2011 ;Holt & Gomulkiewicz, 2004), potentially compromising the effectiveness of kelp conservation, restoration and farming actions taken by decision-makers.

In this study, we used *Laminaria ochroleuca* as a model temperate kelp species with a distribution range in the Northeast Atlantic Ocean and Mediterranean (Assis et al., 2018; Schoenrock et al., 2019; Strasser et al., 2022). Our aim was to analyse intraspecific (population level) variation across a latitudinal gradient of the species distribution (North, Centre and South) but also between shallow (-4m) and deep (-50m) populations using field adults sporophytes but also the next generation (F1s) sporophytes, grown in controlled laboratory conditions, to account for parent field acclimation/exposure. We assessed ecophysiological responses (photosynthesis and growth) to different simulated marine heatwaves (sMHWs) scenarios with interacting effects of temperature and nutrient availability. We additionally analysed the thermal regime and long-term MHW metrics from 5 geographically distinct regions covering the contemporary distribution of the species.

We hypothesize that 1) Nutrient enrichment would ameliorate sporophytes response to high thermal stressed imposed by the sMHW compared to non-enriched treatments; 2) A latitudinal gradient of response to the sMHWs with the South distribution edge being more resilient due

to higher and unique genetic diversity (Assis et al., 2018) and/or field acclimation to warmer sea water; 3) Deep populations lower response to sMHWs in comparison to more shallower populations due to the thermal stability of the deep habitat.

4.3 Methods

4.3.1 Sampling area

In this study, we used 5 regions along the distribution range of *Laminaria ochroleuca* in the eastern Atlantic: North (France, Roscoff), Centre (Spain, Galicia), South (Morocco, El Jadida) and 2 deep (-50m) in Portugal, Azores and Italy, Messina to assess population differentiation across the entire species distribution in both latitude and depth (Fig. 4.1).

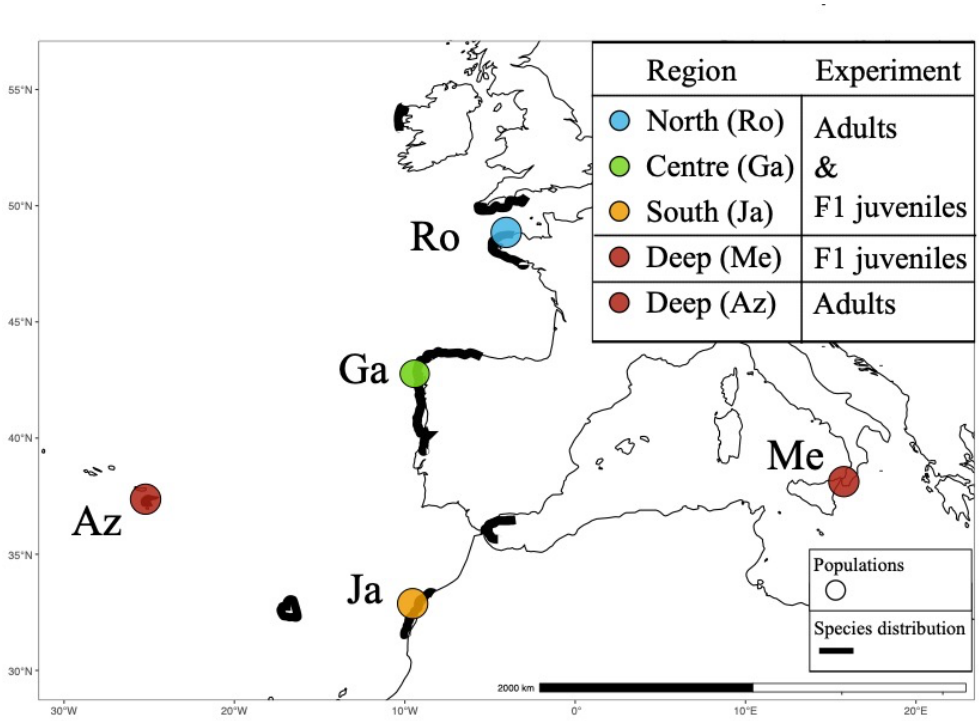

Figure 4.1: *Laminaria ochroleuca* distribution across the Northeast Atlantic and studied regions: North in France, Roscoff (Ro), Centre in Spain, Galicia (Ga), South in Morocco, El Jadida (Ja) and 2 deep populations: Italy, Messina (Me) and Portugal, Azores (Az) (see table S4.1 for population coordinates). Experiments on both adults and F1s juveniles were performed in the North (Ro), Centre (Ga) and South (Ja) regions while Deep (Az) only adult experiment and Deep (Me) only F1s juvenile experiment.

For field adults experiment we used North, Centre, South and Deep Azorean (Az) populations as the Deep Messina population adults did not survive the transport to laboratory. For F1s

juvenile experiments we used North, Centre, South and Deep Messina (Me) populations as the Az population was not reproductive at the time of sampling.

4.3.2 Sampling methodology

Laminaria ochroleuca adults were sampled by snorkelling or scuba in rocky subtidal areas between 1 and 51 m depth with at least 2 m distance between individuals at Roscoff, France (January 2019), Galicia, Spain (May 2019), El Jadida, Morocco (August 2019), Messina, Italy (November 2019) and Azores, Portugal (August 2018) encompassing most of the species distribution range in the NE Atlantic (see Table S4.1 for coordinates) and covering distinct genetic groups (see Assis et al., 2018).

Adult sporophytes were sampled by cutting the stipe junction to the meristem. To avoid excessive sampling impact on low-density deep *L. ochroleuca* populations (Az and Me) 16 and 12 sporophytes were sampled, respectively, while ~40 individuals were sampled from the other locations (Table S4.1). Sporophytes were immediately processed in indoor facilities. Tissue was cleaned of epiphytes with moist paper and 6 discs (2 cm Ø) were cut from the meristematic region and wrapped (per individual) in seawater-moistened paper rolls and placed in independent zip lock bags. Discs were stored between 5 - 8°C and transported in cool boxes within 48h to the experimental facilities at Centro de Ciências do Mar do Algarve (CCMAR), Portugal. Discs from the reproductive tissue (sorus, n = 2) were also collected from each individual when mature sorus was observed and placed in 50 ml falcon tubes containing 2 glass slides and artificial sea water (ASW; Tropic Marin® Classic and Elix H_2O) with 10ml/L GeO_2 (to inhibit diatom growth) at 32 ppm salinity for spore release.

4.3.3 Laboratory F1 juvenile cultivation

Upon arrival at the laboratory, each glass slide from the Falcon tubes with reproductive tissue was individually placed inside a petri dish with ASW with 10 ml/L GeO_2 at 32 ppm and stored in a climatic chamber at 13°C and 8 µmol red light (16:8h Light:Dark) to allow spore germination and vegetative growth of gametophytes without inducing gametogenesis (Fig. 2a). After one week, the medium was changed to ASW with 10 ml/L modified Provasoli enrichment (PES; Provasoli, 1968, modifications: HEPES buffer instead of TRIS, double concentration of

Na_2-glycerophosphate). From each region, 10 individuals with a similar density of gametophytes were selected and half of each slide was scraped into a 15 cm Ø glass petri dish to obtain a homogenous contribution from each individual to a population pool. To induce gametogenesis and sexual reproduction, glass petri dishes were placed in 15 µmol white light (16:8h L:D) and medium was renewed twice a week. When small sporophytes were visible to the naked eye (≈ 1-2 mm), they were scraped into a 5L glass bottle with aeration and cultured in the same medium and light conditions (Fig. 2b). As sporophytes in these conditions usually grow in aggregates, when they reached ≈ 1-2 cm, the stipes were cut with a scalpel to allow homogenous growth of individual sporophytes. When sporophytes reached ≈ 6 - 8 cm, temperature and light intensity were gradually increased from 13 to 17°C at 1°C every other day and from 15 to 30 µmol at 4 µmol every other day, respectively, until they were moved into the experimental setup.

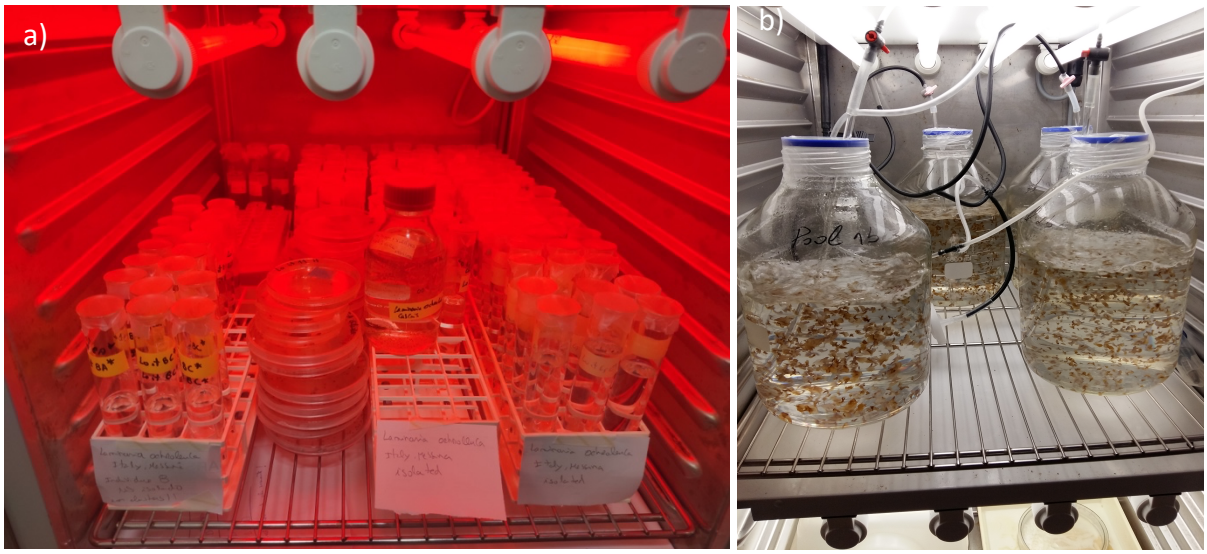

Figure 4.2: a) Gametophytes in vegetative conditions. b) Small F1s juvenile sporophytes growing in white light and aeration.

4.3.4 Ecophysiological (photosynthetic and growth) performance to simulate marine heat waves (sMHW)

Adult meristematic discs (n = 6) from the same individual were placed in a 1 L beaker with 900 mL ASW (Tropic Marin® Classic and Elix H_2O) at 32 ppm salinity, with 10 mL/L modified Provasoli enrichment (PES; Provasoli, 1968, modifications: HEPES buffer instead of TRIS, double concentration of Na_2-glycerophosphate). Circulation of the medium was achieved by aeration (AIR Pump DB-120, Esoair) at 11°C and a 16:8h L:D cycle with irradiance of 15 µmol m^2 s^{-1} (AquaBeam 1500 MW Marine 24 White, Tropical Marine Centre) to allow wound

healing for 18 days. The medium was renewed every 3 days. Temperature and light were gradually increased every other day at 1°C and 2 µmol m^2 s^{-1} steps, until the target temperature of 17°C and irradiance of 30 µmol m^2 s^{-1} were reached.

The factorial experimental design for both adult meristem discs and F1 juveniles consisted of simulated dynamic gradient heat waves with 4 temperatures selected based on modelled MHW data from each site (see MHW section below and Results): 17°C (control) 21°C, 23°C (reported sporophyte upper survival temperature for a 14 day exposure with no thermal ramp [Wiencke et al., 1994]) and 25°C (2°C above the reported sporophyte upper survival temperature) with 4 - 5 replicates per treatment. As anomalously high sea water temperature events are highly correlated with nutrient depletion (Carr & Kearns, 2003; Hayashida et al., 2020), two nutrient treatments were used: PES-enriched and non-enriched ASW. As only 16 individuals were sampled for the Deep Az adults, only the PES-enriched treatment was used in this case. A replicate consisted of a 1 L beaker with 6 discs from the same individual for the adult experiment and 6 F1 juvenile sporophytes for the F1 experiment. Prior to thermal (sMHW) treatments, discs/sporophytes were maintained under control conditions for an additional 5-day acclimation phase to the nutrient-enriched and non-enriched conditions (day -5 in Fig. 4.3).

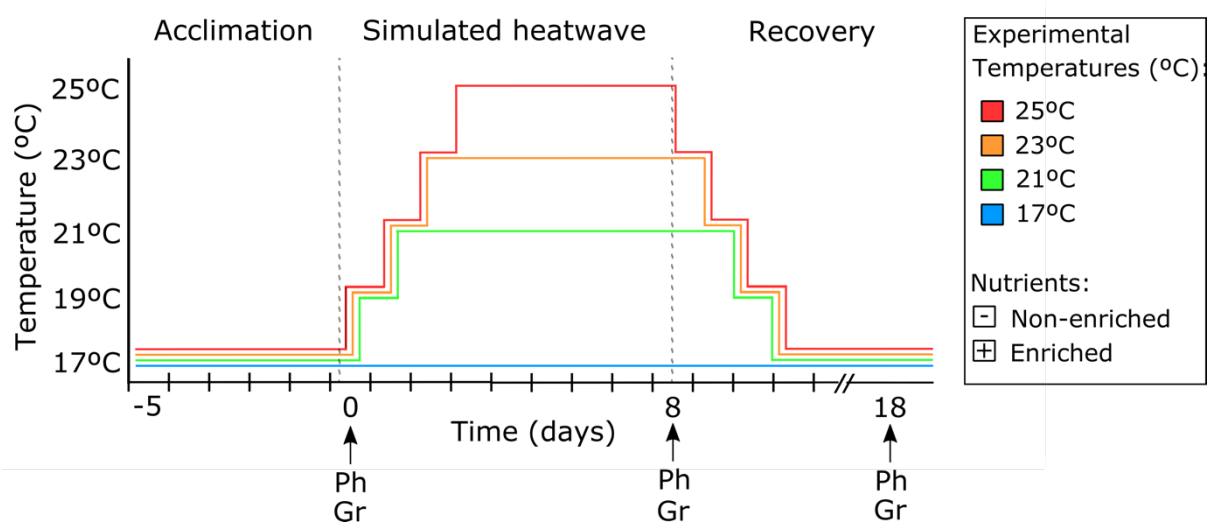

Figure 4.3: Experimental design of simulated heat waves (sMHW) applied in *Laminaria ochroleuca* adult and F1 juvenile sporophytes. Dotted vertical lines define the experimental stages: "Acclimation" from day -5 to 0,

dynamic “Simulated heatwave” from day 0 to 8 and “Recovery” from day 8 to 18. Experimental temperatures were 17°C (control), 21°C, 23°C and 25°C. Nutrient treatments corresponded to Provasoli enriched (+) and non-enriched (-) medium. ↑ indicates sampling for photosynthetic performance (Ph) and growth (Gr) taken on days 0 (control), 8 (end of heat wave [sMHW]) and 18 (end of recovery [RC]).

The sMHW phase started at day 0 with 2°C daily temperature increase until the target maximum temperature for each thermal treatment was reached, followed by 7 days at 21°C, 6 days at 23°C and 5 days at 25°C. At day 8, the recovery (RC) phase started, consisting of a 2°C daily temperature decrease until all treatments reached 17°C. There followed an additional 7 days under control conditions (total RC = 10 days; Fig. 4.3). Each temperature treatment consisted of an independent thermally controlled water bath (Huber Variostat Pilot One, Offenburg, Germany) with a temperature stability of 0.02°C (Fig. 4.4a, b).

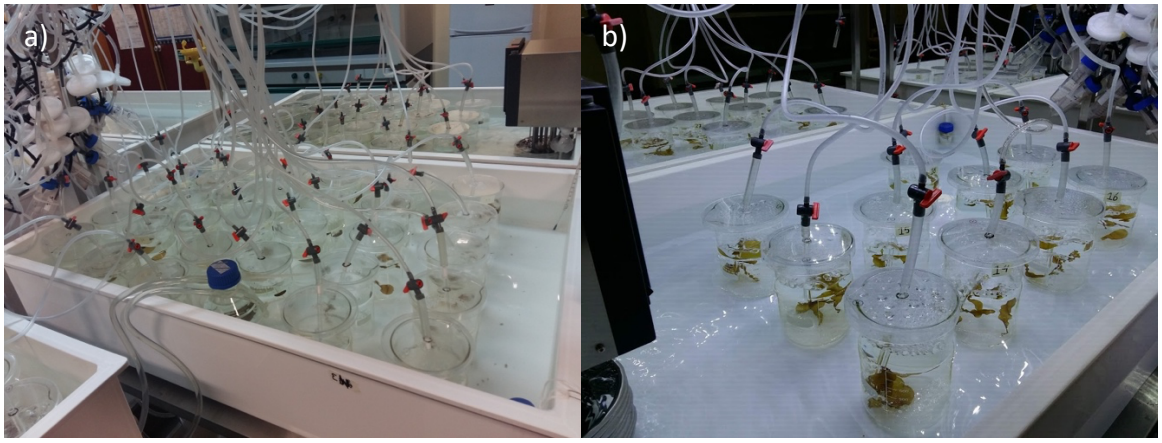

Figure 4.4: Ecophysiological experimental setup for a) field adult sporophytes meristem discs and b) F1 juvenile sporophytes

Measurements for photosynthetic performance and growth were taken at day 0 (control), day 8 (end of sMHW) and day 18 (end of RC). One random sporophyte meristem disc or F1 juvenile per replicate (n = 5) was dark acclimated for 5 min. Maximum photochemical efficiency of photosystem II (F_v/F_m) followed by rapid light curve (RLC; 8 irradiance steps between 4 and 420 µmol photons m^{-2} s^{-1}) were measured using a pulse amplitude modulated fluorometer (Diving PAM, Walz GmbH, Germany) and parameters were calculated using Wincontrol-3 software (Walz GmbH, Germany). The use of fluorometry as a proxy for thermal stress response is reliable (*i.e.* has a significant linear relationship with O_2 production) under sub-saturating irradiances (Duarte et al, 2013; Beer et al., 2014). Sampling always started after discs were exposed to at least 6 hours of light. F_v/F_m corresponds to the maximum quantum yield of photochemistry of photosystem II and was calculated as:

$$\frac{F_v}{F_m} = \frac{(F_m - F_0)}{F_m}$$

Where F_m is the maximum fluorescence level elicited by a saturating light pulse that closes all PSII reaction centres, and F_0 correspond to the minimum fluorescence level measured with a very low intensity modulated measuring light under which PSII reaction centres remain open.

From the RLCs, the maximum relative electron transport rate ($rETR_{max}$) as µmol electrons m^{-2} s^{-1} was calculated as:

$$rETR_{max} = ETR_{mPot}\left(\frac{\alpha}{a + \beta}\right)\left(\frac{\beta}{a + \beta}\right)^{\beta/\alpha}$$

Where ETR_{mPot} corresponds to the maximum potential light-saturated electron transport rate, a is the initial slope of the RLC corresponding to the quantum efficiency of photosynthesis and β corresponds to the photoinhibition parameter (Platt et al., 1980).

Meristem disc and F1 juvenile fresh weight (g) was measured on day 0 (control), day 8 (end of sMHW) and day 18 (end of RC) from a randomly selected disc per replicate (n = 5). Relative growth rate (RGR) was estimated as:

$$RGR\ (g\ day^{-1}) = \left(\frac{ln(sMHW\ or\ RC\ weight(g)) - \ln\ (control\ weight(g))}{Time\ (days)}\right)$$

Where sMHW corresponds to the end of the simulated marine heatwave (day 8), RC to the end of the recovery (day 18) and Time corresponds to the culture period (days).

4.3.5 Regional thermal regimes and MHW metrics

In order to characterize local oceanographic thermal regimes, we calculated the minimum, mean and maximum sea surface temperature (SST, °C) for each region, using Bio-Oracle (Assis et al., 2017; see Table S4.2 for layers used). We used the Global Ocean Physics Reanalysis gridded dataset (Global Monitoring and Forecasting Centre, 2018) generated by the E.U. Copernicus Marine Service (CMEMS) (https://www.copernicus.eu/en) to calculate MHW for

each site of interest. This dataset is the product of a 3D model (NEMOVAR) with a bias correction scheme, that combines satellite and in-situ measurements for a resolution of 0.083-degree covering the period from 01/01/1994 to 31/12/2019.

Following the definition of Hobday *et al.*, (2016), we described a MHW as a discrete prolonged anomalously warm water event of at least 5-day duration, during which daily temperatures exceeded the seasonally varying 90th percentile threshold of the historical baseline climatology. If two events took place less than 3 days apart, they were considered as a single event. The historical baseline climatology for a given day was calculated using an 11-day window centred on that date across all years of the climatology period, while an additional 31-day moving average was applied to smooth the climatology (Hobday et al., 2016). A seasonally varying threshold was preferred to an absolute fixed value, as it allowed the identification of MHW events throughout the year, rather than during the warmest seasons only. Climatologies were produced and MHWs were calculated for each site of interest. Each MHW event was characterised by a set of metrics (Hobday et al., 2016), mean and maximum duration (D_{mean} and D_{max}, days), mean, maximum and cumulative intensity (I_{avrmax}, I_{max} and I_{cum} °C days). MHW frequency was measured as the total number of events occurring during the modelled period (1993-2019).

4.3.6 Statistical analysis

Photosynthetic performance (F_v/F_m and $rETR_{max}$) and relative growth rates (RGR, g day^{-1}) were analysed using the PERMANOVA+ module within PRIMER 7. For the F1 Juvenile experiment, a 4-factor design with temperature (17°C, 21°C, 23°C and 25°C), nutrients (enriched and non-enriched), time (end of the sMHW [day 8] and end of the RC [day 18]) and region (North, Centre, South, Deep [Az] and Deep [Me]) as fixed factors, was used for each response variable. For the adult sporophyte disc experiment, only 16 individuals of the adult Deep [Az] were sampled, and only the enriched treatment was performed for this population. Thus, for the adult experiment we performed 2 separate analyses: 1) all 4 regions with only the enriched treatment, and 2) 3 regions (North, Centre and South) for both enriched and non-enriched treatments.

All Permanova analyses were performed using Euclidian distances, 9999 permutations and Monte Carlo *P*-values were used when unique permutations were < 100. Whenever a

significant main effect or interaction was found ($p < 0.05$), post-hoc pair-wise t-tests were performed to identify differences among treatments levels. PERMDISP analyses were used to test the homogeneity of multivariate dispersions among *a priori* groups.

4.4 Results

Photosynthetic responses (F_v/F_m and $rETR_{max}$) and growth rate (RGR) are presented for both adults (Fig. 4.5-7) and F1 juveniles (Fig. 4.8-10) at the end of the simulated heatwave (sMHW) (day 8) and end of the recovery (RC) (day 18). Values presented are proportional to the respective controls (non-enriched and enriched; day 5, dotted line) to facilitate comparisons between regions and time points.

4.4.1 Field adult experiment

As outlined above (3.2.4), due to the low number of individuals (16) in the Deep (Az) region, statistical analysis of the adult experiment was performed as 2 separate analyses: 1) 3 regions (North, Centre and South, see tables below figures) for both enriched and non-enriched treatments, and 2) all 4 regions with only enriched treatment.

Comparing both enriched and non-enriched treatments excluding the Deep region (North, Centre and South) (Fig. 4.5a-d; 5e, Table S4), post-hoc analysis on the significant interaction between Nutrients x Time x Region highlighted a positive effect of nutrients, with all 3 regions during RC in the enriched treatment presenting average 51-fold higher F_v/F_m values compared to the non-enriched treatment. In the non-enriched treatment and for each region, F_v/F_m values were always higher at the end of the sMHW compared to the RC. When we consider the Temperature x Nutrients interaction (Fig. 4.5e), all the temperatures in the enriched treatment had higher F_v/F_m (6-fold average) compared to the non-enriched treatment.

The maximum quantum yield of adults (Fv/Fm) under enriched conditions showed that the Deep (Az) region was significantly reduced at the higher temperatures (23°C, 25°C) during the sMHW (day 8) compared to the average of the other regions (10.4-fold at 25°C) and temperatures (2.4-fold) (Fig. 4.5c, small and capital letters, respectively). However, the deep

individuals showed the capacity to recover from thermal stress at the end of the RC (day 18) (Fig. 4.5c, d, numbers, Table S4.3).

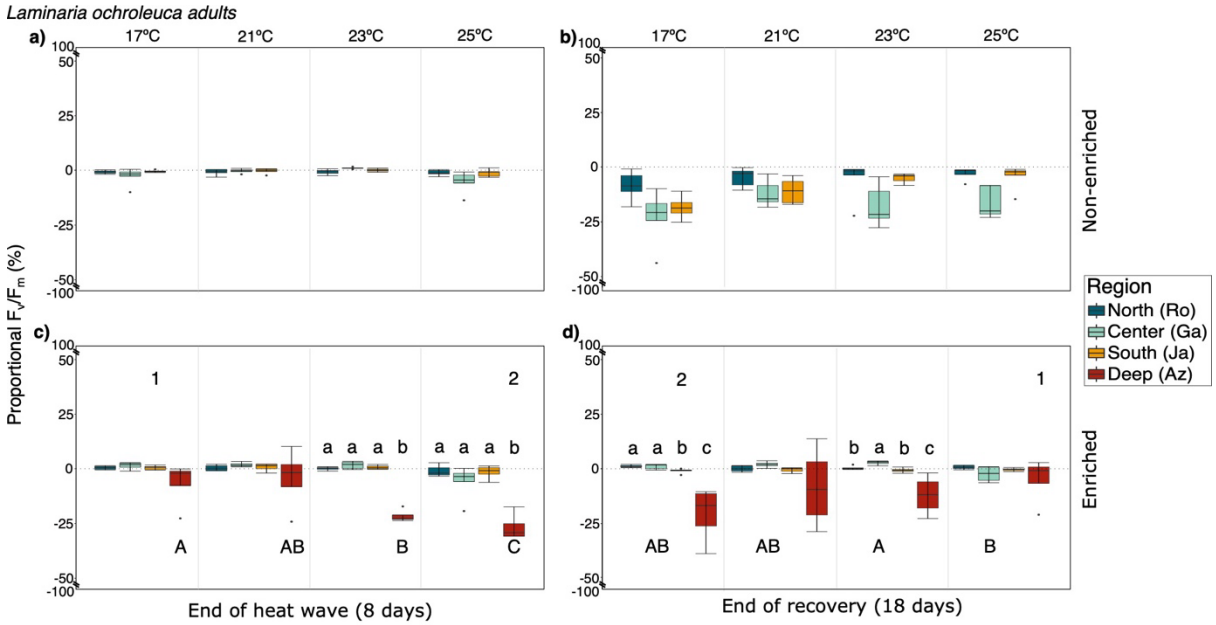

e) Only North, Centre and South

Nutrients	x	Time	x	Region
Enriched > Non-enriched		sHW		North
Enriched > Non-enriched		Recovery		North, Centre, South
Non-enriched		**sHW > Recovery**		North, Centre, South
Enriched		Recovery		**South < North, Center**
Non-enriched		Recovery		**North > Centre**
Non-enriched		Recovery		**Centre < South**

Temperature	x	Region
17°C < 21°C > 25°C		Centre
23°C > 25°C		Centre
17°C < 21°C, 23°C, 25°C		South
17°C		**North > Centre, South**
25°C		**Centre < North, South**

Temperature	x	Time
25°C < 17°C, 21°C, 23°C		sHW
17°C < 21°C, 23°C, 25°C		Recovery
17°C, 21°C, 23°C		**sHW > Recovery**

Temperature	x	Nutrients
25°C < 17°C, 21°C, 23°C		Enriched
17°C < 21°C, 23°C, 25°C		Non-enriched
17°C, 21°C, 23°C, 25°C		**Enriched > Non-enriched**

Figure 4.5: Field adults maximum quantum yield of photosystem II (F_v/F_m) at the end of the simulated heatwave (sMHW) (day 8) (a, c) and recovery (RC) (day 18) (b, d) proportional to day 0 represented by the dotted line at 0 for the North (Roscoff [Ro]), Centre (Galicia [Ga]), South (El Jadida [Ja]) and Deep (Messina [Me]) regions (see table S4.1) at 17°C (control) 21°C , 23°C and 25°C. Top panels (a, b) correspond to non-nutrient enriched (Non-enriched) and bottom panels (c, d) correspond to nutrient enriched (Enriched) treatments. Boxplot with median, 25th and 75th percentiles corresponding to the upper and lower boxes hinges respectively, whiskers corresponding to values no further than the inter-quartile range × 1.5 and outliers as black dots (n=4 or 5). Statistical comparisons presented correspond to 4 regions and for the enriched treatment (Enriched) only as the low number of individuals from the Azores region precluded the use of non-enriched treatment for this region: Small letters (above bars) correspond to significant differences between regions within the same temperature, time point and only for enriched treatment using permutation *P*-value ($p < 0.05$). Capital letters (bellow bars) correspond to significant differences between temperatures within the same region, time point and nutrient-enriched treatment using permutation *P*-value ($p < 0.05$). Numbers correspond to significant differences between time points treatments (end of the sMHW [day 8] and end of the RC

[day 18]) within the same temperature, region and nutrient-enriched treatment using permutation *P*-value ($p < 0.05$) (see table S4.3). e) Summary of post-hoc analysis for North, Centre and South regions (excluding Deep) in both nutrient enriched and non-enriched treatments (see table S4 for more statistical information).

In the enriched treatment at the end of the sMHW (day 8), F_v/F_m of Deep (Az) individuals was 28.4-fold and 10.4-fold at 23°C and 25°C, respectively, compared to the average F_v/F_m from the other regions (Fig. 4.5, small letters, Table S4.3). At the end of RC (day 18), at 23°C, Deep region F_v/F_m was still 15-fold lower compared to the other regions (Fig. 4.5d, small letters) but at 25°C, Deep region F_v/F_m not only did not differ from the other regions but was 5.8-fold higher when compared to the end of the sMHW (day 8) (Fig. 4.5c,d, numbers). Other significant differences among regions for the enriched treatment were only found at 17°C at day 18 where the Deep population 67.3-fold lower F_v/F_m values compared to the average of the other regions (Fig. 4.5, small letters).

For the North, Centre, and South regions (No Deep) and both nutrient treatments (Fig. 4.6a-d; Fig 6e, Table S4.6), $rETR_{max}$ showed a significant Time x Nutrients interaction. The Centre region always performed more poorly than the average $rETR_{max}$ of the other regions, both following sMHW (3.4-fold) and RC (4.9-fold) periods. A positive nutrient addition effect was observed with a 5.0-fold increase in the enriched treatment compared to the non-enriched for all 3 regions (Fig. 4.6e, Nutrients x Region). The Centre region again had lower $rETR_{max}$ values compared to the other regions in both nutrient enriched (4.3-fold) and non-enriched (5.6-fold) treatments. Post-hoc analysis of the Nutrients x Time interaction indicates the effect of the lack of nutrients over time, with individuals in the non-enriched treatment having 20.4-fold higher $rETR_{max}$ during the sMHW compared to the RC (Fig. 4.6e), a pattern already observed in the other photosynthetic parameter F_v/F_m (Fig. 4.6e, Nutrients x Time x Region). No significant interactions were found with factor Temperature.

$rETR_{max}$ showed a similar pattern as F_v/F_m when considering all regions (enriched treatment only), with the Deep region individuals having 3.6-fold and 11.4-fold lower $rETR_{max}$ values at 23°C and 25°C, respectively, following the sMHW compared to the average of the other regions (Fig. 4.6c, small letters, Table S4.5) but were able to fully recover by the end of the RC (Fig. 4.6c,d, numbers).

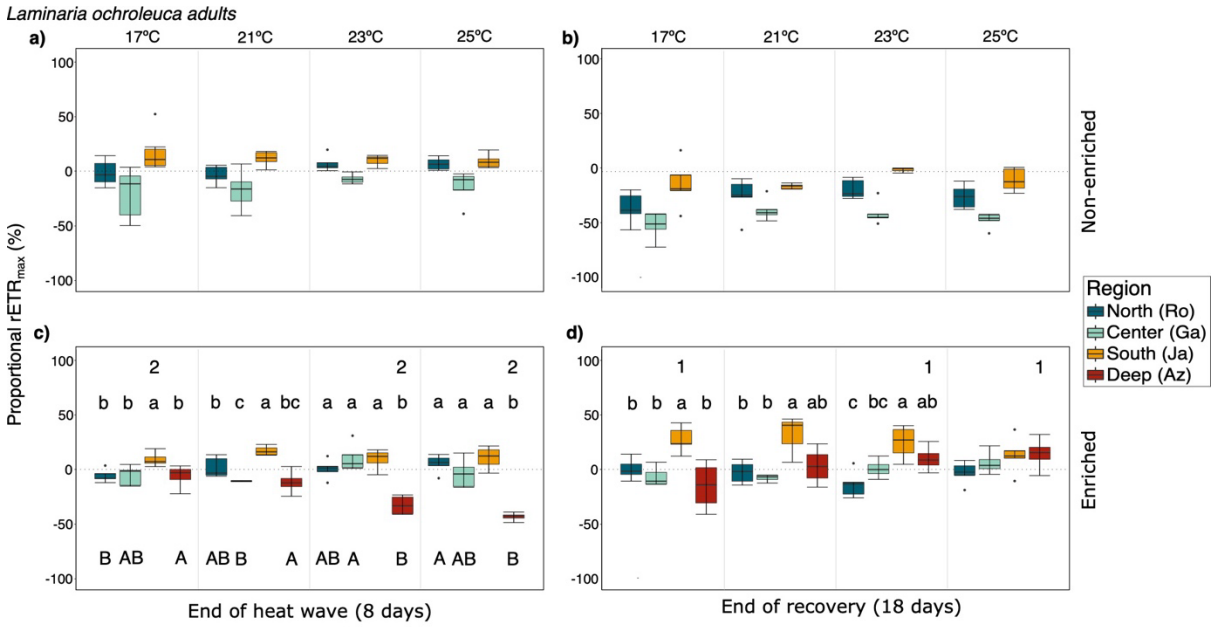

e) **Only North, Centre and South**

Time	x	**Region**
sHW > Recovery		North
sHW > Recovery		Centre
sHW		**North > Centre**
sHW		**North < South > Centre**
Recovery		**North > Centre**
Recovery		**North < South > Centre**
Nutrients	x	**Region**
Enriched > Non-enriched		North, Centre, South
Enriched		**North < South > Centre**
Non-enriched		**North > Centre**
Non-enriched		**North < South > Centre**
Nutrients	x	**Time**
Enriched > Non-enriched		Recovery
Non-enriched		**sHW > Recovery**

Figure 4.6: Field adults relative maximum electron transport rate (rETR$_{max}$) at the end of the simulated heatwave (sMHW) (day 8) (a, c) and recovery (RC) (day 18) (b, d) proportional to day 0 represented by the dotted line at 0 for the North (Roscoff [Ro]), Centre (Galicia [Ga]), South (El Jadida [Ja]) and Deep (Messina [Me]) regions (see table W1) at 17°C (control) 21°C , 23°C and 25°C. Top panels (a, b) correspond to non-nutrient enriched (Non-enriched) and bottom panels (c, d) correspond to nutrient enriched (Enriched) treatments. Boxplot with median, 25th and 75th percentiles corresponding to the upper and lower boxes hinges respectively, whiskers corresponding to values no further than the inter-quartile range × 1.5 and outliers as black dots (n=4 or 5). Statistical comparisons presented correspond to 4 regions and for the enriched treatment (Enriched) only as the low number of individuals from the Azores region precluded the use of non-enriched treatment for this region: Small letters (above bars) correspond to significant differences between regions within the same temperature, time point and only for enriched treatment using permutation *P*-value ($p < 0.05$). Capital letters (bellow bars) correspond to significant differences between temperatures within the same region, time point and nutrient-enriched treatment using permutation *P*-value ($p < 0.05$). Numbers correspond to significant differences between time points treatments (end of the sMHW [day 8] and end of the RC [day 18]) within the same temperature, region and nutrient-enriched treatment using permutation *P*-value ($p < 0.05$) (see table S4.5). e) Summary of post-hoc analysis for North, Centre and South regions (no Deep) in both nutrient enriched and non-enriched treatments (see table S4.6 for more statistical information).

Among thermal treatments following the sMHW (Fig. 4.6c, capital letters, Table S4.5), Deep region had average lower rETR$_{max}$ at the highest's temperatures of 23°C and 25°C compared to the control 17°C and 21°C with 3.6-fold and 5.5-fold, respectively. In contrast, South region

individuals had 7.9-fold and 16.2 higher $rETR_{max}$ at the end of the RC at all temperatures compared to the North and Centre regions, respectively (Fig. 4.6d, small letters), except at the highest temperature of 25°C where no differences were detected.

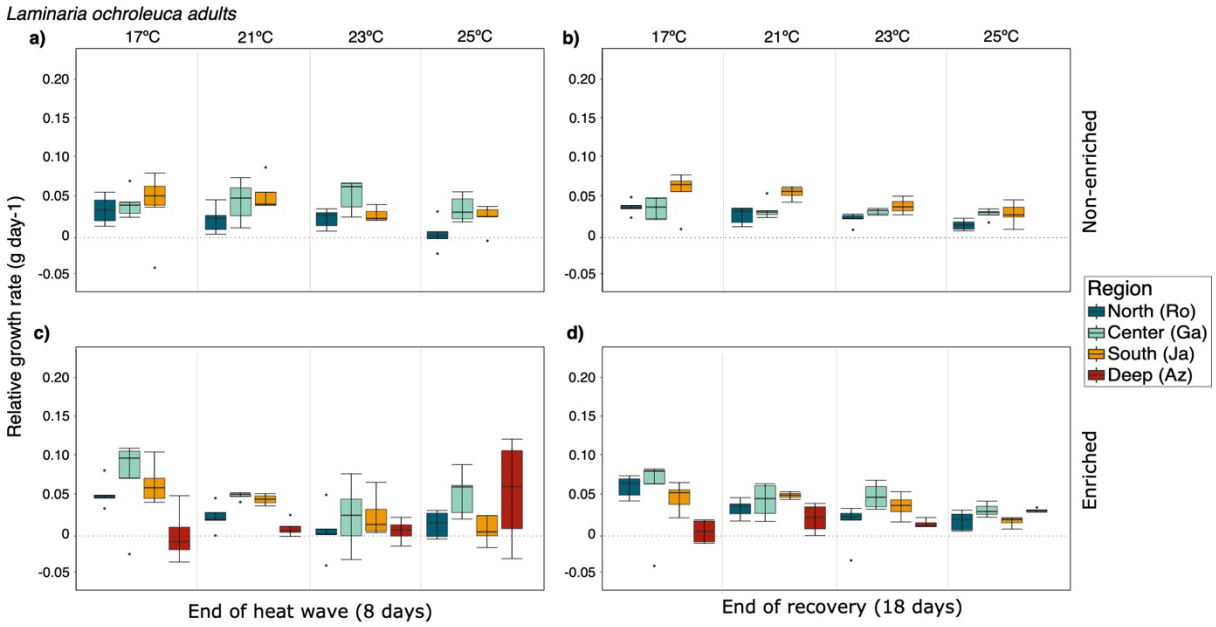

e) **Only North, Centre and South**

Temperature	x	Nutrients
17°C > 21°C, 23°C, 25°C	Enriched	
21°C > 23°C, 25°C	Enriched	
25°C < 17°C, 21°C, 23°C	Non-enriched	
17°C	**Enriched > Non-enriched**	
Region		
North < Centre, South		

Figure 4.7: Field adults relative growth rate (g day^{-1}) at the end of the simulated heatwave (sMHW) (day 8) (a, c) and recovery (RC) (day 18) (b, d) proportional to day 0 represented by the dotted line at 0 for the North (Roscoff [Ro]), Centre (Galicia [Ga]), South (El Jadida [Ja]) and Deep (Messina [Me]) regions (see table W1) at 17°C (control) 21°C , 23°C and 25°C. Top panels (a, b) correspond to non-nutrient enriched (Non-enriched) and bottom panels (c, d) correspond to nutrient enriched (Enriched) treatments. Boxplot with median, 25th and 75th percentiles corresponding to the upper and lower boxes hinges respectively, whiskers corresponding to values no further than the inter-quartile range × 1.5 and outliers as black dots (n=4 or 5). e) Summary of post-hoc analysis for North, Centre and South regions (no Deep) in both nutrient enriched and non-enriched treatments (see table S4.8 for more statistical information).

There were no significant interactions between any factors for fresh weight relative growth rate (RGR) (Fig. 4.7) when the four regions and nutrient enrichment treatment only were tested (Table S4.7).

For the North, Centre and South regions only (no Deep) and both nutrient treatments (Fig. 4.7a-d; Fig. 4.7e, Table S4.8) the 25°C and 23°C were 2-fold lower compared to the 17°C and 21°C in the enriched treatment and 25°C was 1.9 lower compared to the average of all the

other temperatures in the non-enrichment treatment. Nutrient enrichment was only positive for 17°C (1.3-fold) (Fig. 4.7e). No significant interactions were found with factor Time (Table S4.8).

4.4.2 F1 juvenile experiment

There were very clear positive effects of nutrient enrichment on F1 juvenile F_v/F_m compared to the non-enriched treatment for all 4 regions at both the sMHW (day 8) (North = 8.2-fold, Centre = 20.8-fold, South = 37.2-fold and Deep [Me] = 6.7-fold) and RC (day 18) (North = 3.8-fold, Centre = 20.4-fold, South = 15.4-fold and Deep [Me] = 7-fold) (Fig. 4.8a-e, Table S4.9).

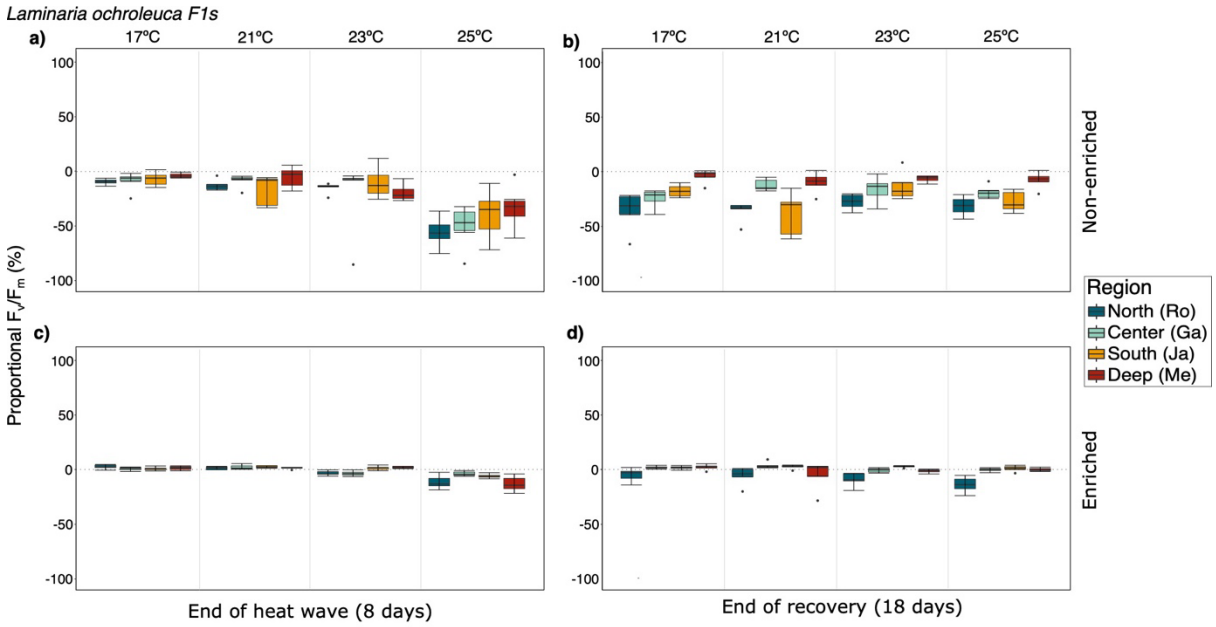

e) North, Centre, South and Deep

Nutrients	x Time	x Region
Enriched > Non-enriched	sHW	North, Centre, South, Deep
Enriched > Non-enriched	Recovery	North, Centre, South, Deep
Enriched	**sHW > Recovery**	North
Enriched	**sHW < Recovery**	Centre, South
Non-enriched	**sHW > Recovery**	North
Non-enriched	**sHW < Recovery**	Deep
Enriched	sHW	**North < South > Deep**
Enriched	Recovery	**North < Center, South, Deep**
Non-enriched	sHW	**North < Deep**
Non-enriched	Recovery	**North < Centre, South, Deep**
Non-enriched	Recovery	**Deep > Centre, South**
Temperature	**x Nutrients**	**x Time**
17°C > 23°C, 25°C	Enriched	sHW
21°C > 23°C, 25°C	Enriched	sHW
23°C > 25°C	Enriched	sHW
17°C > 23°C, 25°C	Enriched	Recovery
17°C > 23°C, 25°C	Non-enriched	sHW
25°C < 21°C, 23°C	Non-enriched	sHW
21°C > 23°C	Non-enriched	Recovery
17°C, 21°C, 23°C, 25°C	**Enriched > Non-enriched**	sHW
17°C, 21°C, 23°C, 25°C	**Enriched > Non-enriched**	Recovery
17°C, 21°C	Non-enriched	**sHW > Recovery**
25°C	Enriched	**sHW < Recovery**
25°C	Non-enriched	**sHW < Recovery**
Temperature	**x Region**	
25°C < 17°C, 21°C, 23°C	North	
25°C < 17°C < 21°C	Centre	
21°C > 25°C	Centre	
17°C > 21°C, 25°C	South	
23°C > 21°C, 25°C	South	
17°C > 21°C, 23°C 25°C	Deep	
25°C < 21°C, 23°C	Deep	
17°C	**North < South, Deep**	
17°C	**Deep > Centre, South**	
21°C	**North < South, Deep**	
21°C	**South < Centre, Deep**	
23°C	**North < South, Deep**	
25°C	**North < Centre, South, Deep**	

Figure 4.8: F1 juvenile maximum quantum yield of photosystem II (F_v/F_m) at the end of the simulated heatwave (sMHW) (day 8) (a, c) and recovery (RC) (day 18) (b, d) proportional to day 0 represented by the dotted line at 0 for the North (Roscoff [Ro]), Centre (Galicia [Ga]), South (El Jadida [Ja]) and Deep (Messina [Me]) regions (see table S4.1) at 17°C (control) 21°C , 23°C and 25°C. Top panels (a, b) correspond to non-nutrient enriched (Non-enriched) and bottom panels (c, d) correspond to nutrient enriched (Enriched) treatments. Boxplot with median, 25th and 75th percentiles corresponding to the upper and lower boxes hinges respectively, whiskers corresponding to values no further than the inter-quartile range × 1.5 and outliers as black dots (n=3 or 5). e) Summary of post-hoc analysis for all regions in both nutrient enriched and non-enriched treatments (see table S4.9 for more statistical information).

The significant Nutrients x Time x Region interaction (Fig. 4.e) indicated that the North was the only region to show lower F_v/F_m values following RC compared to the sMHW in both enriched (2.9-fold) and non-enriched (3.8-fold) treatments. North region individuals also had lower F_v/F_m when compared to the average of the other regions following RC in both enriched (14.1-fold) and non-enriched (1.9-fold) treatments. The Deep samples had (3.5-fold) higher mean F_v/F_m following RC compared to the average of the other regions in the non-enriched treatment (Fig. 4.8e). The Temperature x Nutrients x Time interaction highlights the stress imposed by the highest temperature of 25°C following sMHW (day 8), as all F_v/F_m values are lower compared to all other temperatures in both nutrient-enriched (25°C < 17°C = 21.2-fold, 25°C < 21°C = 16.7-fold, 25°C < 23°C = 31.2-fold) and non-enriched (25°C < 17°C = 6.1-fold, 25°C < 21°C = 4.4-fold, 25°C < 23°C = 2.7-fold) (Fig. 4.8e). Nonetheless, at 25°C following RC (day 18) mean F_v/F_m values were higher compared to the sMHW in both nutrient enriched (2.3-fold) and non-enriched (2-fold) treatments, indicating a general capacity of the juveniles to recover from the greatest heat stress. The 17°C control temperature samples had higher F_v/F_m values compared to those at 23°C and 25°C in both the sMHW enriched (17°C > 23°C = 3.5-fold, 17°C > 25°C = 8.6-fold) and non-enriched treatments (17°C > 23°C = 2.2-fold, 17°C > 25°C = 6.1-fold) and RC enriched (17°C > 23°C = 2.3-fold, 17°C > 25°C = 3.7-fold). However, no differences were found in the RC non-enriched treatment (Fig. 4.8e). Post hoc analysis of the Temperature x Region interaction confirmed that the North region samples had higher sensitivity to the warmer heat waves, with lower F_v/F_m values at 23°C compared to South (8.6-fold) and Deep (5.1-fold) regions and to all regions at 25°C (Centre = 1.5-fold, South = 1.5-fold, Deep = 1.6-fold).

The results comparing $rETR_{max}$ values (Fig. 4.9a-e) showed the sensitivity of the Deep region to the 25°C treatment with lower $rETR_{max}$ values compared to the other temperatures in both nutrient enriched (25°C < 17°C = 3.1-fold, 25°C < 21°C = 3.9-fold, 25°C < 23°C = 20-fold) and non-enriched (25°C < 17°C = 2.2-fold, 25°C < 21°C = 3.9-fold) treatments, except when compared to 23°C in the non-enriched treatment (Fig. 4.9e, Temperature x Nutrients x Region interaction, Table S4.10).

Laminaria ochroleuca F1s

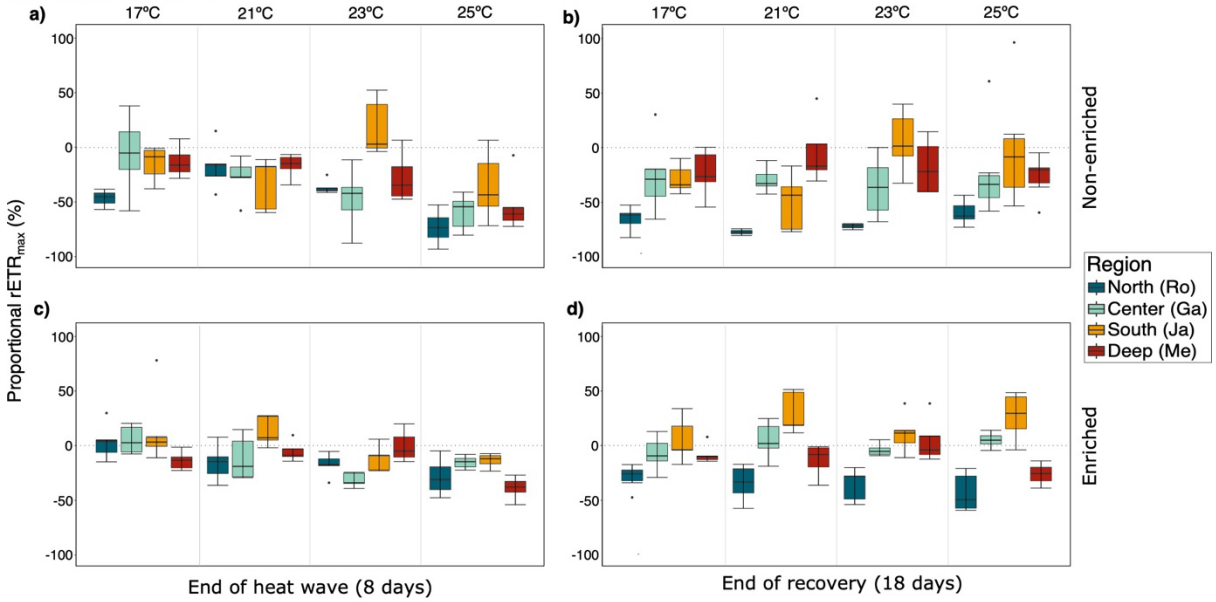

e) North, Centre, South and Deep

Temperature	x	Nutrients	x	Region
17°C > 23°C, 25°C		Enriched		North
23°C < 21°C, 25°C		Enriched		Centre
21°C > 23°C, 25°C		Enriched		South
25°C < 17°C, 21°C, 23°C		Enriched		Deep
25°C < 21°C, 23°C		Non-enriched		North
21°C < 17°C < 23°C		Non-enriched		South
21°C < 23°C		Non-enriched		South
25°C < 17°C, 21°C		Non-enriched		Deep
17°C		**Enriched > Non-enriched**		North, South
21°C		**Enriched > Non-enriched**		North, Centre, South
23°C		**Enriched > Non-enriched**		North, Centre, Deep
25°C		**Enriched > Non-enriched**		North, Centre
17°C		Enriched		**South > North, Deep**
17°C		Non-enriched		**North < Centre, South, Deep**
21°C		Enriched		**North < Centre, South, Deep**
21°C		Enriched		**South > Centre, Deep**
21°C		Non-enriched		**Deep > North, South**
23°C		Enriched		**North < South, Deep**
23°C		Enriched		**Centre < South, Deep**
23°C		Non-enriched		**North < South, Deep**
23°C		Non-enriched		**South > Centre, Deep**
25°C		Enriched		**North < Centre, South**
25°C		Enriched		**South > Centre > Deep**
25°C		Enriched		**South > Deep**
25°C		Non-enriched		**North < Centre, South, Deep**

Time	x	Region
sHW > Recovery		North
sHW		**North < South, Deep**
sHW		**South > Centre, Deep**
Recovery		**North < Centre, South, Deep**
Recovery		**South > Centre, Deep**

Temperature	x	Time
17°C > 23°C, 25°C		sHW
25°C < 21°C, 23°C		sHW
17°C		**sHW > Recovery**
25°C		**sHW < Recovery**

Figure 4.9: F1 juvenile maximum relative electron transport rate ($rETR_{max}$) at the end of the simulated heatwave (sMHW) (day 8) (a, c) and recovery (RC) (day 18) (b, d) proportional to day 0 represented by the dotted line at 0 for the North (Roscoff [Ro]), Centre (Galicia [Ga]), South (El Jadida [Ja]) and Deep (Messina [Me]) regions (see table S4.1) at 17°C (control) 21°C , 23°C and 25°C. Top panels (a, b) correspond to non-nutrient enriched (Non-enriched) and bottom panels (c, d) correspond to nutrient enriched (Enriched) treatments. Boxplot with median, 25th and 75th percentiles corresponding to the upper and lower boxes hinges respectively, whiskers corresponding to values no further than the inter-quartile range × 1.5 and outliers as black dots (n=3 or 5). e) Summary of post-hoc analysis for all regions in both nutrient enriched and non-enriched treatments (see table S4.10 for more statistical information).

Nutrient enrichment had a consistently positive effect on $rETR_{max}$ for the North region at all temperatures (17°C = 4.6-fold, 21°C = 1.4-fold, 23°C = 2-fold, 25°C = 1.8-fold) and the Centre region at 21°C (8.9-fold), 23°C (2.3-fold) and 25°C (8.3-fold) heat waves (Fig. 4.9e). For the South region, nutrient enrichment was positive for the control 17°C (2.3-fold) and 21°C (1.9-fold), while for the Deep region, a positive effect of nutrient addition was only observed at 23°C (11.7-fold). Comparisons among regions showed that the warmest South region had higher $rETR_{max}$ while the cooler North region had lower performance among regions (see Fig. 4.9e; Temperature x Time x Region interaction post-hoc tests among regions). Post-hoc analysis of the Temperature x Time interaction revealed that at 17°C individuals had 3.5-fold higher $rETR_{max}$ following sMHW compared to RC but for individuals at 25°C 2.2-fold higher values were found following RC, indicating 25°C was able to recover from sMHW stress.

Relative growth rates (RGR) were somewhat higher following sMHW compared to RC for all regions (Centre = 1.5-fold, South = 1.2-fold, Deep = 2.8-fold) except North where no difference between time points was found (Fig. 4.10a-e, Time x Region, Table S4.11).

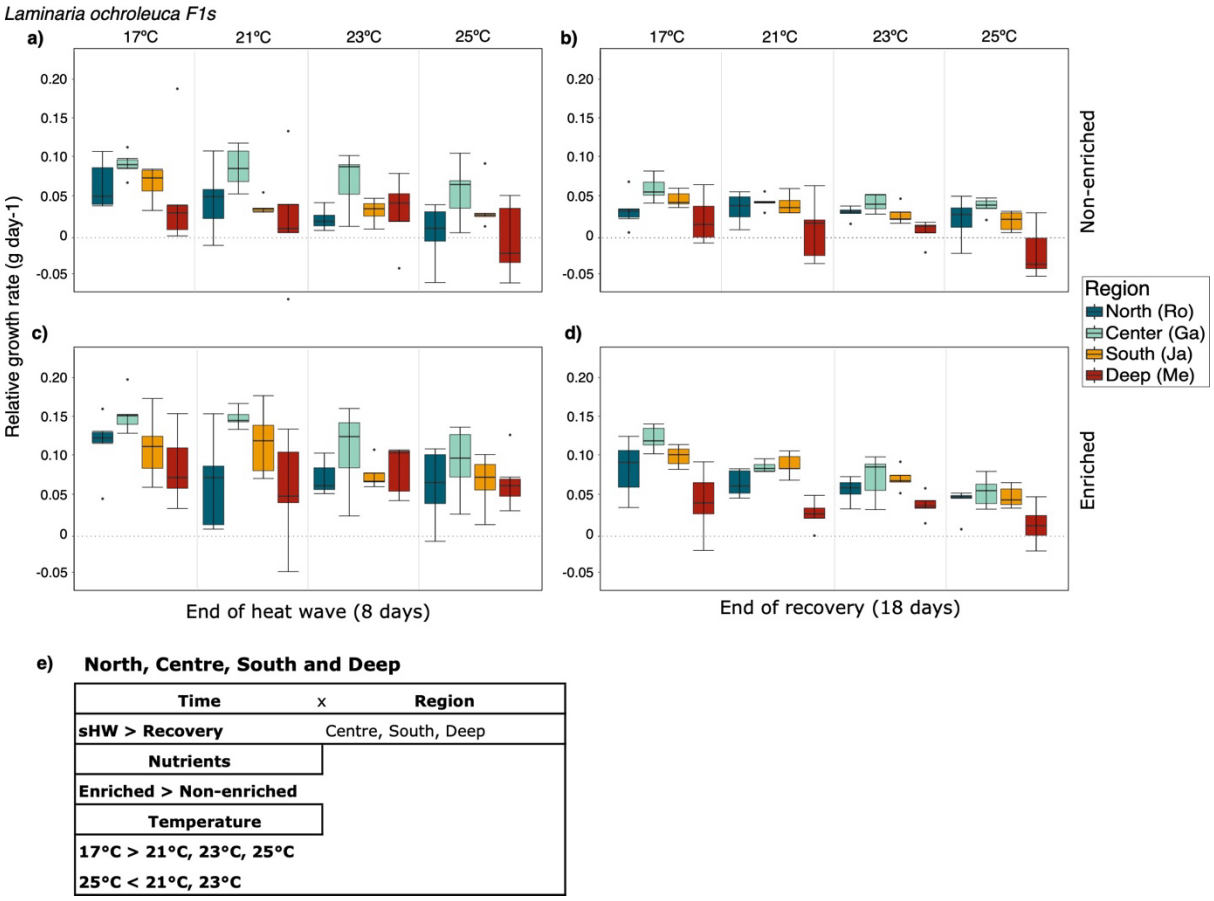

e) North, Centre, South and Deep

Time	x	Region
sHW > Recovery		Centre, South, Deep
Nutrients		
Enriched > Non-enriched		
Temperature		
17°C > 21°C, 23°C, 25°C		
25°C < 21°C, 23°C		

Figure 4.10: F1 juvenile relative growth rate (RGR) at the end of the simulated heatwave (sMHW) (day 8) (a, c) and recovery (RC) (day 18) (b, d) proportional to day 0 represented by the dotted line at 0 for the North (Roscoff [Ro]), Centre (Galicia [Ga]), South (El Jadida [Ja]) and Deep (Messina [Me]) regions (see table S4.1) at 17°C (control) 21°C , 23°C and 25°C. Top panels (a, b) correspond to non-nutrient enriched (Non-enriched) and bottom panels (c, d) correspond to nutrient enriched (Enriched) treatments. Boxplot with median, 25th and 75th percentiles corresponding to the upper and lower boxes hinges respectively, whiskers corresponding to values no further than the inter-quartile range × 1.5 and outliers as black dots (n=3 or 5). e) Summary of post-hoc analysis for all regions in both nutrient enriched and non-enriched treatments (see table S4.11 for more statistical information).

Following the pattern of the photosynthetic measurements, nutrient enrichment had a 2.1-fold positive effect on growth rate compared to the non-enriched treatment (Fig. 4.10e).

Individuals at 17°C control temperature had higher RGR compared to all sMHW temperatures (21°C = 1.2-fold, 23°C = 1.4-fold, 25°C = 2-fold) and the maximum temperature of 25°C had lower RGR values compared to all other temperatures (17°C = 2-fold, 21°C = 1.6-fold, 23°C = 1.4-fold) indicating that 25°C stress had a strong effect on growth, an integrated fitness estimator (Fig. 4.10e).

4.4.3 Regional thermal regimes and MHW metrics

Sea water temperature (SWT, minimum, mean and average maximum) and long-term MHW metrics highlighted regional differences across the Northeast Atlantic between shallow coastal rocky reefs (sea surface temperature (SST), North [Ro], Centre [Ga] and South [Ja]) and between deeper areas (seawater temperature at 50 m depth) in the Atlantic (Az) and Mediterranean (Me) (Fig. 4.11a). As expected, SWT shows an increasing latitudinal trend from North to South, with the highest SWT temperature (24.9°C) predicted at the southern distributional edge (South). In contrast, SWT reflect increasingly stable thermal conditions with depth, with less than 1°C difference between Min and Max SWT at Me. Despite this however, the maximum MHW intensity I_{max} of 5.036°C (temperature anomaly above the climatology; Fig. 4.11b) was predicted for the Deep Me population.

a)

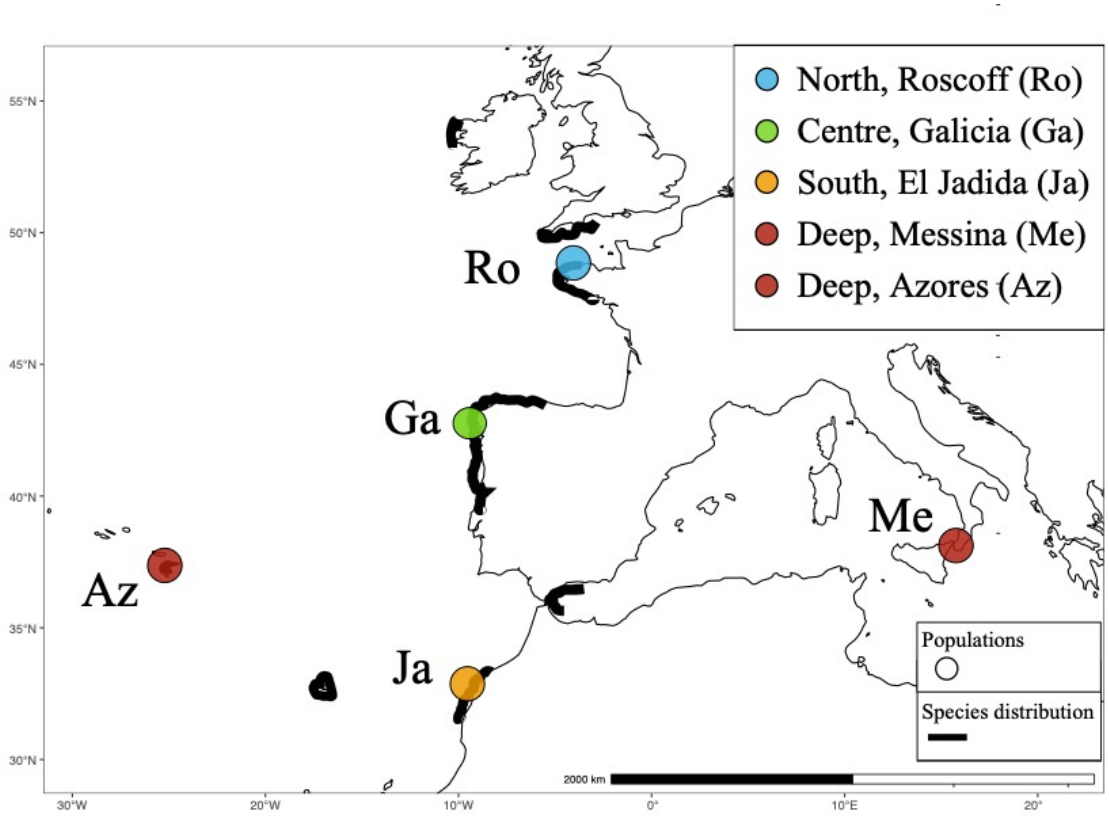

b)

		SWT (°C)			MHW events metrics (1994-2020)				
Region	Depth	Min	Mean	Max	D_{mean} (days)	D_{max} (days)	I_{avrmax} (°C)	I_{max} (°C)	I_{cum} (°C days)
North (Ro)	-4	8.7	13.0	16.7	14	39	1.668	2.847	1226
Center (Ga)	-4	12.3	15.3	19.4	12	55	2.245	4.123	1483
South (Ja)	-1	15.3	19.4	24.9	14	45	1.634	2.529	1171
Deep (Az)	-51	Na	Na	Na	27	117	1.410	2.483	1209
Deep (Me)	-50	13.8	14.2	14.7	16	73	2.125	5.036	1145

Figure 4.11: (A) Sampling locations of field individuals used in ecophysiology experiments: North (Ro) (France, Roscoff), Centre (Ga) (Spain, Galicia), South (Ja) (El Jadida, Morocco), Deep (Az) (Azores, Portugal) and Deep (Me) (Messina, Italy). (B) Minimum, mean and maximum sea water temperature (SWT, °C) for each location calculated using Bio-Oracle (Assis et al., 2017; see Table S4.2). Long-term (1994-2020) marine heatwaves (MHWs) metrics for each location: mean duration (D_{mean}, days), maximum duration (D_{max}, days), average maximum intensity (I_{avrmax}, °C), maximum intensity (I_{avrmax}, °C) and cumulative intensity (I_{cum}, °C). (C) MHW time series from the South region, red lines correspond to MHW periods.

The mean SWT in the South region (19.4°C) was equal to the maximum SWT registered for the Centre region. However, metrics describing MHW intensity (average of the highest

temperature anomalies during MHWs [I_{avrmax}], the single highest temperature value during MHW [I_{max}] and the cumulative intensity [I_{cum}]), and which reflect extreme events relative to local climatological averages, were actually lower for the South region compared to the other shallow Regions (North and Centre; Fig. 4.11b). In fact, all the MHW metrics (except for D_{mean}) were higher in the Centre than the North or South regions (Fig. 4.11b). The two deep regions Az and Me had the higher maximum number of MHW duration (D_{max}) with 117 and 73 days compared to the other regions.

4.5 Discussion

In this study we analysed the ecophysiological and growth responses to sMHWs of the sporophyte phase of *L. ochroleuca*, in both field-sampled adult tissue and *in vitro* cultured F1 juvenile sporophytes. Populations representing the intraspecific variation in thermal regimes across different latitudes and depth distributions were compared, as supported by modelled thermal data from the sampled regions for SWT and MHWs metrics. Our results provide overall support for the negative effects of low nutrient conditions in combination with thermal stress in both ontogenetic development stages. The hypothesis that nutrient enrichment ameliorates thermal stress on sporophytes at the highest temperatures of the sMHWs was confirmed by significant interactions and post-hoc tests for all experimental parameters (F_v/F_m, $rETR_{max}$ and RGR), which were higher in the nutrient-enriched compared to non-enriched treatments. This was expected at least for juvenile sporophytes, as a previous study on *L. ochroleuca* found that nutrient enrichment improved growth (g FW/day) even at sub-optimal temperatures of 20°C, 22°C and 24°C (Franco et al., 2018). A positive effect of nutrient enrichment compensating thermal stress was previously observed in juveniles of other kelp forest-forming species such as *Undaria pinnatifida* (Gao et al., 2013; RGR and survival), *Saccharina japonica* (Gao et al., 2017; O_2 evolution, RGR and nitrogen and chlorophyll content) *Ecklonia cava* (Gao et al., 2016; O_2 evolution, RGR, survival and nitrogen and chlorphyll content). This is very relevant with the increasing number, duration and intensity of MHWs over the last decades (Oliver et al., 2018; Holbrook et al., 2019). As the highest temperature MHWs occur during the warm season and nutrient availability is usually low due to water column stratification (*i.e.* nutrient recycling of the surface water column layer via upwelling of cooler and nutrient-rich deep water is greatly reduced [Fram et al., 2008; Sousa

et al., 2020]) rendering the warmer months the period of highest threat to juvenile kelp sporophytes.

The second hypothesis was that individuals near the South distribution edge would exhibit greater resilience to high temperatures, either due to a plastic or acclimatory response to exposure, or to local adaptation (potentially facilitated by greater genetic diversity compared to the Centre and North regions - see Assis et al., 2018) was not fully confirmed. Although $rETR_{max}$ in both adults and juveniles did indicate that samples from the South outperform those from the North or Centre, the pattern was not consistent across the different treatments, nor was it observed in the response of other parameters (F_v/F_m and RGR). It was previously observed for intertidal *L. ochroleuca* samples that those from the Centre were more resilient than the North to a consecutive heat shock treatment (30°C; Pereira et al., 2015). Intraspecific variation is likely to be subtle, particularly given the Pleistocene cycles of glacial activity that have driven multiple cycles of range expansion-contraction in the Atlantic. While some earlier studies detected no differences between populations of *Laminaria* species in response to thermal stress (Bolton & Lüning, 1982; Kain, 1967), intraspecific variation in thermal response across a broader latitudinal gradient was observed recently in the related Atlantic species *L. digitata* (Liesner et al 2020). Finally, we observed consistently poor performance of North region F1 juveniles (F_v/F_m and $rETR_{max}$) compared to Centre and South regions across RC (day 18) treatments. This cannot be attributed to thermal stress *per se*, but by other factors, amongst which potentially include the impacts on functional performance of reduced genetic diversity (Assis et al. 2018), which would be interesting to explore in future studies.

The 3rd hypothesis that Deep populations are more susceptible to MHWs due to the thermally stable natural environment (Fig. 4.11), with a SWT oscillation of 0.9°C between a minimum of 13.8°C and a average maximum 14.7°C SWT in Deep [Me], was confirmed in the adult sporophyte photosynthetic parameters during the sMHW at 23°C and 25°C in comparison to the other regions and temperatures. Deep (Az) individuals were able to recover from sMHW, suggesting photoinhibition (*i.e.,* regulated) and not photodamage (tissue necrosis and/or damage to the photosynthetic apparatus). This might be an indication of local adaptation of the deep populations to the low PAR availability and thermal stability in their natural environment as light penetration at depth is rapidly attenuated even in clear waters (Kirk, 2011; Beer et al., 2014) and thermal oscillations are very low (0.9°C) thus selection of genotypes that are better suited to grow and reproduce under these conditions might be ongoing. Nonetheless, more

detailed timecourses are required to describe the kinetics of the response(s) and we should also consider the possibility of adult sporophytes long-term acclimation to their environmental conditions (acclimation and not local adaptation) as the *in vitro* cultured F1 sporophytes from a different deep region population (Me) were able to cope with the same temperatures without clear differences to shallower and thermally variable regions. We could also expect the RGR of deep individuals to be lower than their shallower counterparts as growth rates of photosynthetic organisms are lower in deep habitats due to reduced available PAR and relatively low temperatures (Kirk, 2011; Beer et al., 2014). However, this was not observed in either adult or *in vitro* F1 sporophytes. Thus, the impact of increasing number and intensity of MHWs at depth (Deep (Me) I_{max} = 5.036 °C days, i.e., double that of shallower regions [Centre I_{max} = 2.592]) (see also Schaeffer & Roughan, 2017; Fragkopoulou et al., 2023) on deep *L. ochroleuca* populations, in particular on adult sporophytes, might potentially be mitigated by the gametophyte seed bank (see chapter 2, Strasser et al., 2022) and next generation juvenile acclimation to the warmer conditions, especially if nutrient availability is maintained by deep ocean upwelling pulses during MHW events (i.e., the positive effect of nutrient enrichment in our experiments). Nonetheless, such conclusions require further experimental analysis with prolonged MHWs scenarios while integrating other stressors and a continuous monitorization of the known populations. MHW metrics comparisons between the two Deep regions, Az and Me provide information that although in depth and roughly at the same longitudinal, the two habitats differ with the Az seamount top having higher mean and max. duration (D_{mean} *and* D_{max}) of MHW events (27 and 117 days, respectively) while the Me Mediterranean system having higher mean and max MHW intensities in particular I_{max} with more than the double (5.038 °C days) than in Az (2.483 °C days). Thus, comparisons between adult sporophytes from Az and the juvenile F1s from Me need to take into consideration that the regime of MHWs differs between locations.

L. ochroleuca has the broadest known depth range within the genus, able to occupy intertidal pools and shallow coastal areas but also deep open ocean habitats below 60m up to 95m depth (Bartsch et al., 2008). These deep habitats are largely undescribed, and the demography and population genetics of known *L. ochroleuca* deep populations, as well as the environmental parameters have not been well described or monitored to date. In 2019, an expedition to Madeira Island discovered an unknown deep *L. ochroleuca* forest between 73m and 98m (Braga-Henriques et al., 2022), extending the known southern distributional edge of the species at these depths. But our lack of knowledge about these unique habitats and the real impacts of

MHWs on them might endanger the species genetic potential as the South edge and specially the deep *L. ochroleuca* populations harbour ancient and unique gene pools as well as high genetic diversity (Assis et al., 2018). Although range expansion at the Northern distributional edge is predicted by ecological niche models (Assis et al., 2017) and has been observed in the English Channel and Ireland (Smale et al., 2015; Schoenrock et al., 2019) due to warming SWT and anthropogenic introductions, the South edge *L. ochroleuca* populations are predicted to decline in the best RCP scenario (2.6) and almost disappear from these region in the 8.5 RCP scenario (Assis et al., 2017). In addition to the current increase in MHWs, associated biotic stressors that are amplified by the increase in SWT have already been reported to impact *L. ochroleuca* populations, such as increased herbivory (Barrientos et al, 2022; 2023; Franco et al., 2015) and competition with faster growing annual kelps (Pereira et al., 2017; Biskup et al., 2014)**.** Combined stressors might tip these already endangered populations towards collapse, with consequent implications for the biodiversity and ecosystem services provided by perennial kelp forests, such as nutrient turnover, habitat quality and fisheries stocks (Smale et al., 2013; Bertocci et al., 2015; Smith et al., 2023).

To further understand the impacts of MHWs in *L. ochroleuca* in further detail we suggest designing larger scale experiments that assess longer term sMHWs and added pressures from herbivory and competition. Mapping and detailed monitoring (e.g., density, reproduction, temperature, nutrients conditions) of populations across the species distribution with special attention to the South and deep populations. The creation of seed banks from the entire distribution range, especially from southern and deep populations is also crucial to preserve this unique and rich gene pool for future generations. In addition to the current increase in MHWs, associated biotic stressors that are amplified by the increase in SWT have already been reported to impact *L. ochroleuca* populations, such as increased herbivory (Barrientos et al, 2022; 2023; Franco et al., 2015) and competition with faster growing annual kelps (Pereira et al., 2017; Combined stressors might tip these already endangered populations towards collapse, with consequent implications for the biodiversity and ecosystem services provided by perennial kelp forests, such as nutrient turnover, habitat quality and fisheries stocks (Smale et al., 2013; Bertocci et al., 2015; Smith et al., 2023).

To further understand the impacts of MHWs in *L. ochroleuca* in further detail we suggest designing larger scale experiments that assess longer term sMHWs and had added pressures from herbivory and competition. Mapping and detailed monitorization (e.g., density,

reproduction, temperature, nutrients conditions) of populations across the species distribution with special attention to the South and deep populations. The creation of seed ban; Bertocci et al., 2015; Smith et al., 2023).

The two constrains found during this work we would like to highlight are associated with the technical difficulty and rare chances we get to sample the deep populations. As so, adult individuals collect in Messina (Me) were unable to survive the transport from Italy to Portugal for the ecophysiological experiment but were able to release spores. On the other hand, adults collect in Azores (Az) were not reproductive and due to the low number of individuals (16) sampled due to dive time constraints and to impact as less as possible this unique populations, we were forced to select only one nutrient treatment for this region. Nevertheless, we were able to provide for both adults and F1 juvenile sporophytes comparable regional sampling to assess and discuss our results.

Chapter 5

Overview, conclusions and perspectives

5.1 Overview

The aim of this thesis was to address an ongoing major knowledge gap in marine foundation species research: to assess population level intraspecific variation (*i.e.* phenotypic plasticity and/or local adaptation) in marine forest-forming species of kelp (but see Liesner et al., 2020a; 2020b). For this, we tested two kelp species belonging to sister phylogenic clades with different thermal affinities; *Laminaria hyperborea* (cold-temperate clade) and *L. ochroleuca* (warm-temperate clade). For each species, populations were sampled and (for *L. ochroleuca*) established as gametophyte cultures from across the latitudinal gradient of the respective northern, central, and southern regions of their distributions in the northeast Atlantic. We specifically selected these two models because in the overlapping distributional range of the two species (namely the English Channel), warm-temperate *L. ochroleuca* is expanding its northern distribution poleward while out-competing the once dominant *L. hyperborea* (cold-temperate) which is contracting its distribution poleward (Smale et al., 2015). Local thermal regimes and long-term MHW metrics were obtained and analysed to characterize the history of thermal exposure of each population and integrate temperature into the experimental design.

In *L. ochroleuca*, we were also able to experimentally investigate two deep (-50 m) populations together with the shallower coastal (-4 m) populations from the latitudinal gradient. We performed experimental sMHWs using field collected adults, cultured gametophytes originated from meiospores of these adults, and on *in vitro* cultured F1 generation juvenile sporophytes derived from male and female gametophyte crosses. As both gametophytes and F1s sporophytes originated and were grown under common garden conditions (*i.e.* spores from the adults were release in laboratory and gametophytes and later F1s were always grown exposed to the same temperature and light conditions within species) we were able to remove parental field exposure "memory" rendering the comparisons between populations suitable to assess intraspecific variation (notwithstanding the potential for transgenerational carry over effects). Unfortunately, we were unable to collect reproductive tissue from two (North and South) populations of *L. hyperborea* during the period of the PhD study, limiting the analysis of this species to population differentiation between field-collected adult tissue (ecophysiological response) and data analysis on density, size, and structure from natural beds in each region. However, we were able to fill a knowledge gap for *L. hyperborea*, as we perform the first (to our knowledge) genetic

structure analysis across the entire continental distribution range (but see Schoenrock et al., 2020 for the Irish coast). An analysis of genetic structure in *L. ochroleuca* was already described by Assis et al., 2018.

5.2 Conclusions

Genetic analysis highlights similar patterns of diversity in the two *Laminaria* species across the latitudinal gradient, with in both cases the warmer South edge populations displaying rich and unique genetic diversity compared to the corresponding Centre and North regions. As has been argued previously for several seaweed taxa, this is likely the result of the fact that current southern distributional edges of both species actually correspond to long-term regions of persistence across multiple Pleistocene glacial-interglacial cycles, which have therefore acted as refugia over the millennia, harboring ancient populations with unique and rich gene pools (Assis et al., 2018a; 2018b). However, when we assessed the ecophysiological responses of adult sporophytes to sMHWs, the similarity in their patterns of genetic diversity did not translate into similar responses to thermal stress between species. The cold-temperate clade *L. hyperborea* South edge population had 100% mortality at the highest sMHW (23 ºC) at the end of the RC while the Centre and North regions were able to recover. On the other hand, the warm-clade *L. ochroleuca* South edge populations photosynthetic performance did not differ from the Centre and North populations. Such disparate results might be a consequence of South *L. hyperborea* smaller (57% compared to the mean of the other regions) and thinner adult individuals, possibly with low energy and/or nutrient reserves, that were not able to sustain metabolic performance under thermal stress. The field conditions highlighted by the long-term MHW metrics results also indicate a degradation of suitable habitat for *L. hyperborea* at the southern distributional edge, which is in agreement with the continuous range contraction in the region (260 km since 1970 in the coast of Portugal (Ardré, 1970; Monteiro et al., 2022). Indeed, the total disappearance of *L. hyperborea* from the Iberian Peninsula is predicted by species distribution models in future for all RCP scenarios (Assis et al., 2016). Such compelling evidence indicates that unique and diverse southern populations of *L. hyperborea* are under continuous habitat degradation and have shifted from a perennial kelp forest system with large adults to a sparse and patchy distribution of younger, smaller and thinner individuals. Extirpation of these ancient populations, together with their unique and diverse gene pool will greatly reduce the future

genetic potential of the species. The impact on local economies include not only direct reductions in harvestable stocks for industry, but also in biodiversity and other ecosystem services provided by perennial kelp forests (Bertocci et al., 2015; Smale et al., 2013; Vásquez et al., 2014).

We show that nutrient enrichment had a positive effect on the ecophysiological parameters of photosynthesis (F_v/F_m, $rETR_{max}$) and growth in response to sMHWs of *L. ochroleuca* adult and F1 juvenile sporophytes, a pattern previously suggested in *L. ochroleuca* (Franco et al., 2018) and in other kelp species such as *Undaria pinnatifida* (Gao et al., 2013), and *Saccharina japonica* (Gao et al., 2017). Our objective in using non-enriched as well as nutrient enriched (controls) treatments was to mimic the nutrient depleted conditions that can occur during the warm season, when nutrient availability is usually low due to water column stratification (Fram et al., 2008; Sousa et al., 2020) and which can be exacerbated by MHW events (Schaeffer & Roughan, 2017; Holbrook et al., 2019; Garrabou et al., 2022). Thus, our results suggest that locations with strong coastal upwelling regimes such us the Moroccan coast around El Jadida (Lourenço et al., 2016b) or deep seamounts (Santelices, 2007; Assis et al., 2018) have the potential to continue acting as refugia for ancient *L. ochroleuca* populations even under increasingly warm conditions. This is suggested by our SST results for the South region showing that temperatures do not currently exceed the species tolerance. In *L. hyperborea*, although we found no evidence that nutrient enrichment affected ecophysiological responses to the sMHW, care should be taken interpreting these results as adults from the North and Centre regions were collected from the field during September and November, respectively, corresponding to the beginning of the winter dormancy period, in which sporophyte growth stops and uptake of nutrients is greatly reduced (Luning, 1979; Schaffelke & Luning, 1994). Unfortunately, we were unable to perform the experiment in F1 juvenile sporophytes due to the narrow winter reproductive window of the species and rough winter sea conditions. It therefore remains a future goal to assess nutrient enrichment effects under common garden conditions with *in vitro*-derived life stages in *L. hyperborea*.

L. ochroleuca results for both generations (gametophytes [N] and sporophytes [2N]), different ontogenetic stages (adult and juvenile sporophytes) and latitudinal and depth gradients allowed a novel and comprehensive view on the species detailed ecophysiology response to sMHWs (see also *L. digitata* work in Liesner et al., 2020a, b; 2022).

Gametophytes showed intraspecific variation in survival with the North population being the most thermally sensitive, with mortality onset at 23°C, whereas mortality in the remaining populations was only apparent at 27°C. Populations also varied in reproductive success with Spain and Morocco exhibiting very low reproductive success at the end of the recovery from 23°C and 25°C, while after recover from 27°C both populations surpassed France and Italy in reproductive development and sporophyte output. This may indicate potential selection for a stimulation of reproductive output when faced with extreme thermal stress (see Martins et al., 2020 for a similar response in *L.digitata*).

Deep populations of *L. ochroleuca* adult sporophytes highlighted their susceptibility to sMHWs, with lower values of both photosynthetic parameters (F_v/F_m, $rETR_{max}$) in comparison with coastal shallow populations. This may indicate some combination of either photodamage or photoinhibition during the sMHW at 25°C. Photoinhibition (*i.e.,* regulated) is possible as both parameters went back to control levels at the end of the RC, although more detailed timecourses are required to describe the kinetics of the response(s). This might be an indication of local adaptation of the deep populations to the low PAR availability and thermal stability in their natural environment as light penetration at depth is rapidly attenuated even in clear waters (Kirk, 2011; Beer et al., 2014) and thermal oscillations are very low (0.9°C) thus selection of genotypes that are better suited to grow and reproduce under these conditions might be ongoing.

Regional comparisons of F1 juvenile sporophytes highlight overall poor recovery capability of the Northern population in photosynthetic performance (specially $rETR_{max}$) in both nutrient treatments and at all sMHW temperatures (21, 23, 25°C), indicative of photodamage (tissue necrosis and/or damage to the photosynthetic apparatus) a population level differentiation that might be a result of cooler water natural conditions (max. SST = 16.7°C) at the North edge of *L. ochroleuca* distribution.

5.3 Perspectives

Future work should aim to evaluate *L. hyperborea* gametophytes and F1 juvenile sporophytes from the same regions and genetic groups in order to further understand potential intraspecific variability for the species. Since *L. hyperborea* has a dormant adult life period (growth stops and individuals shed the previous year blade [Kain, 1967]) a replication of the

adult experiment using only growing tissue (collected during the warmer season) would further contribute to understanding the dynamic responses of this species to MHWs.
An ongoing work that unfortunately we were not able to finish for this thesis delivery is to further assess interspecific variation using transcriptomic profiles of *L. ochroleuca* F1 juveniles, investigating gene expression variation under our sMHW scenarios.
A clear and alarming result was evidenced by the lack of resilience to sMHWs of *L. hyperborea* South and *L. ochroleuca* Deep ancient populations which are the repository of each species most unique and diverse gene pools. Conservation measurements should minimally include collection of reproductive tissue and gametophyte preservation in biobanks to ensure maintenance of these precious gene pools for future generations and future reforestation programs if populations are wiped out by single stochastic events that is not assumed to be repeated and monitorization of these populations with *in situ* environmental sensors to register oscillations in environmental conditions and integrate such data with field surveys of density, growth, reproduction and other population demographic parameters.

Appendix

Chapter 2 supplementary materials

Table S2.1: Minimum, mean and maximum sea surface temperature (SST) layers downloaded from Bio-Oracle.

Sea Surface temperature (SST)	Layer code
Minimum	BO22_tempmin_ss
Mean	BO22_tempmean_ss
Max	BO22_tempmax_ss

Table S2.2: Geographical origin of the populations of *Laminaria hyperborea* used in analysis or experiments:

Analysis or experiment	**Region - Country** Population (site (code))	**Sampling date**	**Coordinates Lat. and Long.**	**Depth (m)**	**N**
1) Field surveys	**North - Norway**				
1) Field surveys	1	Aug-Sep 1985	70.26919462 21.42356065	-5	
1) Field surveys	3	Aug-Sep 1985	70.72718987 22.93481231	-5	
1) Field surveys	5	Aug-Sep 1985	71.05884294 24.1437489	-5	
1) Field surveys	6	Aug-Sep 1985	70.97658327 24.55737523	-5	
1) Field surveys	7	Aug-Sep 1985	71.10061857 25.27728251	-5	
1) Field surveys	8	Aug-Sep 1985	71.03081329 27.5401996	-5	
1) Field surveys	9	Aug-Sep 1985	71.13163922 27.63869676	-5	
1) Field surveys	10	Aug-Sep 1985	71.07131434 28.27082525	-5	
1) Field surveys	12	Aug-Sep 1985	70.38320366 31.15238902	-5	
1) Field surveys	16	Aug-Sep 1985	70.61575473 26.92679574	-5	
1) Field surveys	18	Aug-Sep 1985	70.07481712 29.63046384	-5	
1) Field surveys	19	Aug-Sep 1985	70.02609744 29.33202823	-5	
1) Field surveys	**Center - France**				
1) Field surveys	Barrou an Trez (BRT)	18/07/2017	-4.06641667 48.72362	-19.5	
1) Field surveys	Men Grasias (MGR)	10-11/07/2017	3.96798333 48.74005	-15	
1) Field surveys	Ricard (RIC)	31/07/2017	-3.89613333 48.69613333	-12	
1) Field surveys	**South – NW Iberian Peninsula**				
1) Field surveys	Mirandas (MIR)	11/06/2019	-8.265104 43.419543	15	
1) Field surveys	Abarenta (ABA)	11/06/2019	-8.295357 43.434113	15.7	
1) Field surveys	Esposende (ESP)	15/06/2019	-8.792684 41.496477	11	
1) Field surveys	Apúlia (APU)	15/06/2019	-8.785738 41.473724	8.5	

2) Experimental ecophysiology	**North - Norway** Mjeldevika	18/09/2019	67.2390000 -014.6127500	-2	47
2) Experimental ecophysiology	**Centre - France** Roscoff	15/11/2018	48.7399083 -003.9695222	-5	40
2) Experimental ecophysiology	**South - Portugal** Esposende	18/05/2020	41.4737240 -008.7857380	-10	33
3) Genetic analysis	**North - Norway**				
3) Genetic analysis	Lofoten (LOF)		68.0244 13.3585		14
3) Genetic analysis	Skjerstadfjorden (SKJ)		67.2757 14.5703		24
3) Genetic analysis	Titran (TIT)		68.0518 13.5305		20
3) Genetic analysis	**Centre – English Channel**				
3) Genetic analysis	Hope Cove (HCO)		50.2430 -3.8702		24
3) Genetic analysis	Guérhéon (GUE)		49.4990 -1.1505		24
3) Genetic analysis	Roscoff (ROS)		48.7295 -3.9873		24
3) Genetic analysis	**South – NW Iberian Peninsula**				
3) Genetic analysis	La Coruñesa (COR)		43.3724 -8.4134		24
3) Genetic analysis	Vila Chã (VCH)		41.2933 -8.7384		22
3) Genetic analysis	Leça da Palmeira (LPA)		41.2021 -8.7172		24

Table S2.3: 9 Microsatellite codes used.

Microsatellite code						
LoIVVIV-15	LoIVVIV-17	LoIVVIV-23	LoIVVIV-24	LoIVVIV-28	Ld148	Ld158
Ld167	Ld704					

Table S2.4: F_v/F_m Main test (All regions, No Recovery (day 18), no 19°C and 21°C)

Factor	**df**	**SS**	**MS**	**Pseudo-F**	**P (perm)**	**Unique perms**
Temperature	1	4697.4	4697.4	148.72	0.0001*	9835
Nutrients	1	143.56	143.56	4.5453	0.0302*	9849
Region	2	2481.3	1240.6	39.279	0.0001*	9953
Temperature x Nutrients	1	270	270	8.5484	0.0017*	9832
Temperature x Region	2	3300.8	1650.4	52.253	0.0001*	9956

Nutrients x Region	2	140.18	70.09	2.2191	0.1148	9946
Temperature x Nutrients x Region	2	202.39	101.2	3.2039	0.0386*	9958
Res	1642.4	31.585				

Table S2.5: F_v/F_m Main test (North and Centre Region)

Factor	df	SS	MS	Pseudo-F	P (perm)	Unique perms
Temperature	3	2340.7	780.24	8.633	0.0001*	9952
Nutrients	1	181.17	181.17	2.0046	0.1641	9832
Time	1	64.086	64.086	0.7091	0.4236	9861
Region	1	58.48	58.48	0.6471	0.4342	9844
Temperature x Nutrients	3	711.22	237.07	2.6231	0.0397*	9952
Temperature x Time	3	61.421	20.474	0.2265	0.8926	9944
Temperature x Region	3	390.49	130.16	1.4402	0.2406	9955
Nutrients x Time	1	50.79	50.79	0.5620	0.4764	9845
Nutrients x Region	1	340.34	340.34	3.7657	0.0464*	9862
Time x Region	1	0.7468	0.746	0.0083	0.9318	9837
Temperature x Nutrients x Time	3	25.492	8.4973	0.0940	0.9666	9952
Temperature x Nutrients x Region	3	270.34	90.113	0.9970	0.4126	9972
Temperature x Time x Region	3	161.68	53.895	0.5963	0.6451	9956
Nutrients x Time x Region	1	248.27	248.27	2.747	0.1048	9862
Temperature x Nutrients x Time x Region	3	316.57	105.52	1.1676	0.3412	9955
Res	125	11297	90.379			

Table S2.6: $rETR_{max}$ Main test (All regions, No Recovery (day 18), no 19°C and 21°C)

Factor	df	SS	MS	Pseudo-F	P (perm)	Unique perms
Temperature	1	5697.9	5697.9	37.42	0.0001*	9839
Nutrients	1	7.86	7.86	0.0516	0.8239	9849
Region	2	11299	5649.4	37.101	0.0001*	9949
Temperature x Nutrients	1	0.7548	0.7548	0.005	0.946	9866
Temperature x Region	2	10345	5172.7	33.97	0.0001*	9957
Nutrients x Region	2	790.35	395.17	2.5952	0.0822	9956
Temperature x Nutrients x Region	2	13.963	6.9814	0.0458	0.9559	9950
Res	52	7918.1	152.27			

Table S2.7: $rETR_{max}$ Main test (North and Centre Region)

Factor	df	SS	MS	Pseudo-F	P (perm)	Unique perms
Temperature	3	29.493	9.8311	0.0515	0.9853	9940
Nutrients	1	4140	4140	21.697	0.0001*	9840
Time	1	2755.7	2755.7	14.442	0.0002*	9844
Region	1	1948	1948	10.209	0.0009*	9833
Temperature x Nutrients	3	809.27	269.76	1.4138	0.2451	9943
Temperature x Time	3	717.64	239.21	1.2537	0.2958	9948
Temperature x Region	3	392.43	130.81	0.68556	0.5573	9963
Nutrients x Time	1	421.9	421.9	2.2111	0.1368	9841
Nutrients x Region	1	326.07	326.07	1.7089	0.1988	9853
Time x Region	1	1.2437	1.2437	0.0065	0.9344	9827
Temperature x Nutrients x Time	3	451.04	150.35	0.78794	0.5107	9956
Temperature x Nutrients x Region	3	1019.7	339.88	1.7813	0.1596	9956
Temperature x Time x Region	3	760.54	253.51	1.3286	0.2627	9941
Nutrients x Time x Region	1	11.089	11.089	0.0581	0.8089	9812
Temperature x Nutrients x Time x Region	3	553.75	184.58	0.96739	0.4182	9953
Res	4	23660	190.81			

Table S2.8: RGR (g day^{-1}) Main test (All regions, No Recovery (day 18), no 19°C and 21°C)

Factor	df	SS	MS	Pseudo-F	P (perm)	Unique perms

Temperature	1	0.0005	0.0005	0.9542	0.3379	9858
Nutrients	1	0.0003	0.0003	0.5123	0.4819	9844
Region	2	0.0023	0.0011	2.1584	0.1212	9956
Temperature x Nutrients	1	0.0000	0.0000	0.0578	0.8094	9836
Temperature x Region	2	0.0102	0.0051	9.7344	0.0005*	9954
Nutrients x Region	2	0.0001	0.0001	0.1363	0.8716	9949
Temperature x Nutrients x Region	2	0.0028	0.0014	2.6698	0.0774	9941
Res	51	0.0268	0.0005			

Table S2.9: RGR (g day^{-1}) Main test (North and Centre Region)

Factor	**df**	**SS**	**MS**	**Pseudo-F**	**P (perm)**	**Unique perms**
Temperature	3	0.0033	0.0011	3.3189	0.0201*	9955
Nutrients	1	0.0000	0.0000	0.0033	0.9535	9832
Time	1	0.0002	0.0002	0.6846	0.417	9837
Region	1	0.0000	0.0000	0.0133	0.9121	9852
Temperature x Nutrients	3	0.0008	0.0003	0.7823	0.5112	9949
Temperature x Time	3	0.0006	0.0002	0.6225	0.6063	9958
Temperature x Region	3	0.0019	0.0006	1.8645	0.1417	9960
Nutrients x Time	1	0.0001	0.0001	0.3084	0.5753	9842
Nutrients x Region	1	0.0003	0.0003	0.8744	0.3505	9822
Time x Region	1	0.0001	0.0001	0.3247	0.5689	9832
Temperature x Nutrients x Time	3	0.0007	0.0002	0.7035	0.559	9938
Temperature x Nutrients x Region	3	0.0002	0.0001	0.2342	0.8697	9959
Temperature x Time x Region	3	0.0008	0.0003	0.7967	0.5011	9941
Nutrients x Time x Region	1	0.0000	0.0000	0.0072	0.3209	9949
Temperature x Nutrients x Time x Region	3	0.0000	0.0000	0.0022	0.5436	9943
Res	121	0.0406	0.0003	3.3189		

Chapter 3 supplementary materials

Figure S3.1: Average density (cm^2) of sexual (A) and asexually (B) formed sporophytes of different populations of *Laminaria ochroleuca* after recovery from different thermal treatments (17°C, 23°C, 25°C, and 27°C). Box plots with median, boxes for 25th and 75th percentiles and whiskers indicating min and max values (n = 4).

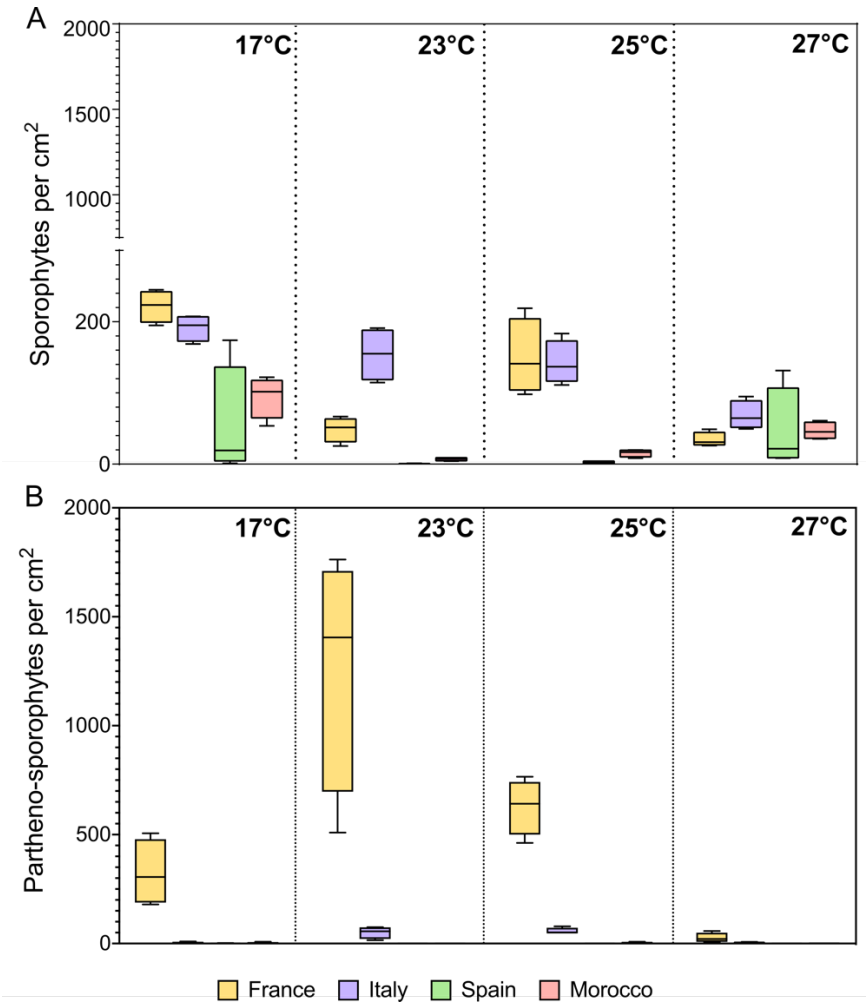

Chapter 4 supplementary materials

Table S4.1: Geographical origin of the adults of *Laminaria ochroleuca* used in analysis or experiments (both field adults and F1 juveniles):

Region - Country Population (site (code))	**Sampling date**	**Coordinates Lat. and Long.**	**Depth (m)**	**N**
North – France – Roscoff (Ro)	31/01/2019	48.6933056, -003.9412583	-4	43
Centre – Spain – Galicia (Ga)	03/05/2019	43.1047222, -009.1694444	-4	41
South – Morocco – El Jadida (Ja)	03/08/2019	33.2467944, -008.5441306	-1	44
Deep: Adults - Portugal – Açores (Az)	27/08/2018	37.0389233, -025.0641667	-51	16
F1 Juveniles – Italy – Messina (Me)	16/11/2019	38.2577710, 015.6277890	-50	12

Table S4.2: Minimum, mean and maximum sea surface temperature (SST) layers downloaded from Bio-Oracle.

Region	Sea water temperature (SWT)	Layer code
North (Ro), Centre (Ga) and South (Ja)	Minimum sea surface	BO22_tempmin_ss
	Mean sea surface	BO22_tempmean_ss
	Max sea surface	BO22_tempmax_ss
Deep (Az) and Deep (Me)	Minimum -50m	BO22_tempmin_bd
	Mean -50m	BO22_tempmean_bd
	Max -50m	BO22_tempmax_bd

Table S4.3: Adults F_v/F_m Main test (Enriched nutrients only, all regions)

Factor	**df**	**SS**	**MS**	**Pseudo-F**	**P (perm)**	**Unique perms**
Temperature	3	277.7	92.55	3.078	0.0266	9954
Time	1	28.9	28.93	0.96213	0.3285	9828
Region	3	3942.1	1314	43.702	0.0001	9953
Temperature x Time	3	554.0	184.66	6.1412	0.0005	9958
Temperature x Region	9	441.9	49.094	1.6327	0.1131	9937
Time x Region	3	51.7	17.232	0.5731	0.6346	9941
Temperature x Time x Region	9	900.5	100.06	3.3276	0.0012	9927
Res	113	3397.7				

Table S4.4: Adults F_v/F_m Main test (Only North, Centre and South)

Factor	**df**	**SS**	**MS**	**Pseudo-F**	**P (perm)**	**Unique perms**
Temperature	3	199.2	66.383	4.1954	0.0056	9956
Nutrients	1	2007.2	2007.2	126.85	0.0001	9811

Time	1	1235.4	1235.4	78.077	0.0001	9822
Region	2	391.3	195.67	12.366	0.0001	9946
Temperature x Nutrients	3	285.5	95.172	6.0149	0.0004	9949
Temperature x Time	3	279.1	93.048	5.8806	0.0008	9964
Temperature x Region	6	272.6	45.437	2.8716	0.01	9946
Nutrients x Time	1	1396.1	1396.1	88.236	0.0001	9824
Nutrients x Region	2	414.5	207.24	13.098	0.0001	9938
Time x Region	2	248.5	124.26	7.8535	0.0006	9944
Temperature x Nutrients x Time	3	123.0	41.012	2.5919	0.054	9962
Temperature x Nutrients x Region	6	59.4	9.9004	0.62571	0.7127	9934
Temperature x Time x Region	6	70.4	11.736	0.74174	0.6277	9948
Nutrients x Time x Region	2	313.0	156.48	9.8895	0.0001	9950
Temperature x Nutrients x Time x Region	6	67.3	11.21	0.70847	0.6472	9932
Res	185	2927.2	15.823			

Table S4.5: Adults $rETR_{max}$ Main test (Enriched nutrients only, all regions)

Factor	**df**	**SS**	**MS**	**Pseudo-F**	**P (perm)**	**Unique perms**
Temperature	3	171.4	57.115	0.4447	0.7197	9955
Time	1	3082.5	3082.5	24.001	0.0001	9826
Region	3	14541	4846.9	37.739	0.0001	9949
Temperature x Time	3	709.1	236.38	1.8405	0.1457	9948
Temperature x Region	9	2481.0	275.67	2.1464	0.03	9940
Time x Region	3	5152.2	1717.4	13.372	0.0001	9943
Temperature x Time x Region	9	6215.5	690.61	5.3772	0.0001	9942
Res	113	14513	128.43			

Table S4.6: Adults $rETR_{max}$ Main test (Only North, Centre and South)

Factor	**df**	**SS**	**MS**	**Pseudo-F**	**P (perm)**	**Unique perms**
Temperature	3	822.9	274.28	2.0576	0.1085	9963
Nutrients	1	17016	17016	127.65	0.0001	9941
Time	1	6772.4	6772.4	50.804	0.0001	9949
Region	2	23838	11919	89.413	0.0001	9960
Temperature x Nutrients	3	522.3	174.09	1.306	0.2804	9966
Temperature x Time	3	94.0	31.322	0.235	0.8581	9962

Temperature x Region	6	1360.7	226.78	1.7012	0.1291	9951
Nutrients x Time	1	11139	11139	83.561	0.0001	9953
Nutrients x Region	2	2710.9	1355.4	10.168	0.0002	9954
Time x Region	2	1583.4	791.72	5.9392	0.0036	9955
Temperature x Nutrients x Time	3	754.7	251.57	1.8872	0.1402	9952
Temperature x Nutrients x Region	6	1541.8	256.97	1.9277	0.0803	9950
Temperature x Time x Region	6	811.4	135.23	1.0145	0.4172	9942
Nutrients x Time x Region	2	66.8	33.388	0.25046	0.7714	9957
Temperature x Nutrients x Time x Region	6	665.1	110.85	0.83158	0.5446	9944
Res	186	24795				

Table S4.7: Adults RGR Fresh weight Main test (Enriched nutrients only, all regions)

Factor	**df**	**SS**	**MS**	**Pseudo-F**	**P (perm)**	**Unique perms**
Temperature	3	172.6	57.5	5.4998	0.0017	9947
Time	1	147.9	147.9	14.135	0.0003	9969
Region	3	544.0	181.3	17.33	0.0001	9964
Temperature x Time	3	42.2	14.1	1.3429	0.2849	9952
Temperature x Region	9	128.8	14.3	1.3678	0.2174	9944
Time x Region	3	75.5	25.2	2.4058	0.0829	9962
Temperature x Time x Region	9	114.2	12.7	1.2127	0.3032	9943
Res	113	1182.3	10.5			

Table S4.8: Adults RGR Fresh weight Main test (Only North, Centre and South)

Factor	**df**	**SS**	**MS**	**Pseudo-F**	**P (perm)**	**Unique perms**
Temperature	3	0.02577	0.00859	17.078	0.0001	9947
Nutrients	1	0.00143	0.00143	2.8519	0.0959	9842
Time	1	0.00057	0.00057	1.1399	0.2915	9854
Region	2	0.01353	0.00677	13.45	0.0001	9952
Temperature x Nutrients	3	0.00522	0.00174	3.4598	0.0187	9952
Temperature x Time	3	0.00054	0.00018	0.35882	0.7829	9948
Temperature x Region	6	0.00523	0.00087	1.7334	0.1143	9950
Nutrients x Time	1	0.00007	0.00007	0.14282	0.7041	9820
Nutrients x Region	2	0.00155	0.00077	1.5379	0.2133	9949
Time x Region	2	0.00243	0.00121	2.4133	0.0921	9946

Temperature x Nutrients x Time	3	0.00207	0.00069	1.3714	0.2552	9959
Temperature x Nutrients x Region	6	0.00112	0.00019	0.37108	0.8957	9944
Temperature x Time x Region	6	0.00073	0.00012	0.24145	0.9621	9933
Nutrients x Time x Region	2	0.00039	0.00019	0.38503	0.6885	9948
Temperature x Nutrients x Time x Region	6	0.00202	0.00034	0.67073	0.678	9952
Res	180	0.09054				

Table S4.9: F1s F_v/F_m Main test

Factor	df	SS	MS	Pseudo-F	P (perm)	Unique perms
Temperature	3	9217.4	3072.5	34.625	0.0001	9951
Nutrients	1	28988	28988	326.68	0.0001	9829
Time	1	16.748	16.748	0.18874	0.667	9834
Region	3	4641.7	1547.2	17.436	0.0001	9946
Temperature x Nutrients	3	2311.3	770.45	8.6824	0.0001	9957
Temperature x Time	3	7138.4	2379.5	26.815	0.0001	9954
Temperature x Region	9	1615.7	179.52	2.0231	0.0355	9948
Nutrients x Time	1	10.826	10.826	0.122	0.7333	9817
Nutrients x Region	3	2206.4	735.45	8.2881	0.0001	9950
Time x Region	3	1975	658.35	7.4191	0.0003	9952
Temperature x Nutrients x Time	3	3160	1053.3	11.87	0.0001	9955
Temperature x Nutrients x Region	9	1372.8	152.54	1.719	0.0829	9941
Temperature x Time x Region	9	516	57.333	0.6461	0.7556	9942
Nutrients x Time x Region	3	718.85	239.62	2.7003	0.0447	9961
Temperature x Nutrients x Time x Region	9	891.92	99.103	1.1168	0.3452	9931
Res	281	24935				

Table S4.10: F1s $rETR_{max}$ Main test

Factor	df	SS	MS	Pseudo-F	P (perm)	Unique perms
Temperature	3	7976.8	2658.9	6.1174	0.0007	9960
Nutrients	1	53260	53260	122.53	0.0001	9832
Time	1	0.7623	0.7623	0.0018	0.9645	9841
Region	3	71863	23954	55.112	0.0001	9961

Temperature x Nutrients	3	1936.8	645.61	1.4853	0.217	9954
Temperature x Time	3	14101	4700.3	10.814	0.0001	9963
Temperature x Region	9	12512	1390.3	3.1986	0.0013	9943
Nutrients x Time	1	958.46	958.46	2.2051	0.1358	9828
Nutrients x Region	3	7821.9	2607.3	5.9986	0.0006	9949
Time x Region	3	16082	5360.8	12.334	0.0001	9959
Temperature x Nutrients x Time	3	3831	1277	2.938	0.0327	9958
Temperature x Nutrients x Region	9	17780	1975.5	4.545	0.0002	9938
Temperature x Time x Region	9	6946.1	771.79	1.7757	0.0733	9929
Nutrients x Time x Region	3	1873.9	624.64	1.4371	0.2305	9958
Temperature x Nutrients x Time x Region	9	5933.7	659.3	1.5168	0.1373	9938
Res	279	1.2127 E5				

Table S4.11: F1s RGR Fresh weight Main test

Factor	**df**	**SS**	**MS**	**Pseudo-F**	**P (perm)**	**Unique perms**
Temperature	3	0.00174	0.00058	0.54696	0.6456	9958
Nutrients	9	0.01134	0.00126	1.1848	0.3054	9935
Time	9	0.00593	0.00066	0.61933	0.783	9930
Region	3	0.00079	0.00026	0.24762	0.8654	9950
Temperature x Nutrients	9	0.00244	0.00027	0.25513	0.9854	9940
Temperature x Time	3	0.00154	0.00051	0.48323	0.6879	9951
Temperature x Region	3	0.00121	0.00040	0.38003	0.7661	9944
Nutrients x Time	9	0.00734	0.00082	0.76728	0.6515	9937
Nutrients x Region	1	0.00414	0.00414	3.8972	0.0501	9838
Time x Region	3	0.00130	0.00043	0.40728	0.736	9938
Temperature x Nutrients x Time	3	0.01140	0.00380	3.5736	0.0123	9943
Temperature x Nutrients x Region	3	0.08617	0.02872	27.01	0.0001	9963
Temperature x Time x Region	1	0.15803	0.15803	148.61	0.0001	9855
Nutrients x Time x Region	1	0.04801	0.04801	45.15	0.0001	9830
Temperature x Nutrients x Time x Region	3	0.12011	0.04004	37.649	0.0001	9948
Res	0.306 25	1.0634E-3				

Bibliography

1) Akita, S., Takano, Y., Nagai, S., Kuwahara, H., Kajihara, R., Tanabe, A. S., & Fujita, D. (2019). Rapid detection of macroalgal seed bank on cobbles: application of DNA metabarcoding using next-generation sequencing. *Journal of Applied Phycology*, *31*(4), 2743–2753. https://doi.org/10.1007/s10811-018-1730-9
2) Alsuwaiyan, N. A., Vranken, S., Filbee-Dexter, K., Cambridge, M., Coleman, M. A., & Wernberg, T. (2021). Genotypic variation in response to extreme events may facilitate kelp adaptation under future climates. *Marine Ecology Progress Series*, *672*(August), 111–121. https://doi.org/10.3354/meps13802
3) Anderson, A. B., Assis, J., Batista, M. B., Serrão, E. A., Guabiroba, H. C., Delfino, S. D. T., … Joyeux, J. C. (2021). Global warming assessment suggests the endemic Brazilian kelp beds to be an endangered ecosystem. *Marine Environmental Research*, *168*, 1–9. https://doi.org/10.1016/j.marenvres.2021.105307
4) Anderson, M. J., Gorley, R. N., & Clarke, K. R. (2014). PERMANOVA+ Primer V7: User Manual. In *Primer-E Ltd., Plymouth, UK*.
5) Applebaum, S. L., Pan, T. C. F., Hedgecock, D., & Manahan, D. T. (2014). Separating the nature and nurture of the allocation of energy in response to global change. *Integrative and Comparative Biology*, *54*(2), 284–295. https://doi.org/10.1093/icb/icu062
6) Arafeh-Dalmau, N., Montaño-Moctezuma, G., Martinez, J. A., Beas-Luna, R., Schoeman, D. S., & Torres-Moye, G. (2019). Extreme Marine Heatwaves alter kelp forest community near its equatorward distribution limit. *Frontiers in Marine Science*, *6*(JUL), 1–18. https://doi.org/10.3389/fmars.2019.00499
7) Arias-Ortiz, A., Serrano, O., Masqué, P., Lavery, P. S., Mueller, U., Kendrick, G. A., … Duarte, C. M. (2018). A marine heatwave drives massive losses from the world's largest seagrass carbon stocks. *Nature Climate Change*, *8*(4), 338–344. https://doi.org/10.1038/s41558-018-0096-y
8) Assis, J., Araújo, M. B., & Serrão, E. A. (2017). Projected climate changes threaten ancient refugia of kelp forests in the North Atlantic. *Global Change Biology*, *24*(1), e55–e66. https://doi.org/10.1111/gcb.13818
9) Assis, J., Coelho, N. C., Lamy, T., Valero, M., Alberto, F., & Serrão, E. Á. (2016). Deep reefs are climatic refugia for genetic diversity of marine forests. *Journal of Biogeography*, *43*(4), 833–844. https://doi.org/10.1111/jbi.12677
10) Assis, J., Lucas, A. V., Barbara, I., & Serrão, E. A. (2016). Future climate change is predicted to shift long - term persistence zones in the cold - temperate kelp Laminaria hyperborea. *Marine Environmental Research*, *113*, 174–182.
11) Assis, J., Serrão, E. Á., Coelho, N. C., Tempera, F., Valero, M., & Alberto, F. (2018). Past climate changes and strong oceanographic barriers structured low-latitude genetic relics for the golden kelp Laminaria ochroleuca. *Journal of Biogeography*, *45*(10), 2326–2336. https://doi.org/10.1111/jbi.13425
12) Assis, J., Tavares, D., Tavares, J., Cunha, A., Alberto, F., & Serrão, E. A. (2009). Findkelp, a GIS-Based Community Participation Project to Assess Portuguese Kelp. *Journal of Coastal Research*, *II*(56), 1469–1473.
13) Assis, J., Tyberghein, L., Bosch, S., Verbruggen, H., Serrão, E. A., & De Clerck, O. (2017). Bio-ORACLE v2.0: Extending marine data layers for bioclimatic modelling. *Global Ecology and Biogeography*, *27*(3), 277–284. https://doi.org/10.1111/geb.12693
14) Atkins, K. E., & Travis, J. M. J. (2010). Local adaptation and the evolution of species' ranges under climate change. *Journal of Theoretical Biology*, *266*(3), 449–457. https://doi.org/10.1016/j.jtbi.2010.07.014
15) Balasubramanian, S., Sureshkumar, S., Lempe, J., & Weigel, D. (2006). Potent induction of Arabidopsis thaliana flowering by elevated growth temperature. *PLoS Genetics*, *2*(7), 0980–0989. https://doi.org/10.1371/journal.pgen.0020106
16) Barner, A. K., Pfister, C. A., & Timothy Wootton, J. (2011). The mixed mating system of the sea palm kelp Postelsia palmaeformis: Few costs to selfing. *Proceedings of the Royal Society B: Biological Sciences*, *278*(1710), 1347–1355. https://doi.org/10.1098/rspb.2010.1928
17) Barrientos, S., Barreiro, R., & Piñeiro-Corbeira, C. (2023). Paradoxical failure of Laminaria ochroleuca (Laminariales, Phaeophyceae) to consolidate a kelp forest inside a Marine National Park. *European Journal of*

Phycology, *58*(1), 72–82. https://doi.org/10.1080/09670262.2022.2065365

18) Barrientos, S., Piñeiro-Corbeira, C., & Barreiro, R. (2022). Temperate Kelp Forest Collapse by Fish Herbivory: A Detailed Demographic Study. *Frontiers in Marine Science*, *9*(January), 1–17. https://doi.org/10.3389/fmars.2022.817021
19) Bartsch, I., Wiencke, C., Bischof, K., Buchholz, C. M., Buck, B. H., Eggert, A., … Wiese, J. (2008). The genus *Laminaria sensu lato* : recent insights and developments. *European Journal of Phycology*, *43*(1), 1–86. https://doi.org/10.1080/09670260701711376
20) Beaumont, N. J., Austen, M. C., Mangi, S. C., & Townsend, M. (2008). Economic valuation for the conservation of marine biodiversity. *Marine Pollution Bulletin*, *56*(3), 386–396. https://doi.org/10.1016/j.marpolbul.2007.11.013
21) Becker, F. G., Cleary, M., Team, R. M., Holtermann, H., The, D., Agenda, N., … (2015) .ح ,فاطمی. Phenotypic Plasticity & Evolution: Causes, Consequences, Controversies. In *Syria Studies* (Vol. 7). https://doi.org/10.1201/9780429343001
22) Beer, S., Björk, M., & Beardall, J. (2014a). Photosynthesis in the marine environment. In *Wiley Blackwell* (Vol. 1). Wiley Blackwell.
23) Beer, S., Björk, M., & Beardall, J. (2014b). *Photosynthesis in the marine environment*. John Wiley & Sons, Ltd.
24) Bellard, C., Bertelsmeier, C., Leadley, P., Thuiller, W., & Courchamp, F. (2012). Impacts of climate change on the future of biodiversity. *Ecology Letters*, *15*(4), 365–377. https://doi.org/10.1111/J.1461-0248.2011.01736.X
25) Bennett, S., Wernberg, T., Connell, S. D., Hobday, A. J., Johnson, C. R., & Poloczanska, E. S. (2016). The "Great Southern Reef": Social, ecological and economic value of Australia's neglected kelp forests. *Marine and Freshwater Research*, *67*(1), 47–56. https://doi.org/10.1071/MF15232
26) Bennett, S., Wernberg, T., Joy, B. A., De Bettignies, T., & Campbell, A. H. (2015). Central and rear-edge populations can be equally vulnerable to warming. *Nature Communications*, *6*, 1–7. https://doi.org/10.1038/ncomms10280
27) Bertocci, I., Araújo, R., Oliveira, P., & Sousa-Pinto, I. (2015). Potential effects of kelp species on local fisheries. *Journal of Applied Ecology*, *52*(5), 1216–1226. https://doi.org/10.1111/1365-2664.12483
28) Birkett, D. A., Maggs, C. A., Dring, M. J., & Boaden, P. J. S. (1998). Infralittoral Reef Biotipes with Kelp Species (volume VII). An overview of dynamic and sensivity characteristics for conservation management of marine SAC's. *Scottish Association of Marine Science (UK Marine SACs Project)*, *VII*(August), 1–174.
29) Biskup, S., Bertocci, I., Arenas, F., & Tuya, F. (2014). Functional responses of juvenile kelps, Laminaria ochroleuca and Saccorhiza polyschides, to increasing temperatures. *Aquatic Botany*, *113*, 117–122. https://doi.org/10.1016/j.aquabot.2013.10.003
30) Blamey, L. K., & Bolton, J. J. (2017). The economic value of South African kelp forests and temperate reefs: Past, present and future. *Journal of Marine Systems*. https://doi.org/10.1016/j.jmarsys.2017.06.003
31) Bolton, J. J., & Lüning, K. (1982). Optimal growth and maximal survival temperatures of Atlantic Laminaria species (Phaeophyta) in culture. *Marine Biology*, *66*(1), 89–94. https://doi.org/10.1007/BF00397259
32) Bolton, John J. (2010). The biogeography of kelps (Laminariales, Phaeophyceae): A global analysis with new insights from recent advances in molecular phylogenetics. *Helgoland Marine Research*, *64*(4), 263–279. https://doi.org/10.1007/s10152-010-0211-6
33) Braga-Henriques, A., Buhl-Mortensen, P., Tokat, E., Martins, A., Silva, T., Jakobsen, J., … Biscoito, M. (2022). Benthic community zonation from mesophotic to deep sea: Description of first deep-water kelp forest and coral gardens in the Madeira archipelago (central NE Atlantic). *Frontiers in Marine Science*, *9*(September), 1–25. https://doi.org/10.3389/fmars.2022.973364
34) Bringloe, T. T., Bartlett, C. A. B., Bergeron, E. S., Cripps, K. S. A., Daigle, N. J., Gallagher, P. O., … Saunders, G. W. (2018). Detecting Alaria esculenta and Laminaria digitata (Laminariales, Phaeophyceae) gametophytes in red algae, with consideration of distribution patterns in the intertidal zone. *Phycologia*, *57*(1), 1–8. https://doi.org/10.2216/17-66.1

35) Bringloe, T. T., Starko, S., Wade, R. M., Vieira, C., Kawai, H., De Clerck, O., … Verbruggen, H. (2020). Phylogeny and Evolution of the Brown Algae. *Critical Reviews in Plant Sciences*, *0*(0), 1–41. https://doi.org/10.1080/07352689.2020.1787679

36) Bruhn, J., & Gerard, V. A. (1996). Photoinhibition and recovery of the kelp Laminaria saccharina at optimal and superoptimal temperatures. *Marine Biology*, *125*(4), 639–648. https://doi.org/10.1007/BF00349245

37) Buonomo, R., Assis, J., Fernandes, F., Engelen, A. H., Airoldi, L., & Serrão, E. A. (2016). Habitat continuity and stepping-stone oceanographic distances explain population genetic connectivity of the brown alga Cystoseira amentacea. *Molecular Ecology*, *26*(3), 766–780. https://doi.org/10.1111/mec.13960

38) Carr, M. E., & Kearns, E. J. (2003). Production regimes in four Eastern Boundary Current systems. *Deep-Sea Research Part II: Topical Studies in Oceanography*, *50*(22–26), 3199–3221. https://doi.org/10.1016/j.dsr2.2003.07.015

39) Casado-Amezúa, P., Araújo, R., Bárbara, I., Bermejo, R., Borja, Díez, I., … Martínez, B. (2019). Distributional shifts of canopy-forming seaweeds from the Atlantic coast of Southern Europe. *Biodiversity and Conservation*, *28*(5), 1151–1172. https://doi.org/10.1007/s10531-019-01716-9

40) Chapman, A. R. . (1986). Population and Community Ecology of Seaweeds. In J. H. S. Blaxter & A. J. Southward (Eds.), *Advances in Marine Biology* (Volume 23, pp. 1–161). https://doi.org/https://doi.org/10.1016/S0065-2881(08)60108-X

41) Cheung, W. W. L., Frölicher, T. L., Lam, V. W. Y., Oyinlola, M. A., Reygondeau, G., Rashid Sumaila, U., … Wabnitz, C. C. C. (2021). Marine high temperature extremes amplify the impacts of climate change on fish and fisheries. *Science Advances*, *7*(40), 1–16. https://doi.org/10.1126/sciadv.abh0895

42) Clarke, K. R., Gorley, R. N., Sommerfield, P. J., & Warwick, R. M. (2014). *Change in marine communities - statistical analysis*.

43) Coleman, F. C., & Williams, S. L. (2002). Overexploiting marine ecosystem engineers: Potential consequences for biodiversity. *Trends in Ecology and Evolution*, *17*(1), 40–44. https://doi.org/10.1016/S0169-5347(01)02330-8

44) Coleman, M. A. (2013). Connectivity of the Habitat-Forming Kelp, Ecklonia radiata within and among Estuaries and Open Coast. *PLOS ONE*, *8*(5), e64667. https://doi.org/10.1371/JOURNAL.PONE.0064667

45) Colin, C., Leblanc, C., Wagner, E., Delage, L., Leize-Wagner, E., Dorsselaer, A. Van, … Potin, P. (2003). The Brown Algal Kelp Laminaria digitata Features Distinct Bromoperoxidase and Iodoperoxidase Activities *. *Journal of Biological Chemistry*, *278*(26), 23545–23552. https://doi.org/10.1074/JBC.M300247200

46) D.A. Birkett, C.A. Maggs, M. J. D. and P. J. S. B. R. S. (1998). *Infralittoral Reef Biotopes with Kelp Species (volume VII). An overview of dynamic and sensitivity characteristics for conservation management of marine SACs*. *VII*(August), 1–174.

47) Dayton, P. K. (1985). Ecology of Kelp Communities. *Annual Review of Ecology and Systematics*, *16*(1985), 215–245.

48) Denny, M. (2017). The fallacy of the average: On the ubiquity, utility and continuing novelty of Jensen's inequality. *Journal of Experimental Biology*, *220*(2), 139–146. https://doi.org/10.1242/jeb.140368

49) Des Roches, S., Pendleton, L. H., Shapiro, B., & Palkovacs, E. P. (2021). Conserving intraspecific variation for nature's contributions to people. *Nature Ecology & Evolution*, *5*(5), 574–582. https://doi.org/10.1038/s41559-021-01403-5

50) Desmond, M. J., Pritchard, D. W., & Hepburn, C. D. (2015). Light limitation within southern New Zealand kelp forest communities. *PLoS ONE*, *10*(4), 1–18. https://doi.org/10.1371/journal.pone.0123676

51) Dieck, I. T. (1992). North Pacific and North Atlantic digitate Laminaria species (Phaeophyta): hybridization experiments and temperature responses. *Phycologia*, *31*(2), 147–163. https://doi.org/10.2216/i0031-8884-31-2-147.1

52) Duarte, C. M., Gattuso, J., Hancke, K., Gundersen, H., & Filbee-Dexter, K. (2022). Global estimates of the extent

and production of algal forests. *Global Biogeochemical Cycles*, *in press*(May). https://doi.org/10.1111/geb.13515

53) Duarte, G. A. S., Villela, H. D. M., Deocleciano, M., Silva, D., Barno, A., Cardoso, P. M., … Peixoto, R. S. (2020). Heat Waves Are a Major Threat to Turbid Coral Reefs in Brazil. *Frontiers in Marine Science*, *7*(March), 1–8. https://doi.org/10.3389/fmars.2020.00179
54) Duarte, P., Ramos, M., Calado, G., & Jesus, B. (2013). Laminaria hyperborea photosynthesis-irradiance relationship measured by oxygen production and pulse-amplitude-modulated chlorophyll fluorometry. *Aquatic Biology*, *19*(1), 29–44. https://doi.org/10.3354/ab00515
55) Earl, D. A., & vonHoldt, B. M. (2012). STRUCTURE HARVESTER: A website and program for visualizing STRUCTURE output and implementing the Evanno method. *Conservation Genetics Resources*, *4*(2), 359–361. https://doi.org/10.1007/s12686-011-9548-7
56) Edgar, G. J., Alexander, T. J., Lefcheck, J. S., Bates, A. E., Kininmonth, S. J., Thomson, R. J., … Stuart-Smith, R. D. (2017). Abundance and local-scale processes contribute to multi-phyla gradients in global marine diversity. *Science Advances*, *3*(10). https://doi.org/10.1126/sciadv.1700419
57) Edwards, M. S. (2022). It's the Little Things: The Role of Microscopic Life Stages in Maintaining Kelp Populations. *Frontiers in Marine Science*, *9*(April), 1–20. https://doi.org/10.3389/fmars.2022.871204
58) Eger, A. M., Marzinelli, E. M., Beas-Luna, R., Blain, C. O., Blamey, L. K., Byrnes, J. E. K., … Vergés, A. (2023). The value of ecosystem services in global marine kelp forests. *Nature Communications*, *14*(1). https://doi.org/10.1038/s41467-023-37385-0
59) Ehlers, A., Worm, B., & Reusch, T. B. H. (2008). Importance of genetic diversity in eelgrass Zostera marina for its resilience to global warming. *Marine Ecology Progress Series*, *355*(May 2014), 1–7. https://doi.org/10.3354/meps07369
60) Elliott Smith, E. A., & Fox, M. D. (2022). Characterizing energy flow in kelp forest food webs: a geochemical review and call for additional research. *Ecography*, *2022*(6), 1–16. https://doi.org/10.1111/ecog.05566
61) Erlandson, J. M., Braje, T. J., Gill, K. M., & Graham, M. H. (2015). Ecology of the Kelp Highway: Did Marine Resources Facilitate Human Dispersal From Northeast Asia to the Americas? *Journal of Island and Coastal Archaeology*, *10*(3), 392–411. https://doi.org/10.1080/15564894.2014.1001923
62) Erlandson, J., Rick, T., & Estes, J. (2005). Sea otters, shellfish, and humans: 10,000 years of ecological interaction on San Miguel Island, California. *Journal of Archaeological Science*, *6*(January 2014), 58–68. Retrieved from http://iws.org/CISProceedings/6th_CIS_Proceedings/Erlandson_et_al.pdf
63) Erwin, D. H. (1998). The end and the beginning: Recoveries from mass extinctions. *Trends in Ecology and Evolution*, *13*(9), 344–349. https://doi.org/10.1016/S0169-5347(98)01436-0
64) Evanno, G., Regnaut, S., & Goudet, J. (2005). Detecting the number of clusters of individuals using the software structure: a simulation study. *Molecular Ecology*, *14*(8), 2611–2620. https://doi.org/https://doi.org/10.1111/j.1365-294X.2005.02553.x
65) Fernández, C. (2011). The retreat of large brown seaweeds on the north coast of Spain: The case of Saccorhiza polyschides. *European Journal of Phycology*, *46*(4), 352–360. https://doi.org/10.1080/09670262.2011.617840
66) Filbee-Dexter, K., Wernberg, T., Grace, S. P., Thormar, J., Fredriksen, S., Narvaez, C. N., … Norderhaug, K. M. (2020). Marine heatwaves and the collapse of North Atlantic kelp forests. *Scientific Reports*, *10*(13388), 1–11. https://doi.org/https://doi.org/10.1038/s41598-020-70273-x
67) Filbee-Dexter, Karen, Feehan, C. J., & Scheibling, R. E. (2016). Large-scale degradation of a kelp ecosystem in an ocean warming hotspot. *Marine Ecology Progress Series*, *543*(February), 141–152. https://doi.org/10.3354/meps11554
68) Filbee-Dexter, Karen, & Wernberg, T. (2018). Rise of Turfs: A New Battlefront for Globally Declining Kelp Forests. *BioScience*, *68*(2), 64–76. https://doi.org/10.1093/biosci/bix147
69) Flores-Moya, A. (2012). *Warm Temperate Seaweed Communities: A Case Study of Deep Water Kelp Forests from*

the Alboran Sea (SW Mediterranean Sea) and the Strait of Gibraltar. https://doi.org/10.1007/978-3-642-28451-9_15

70) Frade, P. R., Bongaerts, P., Englebert, N., Rogers, A., Gonzalez-Rivero, M., & Hoegh-Guldberg, O. (2018). Deep reefs of the Great Barrier Reef offer limited thermal refuge during mass coral bleaching. *Nature Communications*, *9*(1), 1–8. https://doi.org/10.1038/s41467-018-05741-0

71) Fragkopoulou, E., Sen Gupta, A., Costello, M. J., Wernberg, T., Araújo, M. B., Serrão, E. A., … Assis, J. (2023). Marine biodiversity exposed to prolonged and intense subsurface heatwaves. *Nature Climate Change*, *13*(10), 1114–1121. https://doi.org/10.1038/s41558-023-01790-6

72) Fram, J. P., Stewart, H. L., Brzezinski, M. A., Gaylord, B., Reed, D. C., Williams, S. L., & MacIntyre, S. (2008). Physical pathways and utilization of nitrate supply to the giant kelp, Macrocystis pyrifera. *Limnology and Oceanography*, *53*(4), 1589–1603. https://doi.org/10.4319/lo.2008.53.4.1589

73) Franco, J. N., Tuya, F., Bertocci, I., Rodríguez, L., Martínez, B., Sousa-Pinto, I., & Arenas, F. (2018). The 'golden kelp' Laminaria ochroleuca under global change: Integrating multiple eco-physiological responses with species distribution models. *Journal of Ecology*, *106*(1), 47–58. https://doi.org/10.1111/1365-2745.12810

74) Franco, J. N., Wernberg, T., Bertocci, I., Duarte, P., Jacinto, D., Vasco-Rodrigues, N., & Tuya, F. (2015). Herbivory drives kelp recruits into "hiding" in a warm ocean climate. *Marine Ecology Progress Series*, *536*(September), 1–9. https://doi.org/10.3354/meps11445

75) Franco, J. N., Wernberg, T., Bertocci, I., Jacinto, D., Maranhão, P., Pereira, T., … Tuya, F. (2017). Modulation of different kelp life stages by herbivory: compensatory growth versus population decimation. *Marine Biology*, *164*(8), 1–10. https://doi.org/10.1007/s00227-017-3196-8

76) G, M. D., Gassmann, G., & Lunning, K. (1979). Isolation of a spermatozoid-releasing and -attracting substance from female gametophytes of Laminaria digitata. *Nature*, *279*(5712), 430–431. https://doi.org/10.1038/279430a0

77) Gao, X., Endo, H., Nagaki, M., & Agatsuma, Y. (2016). Growth and survival of juvenile sporophytes of the kelp Ecklonia cava in response to different nitrogen and temperature regimes. *Fisheries Science*, *82*(4), 623–629. https://doi.org/10.1007/s12562-016-0998-4

78) Gao, X., Endo, H., Nagaki, M., & Agatsuma, Y. (2017). Interactive effects of nutrient availability and temperature on growth and survival of different size classes of Saccharina japonica (Laminariales , Phaeophyceae). *Phycologia*, *56*(January), 253–260. https://doi.org/10.2216/16-91.1

79) Gao, X., Endo, H., Taniguchi, K., & Agatsuma, Y. (2013). Combined effects of seawater temperature and nutrient condition on growth and survival of juvenile sporophytes of the kelp Undaria pinnatifida (Laminariales; Phaeophyta) cultivated in northern Honshu, Japan. *Journal of Applied Phycology*, *25*(1), 269–275. https://doi.org/10.1007/s10811-012-9861-x

80) Garbary, D. J., Kim, K. Y., Klinger, T., & Duggins, D. (1999). Red algae as hosts for endophytic kelp gametophytes. *Marine Biology*, *135*(1), 35–40. https://doi.org/10.1007/s002270050598

81) García-Sánchez, M. J., Delgado-Huertas, A., Fernández, J. A., & Flores-Moya, A. (2016). Photosynthetic use of inorganic carbon in deep-water kelps from the Strait of Gibraltar. *Photosynthesis Research*, *127*(3), 295–305. https://doi.org/10.1007/s11120-015-0184-z

82) Garrabou, J., Coma, R., Bensoussan, N., Bally, M., Chevaldonné, P., Cigliano, M., … Cerrano, C. (2009). Mass mortality in Northwestern Mediterranean rocky benthic communities: Effects of the 2003 heat wave. *Global Change Biology*, *15*(5), 1090–1103. https://doi.org/10.1111/j.1365-2486.2008.01823.x

83) Garrabou, Joaquim, Gómez-, D., Medrano, A., Cerrano, C., Ponti, M., Schlegel, R., … Anton, P. I. (2022). Marine heatwaves drive recurrent mass mortalities in the Mediterranean Sea. *Global Change Biology*, (May), 1–18. https://doi.org/10.1111/gcb.16301

84) Glaubitz, C. J. (2004). convert: A user-friendly program to reformat diploid genotypic data for commonly used population genetic software packages. *Molecular Ecology*, *4*(2), 309–310. https://doi.org/https://doi.org/10.1111/j.1471-8286.2004.00597.x

85) Global Monitoring and Forecasting Center. (2018). GLORYS12V1-Global Ocean Physical Reanalysis Product.
86) Graham, M. H., Vasquez, J. A., & Buschmann, A. . (2007). Oceanography and marine biology: An annual review. In *Oceanography and Marine Biology: An Annual Review* (Vol. 49, pp. 39–88). https://doi.org/10.1016/0025-326x(94)90189-9
87) Gu, Z., Eils, R., & Schlesner, M. (2016). Complex heatmaps reveal patterns and correlations in multidimensional genomic data. *Bioinformatics*, *32*(18), 2847–2849. https://doi.org/10.1093/bioinformatics/btw313
88) Guzinski, J., Ballenghien, M., Daguin-Thiébaut, C., Lévêque, L., & Viard, F. (2018). Population genomics of the introduced and cultivated Pacific kelp Undaria pinnatifida: Marinas—not farms—drive regional connectivity and establishment in natural rocky reefs. *Evolutionary Applications*, *11*(9), 1582–1597. https://doi.org/10.1111/eva.12647
89) Hayashida, H., Matear, R. J., & Strutton, P. G. (2020). Background nutrient concentration determines phytoplankton bloom response to marine heatwaves. *Global Change Biology*, *26*(9), 4800–4811. https://doi.org/10.1111/gcb.15255
90) Hays, C. G., Hanley, T. C., Hughes, A. R., Truskey, S. B., Zerebecki, R. A., & Sotka, E. E. (2021). Local adaptation in marine foundation species at microgeographic scales. *Biological Bulletin*, *241*(1), 16–29. https://doi.org/10.1086/714821
91) Hereward, H. F. R., King, N. G., & Smale, D. A. (2020). Intra-Annual Variability in Responses of a Canopy Forming Kelp to Cumulative Low Tide Heat Stress: Implications for Populations at the Trailing Range Edge. *Journal of Phycology*, *56*(1), 146–158. https://doi.org/10.1111/jpy.12927
92) Hewitt, G. M. (1996). Some genetic consequences of ice ages, and their role in divvergence and speciation. *Biological Journal of the Linnean Society*, *58*(March), 247–276.
93) Himes-Cornell, A., Grose, S. O., & Pendleton, L. (2018). Mangrove ecosystem service values and methodological approaches to valuation: Where do we stand? *Frontiers in Marine Science*, *5*(OCT), 1–15. https://doi.org/10.3389/fmars.2018.00376
94) Hobday, A. J., Alexander, L. V., Perkins, S. E., Smale, D. A., Straub, S. C., Oliver, E. C. J., … Wernberg, T. (2016). A hierarchical approach to defining marine heatwaves. *Progress in Oceanography*, *141*, 227–238. https://doi.org/10.1016/j.pocean.2015.12.014
95) Holbrook, N. J., Scannell, H. A., Sen Gupta, A., Benthuysen, J. A., Feng, M., Oliver, E. C. J., … Wernberg, T. (2019). A global assessment of marine heatwaves and their drivers. *Nature Communications*, *10*(1), 1–13. https://doi.org/10.1038/s41467-019-10206-z
96) Hollarsmith, J. A., Buschmann, A. H., Camus, C., & Grosholz, E. D. (2020). Varying reproductive success under ocean warming and acidification across giant kelp (Macrocystis pyrifera) populations. *Journal of Experimental Marine Biology and Ecology*, *522*(May 2019), 151247. https://doi.org/10.1016/j.jembe.2019.151247
97) Holt, R. D., & Gomulkiewicz, R. (2004). Conservation Implications of Niche Conservatism and Evolution in Heterogeneous Environments. In F. R, D. U, & C. D (Eds.), *Evolutionary Conservation Biology* (pp. 244–264). https://doi.org/10.1017/cbo9780511542022.018
98) Hop, H., Wiencke, C., Vögele, B., & Kovaltchouk, N. A. (2012). Species composition, zonation, and biomass of marine benthic macroalgae in Kongsfjorden, Svalbard. *Botanica Marina*, *55*(4), 399–4141. https://doi.org/https://doi.org/10.1515/bot-2012-0097
99) Hoppit, G., & Schmidt, D. N. (2022). A Regional View of the Response to Climate Change: A Meta-Analysis of European Benthic Organisms' Responses. *Frontiers in Marine Science*, *9*(June), 1–13. https://doi.org/10.3389/fmars.2022.896157
100) Hu, N., Bourdeau, P. E., Harlos, C., Liu, Y., & Hollander, J. (2022). Meta-analysis reveals variance in tolerance to climate change across marine trophic levels. *Science of the Total Environment*, *827*(March), 154244. https://doi.org/10.1016/j.scitotenv.2022.154244
101) Hubbard, C. B., Garbary, D. J., Kim, K. Y., & Chiasson, D. M. (2004). Host specificity and growth of kelp

gametophytes symbiotic with filamentous red algae (Ceramiales, Rhodophyta). *Helgoland Marine Research*, *58*(1), 18–25. https://doi.org/10.1007/s10152-003-0162-2

102) Ivany, L. C., Patterson, W. P., & Lohmann, K. C. (2000). Cooler winters as a possible cause of mass extinctions at the Eocene/Oligocene boundary. *Nature*, *407*(6806), 887–890. https://doi.org/10.1038/35038044

103) Johansson, M. L., Alberto, F., Reed, D. C., Raimondi, P. T., Coelho, N. C., Young, M. A., … Serrão, E. A. (2015). Seascape drivers of Macrocystis pyrifera population genetic structure in the northeast Pacific. *Molecular Ecology*, *24*(19), 4866–4885. https://doi.org/10.1111/mec.13371

104) Jones, T., Parrish, J. K., Peterson, W. T., Bjorkstedt, E. P., Bond, N. A., Ballance, L. T., … Harvey, J. (2018). Massive Mortality of a Planktivorous Seabird in Response to a Marine Heatwave. *Geophysical Research Letters*, *45*(7), 3193–3202. https://doi.org/10.1002/2017GL076164

105) Kain, J. M. (1967). Populations of Laminaria hyperborea at various latitudes. *Helgoländer Wissenschaftliche Meeresuntersuchungen*, *15*(1–4), 489–499. https://doi.org/10.1007/BF01618645

106) Kim, J. K., Kraemer, G. P., & Yarish, C. (2015). Use of sugar kelp aquaculture in Long Island Sound and the Bronx River Estuary for nutrient extraction. *Marine Ecology Progress Series*, *531*(July), 155–166. https://doi.org/10.3354/meps11331

107) King, N. G., McKeown, N. J., Smale, D. A., & Moore, P. J. (2018). The importance of phenotypic plasticity and local adaptation in driving intraspecific variability in thermal niches of marine macrophytes. *Ecography*, *41*(9), 1469–1484. https://doi.org/10.1111/ecog.03186

108) King, N. G., McKeown, N. J., Smale, D. A., Wilcockson, D. C., Hoelters, L., Groves, E. A., … Moore, P. J. (2019a). Evidence for different thermal ecotypes in range centre and trailing edge kelp populations. *Journal of Experimental Marine Biology and Ecology*, *514–515*(March), 10–17. https://doi.org/10.1016/j.jembe.2019.03.004

109) King, N. G., McKeown, N. J., Smale, D. A., Wilcockson, D. C., Hoelters, L., Groves, E. A., … Moore, P. J. (2019b). Evidence for different thermal ecotypes in range centre and trailing edge kelp populations. *Journal of Experimental Marine Biology and Ecology*, *514–515*, 10–17. https://doi.org/10.1016/j.jembe.2019.03.004

110) King, N. G., Moore, P. J., Thorpe, J. M., & Smale, D. A. (2023). Consistency and Variation in the Kelp Microbiota: Patterns of Bacterial Community Structure Across Spatial Scales. *Microbial Ecology*, *85*(4), 1265–1275. https://doi.org/10.1007/s00248-022-02038-0

111) Kirk, J. T. O. (2011). *Light and Photosynthesis in Aquatic Ecosystems* (Cambridge University Press, Ed.).

112) Krause-Jensen, D., & Duarte, C. M. (2016). Substantial role of macroalgae in marine carbon sequestration. *Nature Geoscience*, *9*(10), 737–742. https://doi.org/10.1038/ngeo2790

113) Krumhansl, K. A., Okamoto, D. K., Rassweiler, A., Novak, M., Bolton, J. J., Cavanaugh, K. C., … Byrnes, J. E. K. (2016). Global patterns of kelp forest change over the past half-century. *Proceedings of the National Academy of Sciences of the United States of America*, *113*(48), 13785–13790. https://doi.org/10.1073/pnas.1606102113

114) Ladah, L. B., Zertuche-González, J. A., & Hernandez-Carmona, G. (1999). Giant kelp (Macrocystis pyrifera, Phaeophyceae) recruitment near its southern limit in Baja California after mass disappearance during ENSO 1997-1998. *Journal of Phycology*, *35*(6), 1106–1112. https://doi.org/10.1046/j.1529-8817.1999.3561106.x

115) Lane, C. E., Mayes, C., Druehl, L. D., & Saunders, G. W. (2006). A MULTI-GENE MOLECULAR INVESTIGATION OF THE KELP (LAMINARIALES, PHAEOPHYCEAE) SUPPORTS SUBSTANTIAL TAXONOMIC RE-ORGANIZATION1. *Journal of Phycology*, *42*(2), 493–512. https://doi.org/10.1111/J.1529-8817.2006.00204.X

116) Layton, C., Shelamoff, V., Cameron, M. J., Tatsumi, M., Wright, J. T., & Johnson, C. R. (2019). Resilience and stability of kelp forests: The importance of patch dynamics and environment-engineer feedbacks. *PLoS ONE*, *14*(1). https://doi.org/10.1371/journal.pone.0210220

117) Leclerc, J., Riera, P., Laurans, M., Leroux, C., Lévêque, L., & Davoult, D. (2015). Community, trophic structure and functioning in two contrasting *Laminaria hyperborea forests*. *Estuarine, Coastal and Shelf Science*, *152*, 11–

22. https://doi.org/10.1016/j.ecss.2014.11.005

118) Liesner, D., Fouqueau, L., Valero, M., Roleda, M., Pearson, G., Bischof, K. ;, … Bartsch, I. (2020). Heat stress responses and population genetics of the kelp Laminaria digitata (Phaeophyceae) across latitudes reveal differentiation among North Atlantic populations. *Ecology and Evolution*, (March), 1–62. https://doi.org/ECE-2020-03-00366.R1

119) Liesner, D., Pearson, G. A., Bartsch, I., Rana, S., Harms, L., Heinrich, S., … Valentin, K. (2022). Increased Heat Resilience of Intraspecific Outbred Compared to Inbred Lineages in the Kelp Laminaria digitata: Physiology and Transcriptomics. *Frontiers in Marine Science*, *9*(March), 1–20. https://doi.org/10.3389/fmars.2022.838793

120) Liesner, D., Shama, L. N. S., Diehl, N., Valentin, K., & Bartsch, I. (2020). Thermal Plasticity of the Kelp Laminaria digitata (Phaeophyceae) Across Life Cycle Stages Reveals the Importance of Cold Seasons for Marine Forests. *Frontiers in Marine Science*, *7*(June). https://doi.org/10.3389/fmars.2020.00456

121) Linhart, Y. B., & Grant, M. C. (1996). Evolutionary significance of local genetic differentiation in plants. *Annual Review of Ecology and Systematics*, *27*, 237–277. https://doi.org/10.1146/annurev.ecolsys.27.1.237

122) Lourenço, C. R., Nicastro, K. R., McQuaid, C. D., Chefaoui, R. M., Assis, J., Taleb, M. Z., & Zardi, G. I. (2017). Evidence for rangewide panmixia despite multiple barriers to dispersal in a marine mussel. *Scientific Reports 2017 7:1*, *7*(1), 1–16. https://doi.org/10.1038/s41598-017-10753-9

123) Lourenço, C. R., Zardi, G. I., McQuaid, C. D., Serrão, E. A., Pearson, G. A., Jacinto, R., & Nicastro, K. R. (2016a). Upwelling areas as climate change refugia for the distribution and genetic diversity of a marine macroalga. *Journal of Biogeography*, *43*(8), 1595–1607. https://doi.org/10.1111/jbi.12744

124) Lourenço, C. R., Zardi, G. I., McQuaid, C. D., Serrão, E. A., Pearson, G. A., Jacinto, R., & Nicastro, K. R. (2016b). Upwelling areas as climate change refugia for the distribution and genetic diversity of a marine macroalga. *Journal of Biogeography*, *43*(8), 1595–1607. https://doi.org/10.1111/jbi.12744

125) Luning, K. (1979). Growth Strategies of Three Laminaria Species (Phaeophyceae) Inhabiting Different Depth Zones in the Sublittoral Region of Helgoland (North Sea). *Marine Ecology*, *1*, 195–207.

126) Lüning, K. (1969). Growth of amputated and dark-exposed individuals of the brown alga Laminaria hyperborea. *Marine Biology*, *2*(3), 218–223. https://doi.org/10.1007/BF00351143

127) Lüning, K., & Dring, M. J. (1972). Reproduction induced by blue light in female gametophytes of Laminaria saccharina. *Planta*, *104*(3), 252–256. https://doi.org/10.1007/BF00387080

128) Lüning, Klaus. (1980). Critical Levels of Light and Temperature Regulating the Gametogenesis of Three Laminaria Species (Phaeophyceae). *Journal of Phycology*, *16*(1), 1–15. https://doi.org/10.1111/j.1529-8817.1980.tb02992.x

129) Manent, P., Bañolas, G., Alberto, F., Curbelo, L., Espino, F., & Tuya, F. (2020). Long-term seagrass degradation: Integrating landscape, demographic, and genetic responses. *Aquatic Conservation: Marine and Freshwater Ecosystems*, *30*(6), 1111–1120. https://doi.org/10.1002/aqc.3325

130) Martins, N., Pearson, G. A., Bernard, J., Serrão, E. A., & Bartsch, I. (2020). Thermal traits for reproduction and recruitment differ between Arctic and Atlantic kelp Laminaria digitata. *PLOS ONE*, *15*(6), 1–19. https://doi.org/10.1371/journal.pone.0235388

131) McPherson, M. L., Finger, D. J. I., Houskeeper, H. F., Bell, T. W., Carr, M. H., Rogers-Bennett, L., & Kudela, R. M. (2021). Large-scale shift in the structure of a kelp forest ecosystem co-occurs with an epizootic and marine heatwave. *Communications Biology*, *4*(1), 1–9. https://doi.org/10.1038/s42003-021-01827-6

132) Meirmans, P. G. (2020). genodive version 3.0: Easy-to-use software for the analysis of genetic data of diploids and polyploids. *Molecular Ecology Resources*, *20*(4), 1126–1131. https://doi.org/10.1111/1755-0998.13145

133) Michèle Barbier, Bénédicte Charrier, Rita Araujo, Susan L. Holdt, B. J. & C. R. (2019). *Pegasus - Phycomorph European Guideline for a Sustainable Aquaculture of Seaweeds Edited by Michèle Barbier & Bénédicte Charrier*. (July).

134) Mikhaylova, T. A., & Shtrik, V. A. (2007). Macroepiphytes of Laminaria hyperborea (Laminariaceae) in the Barents

and the White Sea. *Botanicheskiy Zhurnal*, *98*(12), 1818–1828.

135) Miller, A. D., Coleman, M. A., Clark, J., Cook, R., Naga, Z., Doblin, M. A., … Bellgrove, A. (2019). Local thermal adaptation and limited gene flow constrain future climate responses of a marine ecosystem engineer. *Evolutionary Applications*, *13*(5), 918–934. https://doi.org/10.1111/eva.12909

136) Minich, J. J., Morris, M. M., Brown, M., Doane, M., Edwards, S., Michael, T. P., & Dinsdale, E. A. (2018). *Elevated temperature drives kelp microbiome dysbiosis , while elevated carbon dioxide induces water microbiome disruption*. 1–23.

137) Monteiro, C., Pereira, J., Seabra, R., & Lima, F. P. (2022). Fine-scale survey of intertidal macroalgae reveals recent changes in a cold-water biogeographic stronghold. *Frontiers in Marine Science*, *9*(July), 1–15. https://doi.org/10.3389/fmars.2022.880074

138) Motomura, T., & Sakai, Y. (1984). Ultrastructural studies of gametogenesis in Laminaria angustata (Laminariales, Phaeophyta) regulated by iron concentration in the medium. *Phycologia*, *23*(3), 331–343. https://doi.org/DOI: 10.2216/i0031-8884-23-3-331.1

139) Neige, P. (2015). The Phenomenon of Evolutionary Radiation. In *Events of Increased Biodiversity* (pp. 47–64). https://doi.org/https://doi.org/10.1016/B978-1-78548-029-4.50003-6

140) Neiva, J., Pearson, G. A., Valero, M., & Serrão, E. A. (2010). Surfing the wave on a borrowed board: Range expansion and spread of introgressed organellar genomes in the seaweed Fucus ceranoides L. *Molecular Ecology*, *19*(21), 4812–4822. https://doi.org/10.1111/j.1365-294X.2010.04853.x

141) Neiva, J., Serrão, E. A., Paulino, C., Gouveia, L., Want, A., Tamigneaux, É., … Valero, M. (2020). Genetic structure of amphi-Atlantic Laminaria digitata (Laminariales, Phaeophyceae) reveals a unique range-edge gene pool and suggests post-glacial colonization of the NW Atlantic. *European Journal of Phycology*, *55*(4), 517–528. https://doi.org/10.1080/09670262.2020.1750058

142) Nimbs, M. J., Wernberg, T., Davis, T. R., Champion, C., & Coleman, M. A. (2023). Climate change threatens unique evolutionary diversity in Australian kelp refugia. *Scientific Reports*, *13*(1), 1–9. https://doi.org/10.1038/s41598-023-28301-z

143) Oliver, E. C. J., Donat, M. G., Burrows, M. T., Moore, P. J., Smale, D. A., Alexander, L. V., … Wernberg, T. (2018). Longer and more frequent marine heatwaves over the past century. *Nature Communications*, *9*(1), 1–12. https://doi.org/10.1038/s41467-018-03732-9

144) Parmesan, C., & Yohe, G. (2003). A globally coherent fingerprint of climate change impacts across natural systems. *Nature*, *421*(6918), 37–42. https://doi.org/10.1038/nature01286

145) Pearman, P. B., D'Amen, M., Graham, C. H., Thuiller, W., & Zimmermann, N. E. (2010). Within-taxon niche structure: niche conservatism, divergence and predicted effects of climate change. *Ecography*, *33*(6), 990–1003. https://doi.org/10.1111/J.1600-0587.2010.06443.X

146) Pecl, G. T., Araújo, M. B., Bell, J. D., Blanchard, J., Bonebrake, T. C., Chen, I. C., … Williams, S. E. (2017). Biodiversity redistribution under climate change: Impacts on ecosystems and human well-being. *Science*, *355*(6332). https://doi.org/10.1126/science.aai9214

147) Pedersen, M. F., Nejrup, L. B., Fredriksen, S., Christie, H., & Norderhaug, K. M. (2012). Effects of wave exposure on population structure, demography, biomass and productivity of the kelp Laminaria hyperborea. *Marine Ecology Progress Series*, *451*(December 2013), 45–60. https://doi.org/10.3354/meps09594

148) Pereira, T. R., Engelen, A. H., Pearson, G. A., Valero, M., & Serrão, E. A. (2015). Response of kelps from different latitudes to consecutive heat shock. *Journal of Experimental Marine Biology and Ecology*, *463*, 57–62. https://doi.org/10.1016/j.jembe.2014.10.022

149) Pereira, T. R., Engelen, A. H., Pearson, G. A., Valero, M., & Serrão, E. A. (2017). Population dynamics of temperate kelp forests near their low-latitude limit. *Aquatic Botany*, *139*, 8–18. https://doi.org/10.1016/j.aquabot.2017.02.006

150) Pereyra, R. T., Huenchuñir, C., Johansson, D., Forslund, H., Kautsky, L., Jonsson, P. R., & Johannesson, K. (2013).

Parallel speciation or long-distance dispersal? Lessons from seaweeds (Fucus) in the Baltic Sea. *Journal of Evolutionary Biology*, *26*(8), 1727–1737. https://doi.org/10.1111/JEB.12170

151) Perez, T., Garrabou, J., Harmelin, J., & Vacelet, J. (2000). Mortalité massive d ' invertébrés marins : un événement sans précédent en Méditerranée nord-occidentale. *Comptes Rendus de l'Académie Des Sciences— Series III— Sciences de La Vie*, *323*, 853–865. https://doi.org/https://doi.org/10.1016/S0764 - 4469(00)01237 - 3

152) Perkins-Kirkpatrick, S. E., & Lewis, S. C. (2020). Increasing trends in regional heatwaves. *Nature Communications*, *11*(1), 1–8. https://doi.org/10.1038/s41467-020-16970-7

153) Pessarrodona, A., Assis, J., Filbee-Dexter, K., Burrows, M. T., Gattuso, J. P., Duarte, C. M., … Wernberg, T. (2022). Global seaweed productivity. *Science Advances*, *8*(37). https://doi.org/10.1126/sciadv.abn2465

154) Pessarrodona, A., Foggo, A., & Smale, D. A. (2019). Can ecosystem functioning be maintained despite climate-driven shifts in species composition? Insights from novel marine forests. *Journal of Ecology*, *107*(1), 91–104. https://doi.org/10.1111/1365-2745.13053

155) Platt, T., Gallegos, C. L., & Harrison, W. G. (1980). Photoinhibition of Photosynthesis in Natural Assemblages of Marine Phytoplankton. *Journal of Marine Research*, *38*(4), 687–701.

156) Provasoli, L. (1968). Provasoli L. Media and prospects for the cultivation of marine algae. *Proceedings of the US Japan Conference; 1966; Hakone. Tokyo: Japanese Society of Plant Physiology*, 63–75.

157) Raimondi, P. T., Reed, D. C., & Washburn, L. (2004). Effects of self-fertilization in the giant kelp, Macrocystis pyrifera. *Ecology*, *85*(12), 3267–3276. https://doi.org/https://doi.org/10.1890/03-0559

158) Ramos, M., Bertocci, I., Tempera, F., Calado, G., Albuquerque, M., & Duarte, P. (2016). Patterns in megabenthic assemblages on a seamount summit (Ormonde Peak, Gorringe Bank, Northeast Atlantic). *Marine Ecology*, *37*(5), 1057–1072. https://doi.org/10.1111/MAEC.12353

159) Reed, D. C., Rassweiler, A., & Arkema, K. K. (2008). Biomass rather than growth rate determines variation in net primary production by giant kelp. *Ecology*, *89*(9), 2493–2505. https://doi.org/10.1890/07-1106.1

160) Reed, T. E., Schindler, D. E., & Waples, R. S. (2011). Interacting Effects of Phenotypic Plasticity and Evolution on Population Persistence in a Changing Climate. *Conservation Biology*, *25*(1), 56–63. https://doi.org/10.1111/j.1523-1739.2010.01552.x

161) Rinde, E., & Sjøtun, K. (2005). Demographic variation in the kelp Laminaria hyperborea along a latitudinal gradient. *Marine Biology*, *146*(6), 1051–1062. https://doi.org/10.1007/s00227-004-1513-5

162) Robuchon, M., Couceiro, L., Peters, A. F., Destombe, C., & Valero, M. (2014). Examining the bank of microscopic stages in kelps using culturing and barcoding. *European Journal of Phycology*, *49*(1), 128–133. https://doi.org/10.1080/09670262.2014.892635

163) Rosman, J. H., Koseff, J. R., Monismith, S. G., & Grover, J. (2007). A field investigation into the effects of a kelp forest (Macrocystis pyrifera) on coastal hydrodynamics and transport. *Journal of Geophysical Research: Oceans*, *112*(2). https://doi.org/10.1029/2005JC003430

164) Rothman, M. D., Mattio, L., Anderson, R. J., & Bolton, J. J. (2017). A phylogeographic investigation of the kelp genus Laminaria (Laminariales, Phaeophyceae), with emphasis on the South Atlantic Ocean. *Journal of Phycology*, *53*(4), 778–789. https://doi.org/10.1111/jpy.12544

165) Santelices, B. (2007). The discovery of kelp forests in deep-water habitats of tropical regions. *Proceedings of the National Academy of Sciences*, *104*(49), 19163–19164. https://doi.org/10.1073/PNAS.0708963104

166) Schaeffer, A., & Roughan, M. (2017). Subsurface intensification of marine heatwaves off southeastern Australia: The role of stratification and local winds. *Geophysical Research Letters*, *44*(10), 5025–5033. https://doi.org/10.1002/2017GL073714

167) Schaffelke, B., & Luning, K. (1994). A circannual rhythm controls seasonal growth in the kelps laminaria hyperborea and l digitata from helgoland (North sea). *European Journal of Phycology*, *29*(1), 49–56. https://doi.org/10.1080/09670269400650471

168) Schiel, D. R., & Foster, M. S. (2015). *The Biology and Ecology of Giant Kelp Forests*. Retrieved from https://books.google.com.au/books?id=dO_LBwAAQBAJ

169) Schirpke, U., Kohler, M., Leitinger, G., Fontana, V., Tasser, E., & Tappeiner, U. (2017). Future impacts of changing land-use and climate on ecosystem services of mountain grassland and their resilience. *Ecosystem Services*, *26*, 79–94. https://doi.org/10.1016/j.ecoser.2017.06.008

170) Schoenrock, K. M., O' Connor, A. M., Mauger, S., Valero, M., Neiva, J., Serrão, E., & Krueger-Hadfield, S. A. (2020). Genetic diversity of a marine foundation species, Laminaria hyperborea (Gunnerus) Foslie, along the coast of Ireland. *European Journal of Phycology*, *55*(3), 310–326. https://doi.org/10.1080/09670262.2020.1724338

171) Schoenrock, K. M., O'Callaghan, T., O'Callaghan, R., & Krueger-Hadfield, S. A. (2019). First record of Laminaria ochroleuca Bachelot de la Pylaie in Ireland in Béal an Mhuirthead, county Mayo. *Marine Biodiversity Records*, *12*(1), 1–8. https://doi.org/10.1186/s41200-019-0168-3

172) Silva, C. F., Pearson, G. A., Serrão, E. A., Bartsch, I., & Martins, N. (2022). Microscopic life stages of Arctic kelp differ in their resilience and reproductive output in response to Arctic seasonality. *European Journal of Phycology*, *00*(00), 1–15. https://doi.org/10.1080/09670262.2021.2014983

173) Sjortun, K., & Fredriksen, S. (1995). Growth allocation in Laminaria hyperborea. *Marine Ecology Progress Series*, *126*(1971), 213–222.

174) Sjøtun, K., Christie, H., & Fosså, J. H. (2006). The combined effect of canopy shading and sea urchin grazing on recruitment in kelp forest (Laminaria hyperborea). *Marine Biology Research*, *2*(1), 24–32. https://doi.org/10.1080/17451000500537418

175) Sjøtun, K., Fredriksen, S., & Rueness, J. (2010). Seasonal growth and carbon and nitrogen content in canopy and first-year plants of Laminaria hyperborea (Laminariales, Phaeophyceae). *Phycologia*, *35*(1), 1–8. https://doi.org/10.2216/i0031-8884-35-1-1.1

176) Sjøtun, K., S, F., Rueness, J., & Lein, T. E. (1995). Ecological studies of the kelp Laminaria hyperborea (Gunnerus) Foslie in Norway. *In: Ecology of Fjords and Coastal Waters. HR Skjodahl, C Hopkins, KE Erikstad, HP Leinaas (Eds). Elsevier Science B. V.*, (January), 525–536.

177) Smale, D. A., & Wernberg, T. (2013). Extreme climatic event drives range contraction of a habitat-forming species. *Proceedings of the Royal Society B: Biological Sciences*, *280*(1754), 20122829–20122829. https://doi.org/10.1098/rspb.2012.2829

178) Smale, Dan A., Burrows, M. T., Moore, P., O'Connor, N., & Hawkins, S. J. (2013). Threats and knowledge gaps for ecosystem services provided by kelp forests: A northeast Atlantic perspective. *Ecology and Evolution*, *3*(11), 4016–4038. https://doi.org/10.1002/ece3.774

179) Smale, Dan A., & Vance, T. (2015). Climate-driven shifts in species' distributions may exacerbate the impacts of storm disturbances on North-east Atlantic kelp forests. *Marine and Freshwater Research*, *67*(1), 65–74. https://doi.org/10.1071/MF14155

180) Smale, Dan A., Wernberg, T., Oliver, E. C. J., Thomsen, M., Harvey, B. P., Straub, S. C., … Moore, P. J. (2019). Marine heatwaves threaten global biodiversity and the provision of ecosystem services. *Nature Climate Change*, *9*(4), 306–312. https://doi.org/10.1038/s41558-019-0412-1

181) Smale, Dan A., Wernberg, T., Oliver, E. C. J., Thomsen, M., Harvey, B. P., Straub, S. C., … Moore, P. J. (2019). Marine heatwaves threaten global biodiversity and the provision of ecosystem services. *Nature Climate Change 2019 9:4*, *9*(4), 306–312. https://doi.org/10.1038/s41558-019-0412-1

182) Smale, Dan A., Wernberg, T., & Vanderklift, M. A. (2017). Regional-scale variability in the response of benthic macroinvertebrate assemblages to a marine heatwave. *Marine Ecology Progress Series*, *568*, 17–30. https://doi.org/10.3354/meps12080

183) Smale, Dan A., Wernberg, T., Yunnie, A. L. E., & Vance, T. (2015). The rise of Laminaria ochroleuca in the Western English Channel (UK) and comparisons with its competitor and assemblage dominant Laminaria hyperborea. *Marine*

Ecology, *36*(4), 1033–1044. https://doi.org/10.1111/maec.12199

184) Smith, K. E., Burrows, M. T., Hobday, A. J., King, N. G., Moore, P. J., Sen Gupta, A., … Smale, D. A. (2023). Biological Impacts of Marine Heatwaves. *Annual Review of Marine Science*, *15*(December 2022), 119–145. https://doi.org/10.1146/annurev-marine-032122-121437

185) Sousa, M. C., Ribeiro, A., Des, M., Gomez-Gesteira, M., deCastro, M., & Dias, J. M. (2020). NW Iberian Peninsula coastal upwelling future weakening: Competition between wind intensification and surface heating. *Science of the Total Environment*, *703*, 134808. https://doi.org/10.1016/j.scitotenv.2019.134808

186) Starko, S., Soto Gomez, M., Darby, H., Demes, K. W., Kawai, H., Yotsukura, N., … Martone, P. T. (2019). A comprehensive kelp phylogeny sheds light on the evolution of an ecosystem. *Molecular Phylogenetics and Evolution*, *136*(April), 138–150. https://doi.org/10.1016/j.ympev.2019.04.012

187) Steneck, R., Graham, M. H., Bourque, B. J., Corbett, D., Erlandson, J. M., Estes, J. A., & Tegner, M. J. (2002). Kelp Forest Ecosystems : Biodiversity , Stability , Resilience and Future. *Environmental Conservation*, *29*(4), 436–459. https://doi.org/10.1017/S0376892902000322

188) Steneck, R. S., Graham, M. H., Bourque, B. J., Corbett, D., Erlandson, J. M., Estes, J. A., & Tegner, M. J. (2002, December). Kelp forest ecosystems: Biodiversity, stability, resilience and future. *Environmental Conservation*, Vol. 29, pp. 436–459. https://doi.org/10.1017/S0376892902000322

189) Stewart, J. R., Lister, A. M., Barnes, I., & Dalén, L. (2010). Refugia revisited: Individualistic responses of species in space and time. *Proceedings of the Royal Society B: Biological Sciences*, *277*(1682), 661–671. https://doi.org/10.1098/rspb.2009.1272

190) Strasser, F., Barreto, L. M., & Kaidi, S. (2022). *Population level variation in reproductive development and output in the golden kelp Laminaria ochroleuca under marine heat wave scenarios*. (September), 1–15. https://doi.org/10.3389/fmars.2022.943511

191) Stuart-Smith, R. D., Edgar, G. J., & Bates, A. E. (2017). Thermal limits to the geographic distributions of shallow-water marine species. *Nature Ecology & Evolution*, *1*, 1846–1852. https://doi.org/10.1038/s41559-017-0353-x

192) Tan, T. T., Song, S. L., Poong, S. W., Ward, G. M., Brodie, J., & Lim, P. E. (2020). The effect of grazing on the microbiome of two commercially important agarophytes, Gracilaria firma and G. salicornia (Gracilariaceae, Rhodophyta). *Journal of Applied Phycology*, *32*(4), 2549–2559. https://doi.org/10.1007/s10811-020-02062-y

193) Teagle, H., Hawkins, S. J., Moore, P. J., & Smale, D. A. (2017). The role of kelp species as biogenic habitat formers in coastal marine ecosystems. *Journal of Experimental Marine Biology and Ecology*, *492*, 81–98. https://doi.org/10.1016/j.jembe.2017.01.017

194) tom Dieck, I. (1992). North Pacific and North Atlantic digitate Laminaria species (Phaeophyta): hybridization experiments and temperature responses. *Phycologia*, *31*(1992), 147–163.

195) tom Dieck, I. (1993). Temperature tolerance and survival in darkness of kelp gametophytes (Laminariales, Phaeophyta) - Ecological and biogeographical implications. *Marine Ecology Progress Series*, *100*(3), 253–264. https://doi.org/10.3354/meps100253

196) Tonsor, S. J., Scott, C., Boumaza, I., Liss, T. R., Brodsky, J. L., & Vierling, E. (2008). Heat shock protein 101 effects in A. thaliana: Genetic variation, fitness and pleiotropy in controlled temperature conditions. *Molecular Ecology*, *17*(6), 1614–1626. https://doi.org/10.1111/j.1365-294X.2008.03690.x

197) Tuya, F., Cacabelos, E., Duarte, P., Jacinto, D., Castro, J. J., Silva, T., … Wernberg, T. (2012). Patterns of landscape and assemblage structure along a latitudinal gradient in ocean climate. *Marine Ecology Progress Series*, *466*, 9–19. https://doi.org/10.3354/meps09941

198) Valladares, F., Matesanz, S., Guilhaumon, F., Araújo, M. B., Balaguer, L., Benito-Garzón, M., … Zavala, M. A. (2014). The effects of phenotypic plasticity and local adaptation on forecasts of species range shifts under climate change. *Ecology Letters*, *17*(11), 1351–1364. https://doi.org/10.1111/ele.12348

199) Vargas, C. A., Lagos, N. A., Lardies, M. A., Duarte, C., Manríquez, P. H., Aguilera, V. M., … Dupont, S. (2017).

Species-specific responses to ocean acidification should account for local adaptation and adaptive plasticity. *Nature Ecology and Evolution*, *1*(4), 1–7. https://doi.org/10.1038/s41559-017-0084

200) Vásquez, J. A., Zuñiga, S., Tala, F., Piaget, N., Rodríguez, D. C., & Vega, J. M. A. (2014). Economic valuation of kelp forests in northern Chile: values of goods and services of the ecosystem. *Journal of Applied Phycology*, *26*(2), 1081–1088. https://doi.org/10.1007/s10811-013-0173-6

201) Vassallo, P., Paoli, C., Rovere, A., Montefalcone, M., Morri, C., & Bianchi, C. N. (2013). The value of the seagrass Posidonia oceanica: A natural capital assessment. *Marine Pollution Bulletin*, *75*(1–2), 157–167. https://doi.org/10.1016/j.marpolbul.2013.07.044

202) Vea, J., & Ask, E. (2011). Creating a sustainable commercial harvest of Laminaria hyperborea, in Norway. *Journal of Applied Phycology*, *23*(3), 489–494. https://doi.org/10.1007/s10811-010-9610-y

203) Veenhof, R. J., Champion, C., Dworjanyn, S. A., Wernberg, T., Minne, A. J. P., Layton, C., … Coleman, M. A. (2022). Kelp gametophytes in changing oceans. In *Oceanography and Marine Biology: An Annual Review, Volume 60*. https://doi.org/10.1201/9781003288602-7

204) Veenhof, R. J., Dworjanyn, S. A., Champion, C., & Coleman, M. A. (2022). Grazing and Recovery of Kelp Gametophytes Under Ocean Warming. *Frontiers in Marine Science*, *9*(April), 1–12. https://doi.org/10.3389/fmars.2022.866136

205) Voerman, S. E., Llera, E., & Rico, J. M. (2013). Climate driven changes in subtidal kelp forest communities in NW Spain. *Marine Environmental Research*, *90*, 119–127. https://doi.org/10.1016/j.marenvres.2013.06.006

206) Wernberg, T. (2021). *Marine Heatwave Drives Collapse of Kelp Forests in Western Australia*. https://doi.org/10.1007/978-3-030-71330-0_12

207) Wernberg, T., Coleman, M. A., Bennett, S., Thomsen, M. S., Tuya, F., & Kelaher, B. P. (2018). Genetic diversity and kelp forest vulnerability to climatic stress. *Scientific Reports*, *8*(1), 1–8. https://doi.org/10.1038/s41598-018-20009-9

208) Wernberg, T., Kendrick, G. A., & Toohey, B. D. (2005). Modification of the physical environment by an Ecklonia radiata (Laminariales) canopy and implications for associated foliose algae. *Aquatic Ecology*, *39*(4), 419–430. https://doi.org/10.1007/s10452-005-9009-z

209) Wernberg, T., Krumhansl, K., Filbee-Dexter, K., & Pedersen, M. F. (2019). Chapter 3: Status and trends for the World´s Kelp Forests. In *World Seas: An Environmental Evaluation* (pp. 57–78).

210) Wernberg, T., Smale, D. A., Tuya, F., Thomsen, M. S., Langlois, T. J., Bettignies, T. de, … Rousseaux, C. S. (2012). An extreme climatic event alters marine ecosystem structure in a global biodiversity hotspot. *Nature Climate Change*, *3*(1), 78–82. https://doi.org/10.1038/nclimate1627

211) Wiencke, C., Bischoff, B., Bartsch, I., Peters, A. F., & Breeman, A. M. (1994). Temperature Requirements and Biogeography of Antarctic, Arctic and Amphiequatorial Seaweeds. *Botanica Marina*, *37*(3), 247–260. https://doi.org/10.1515/botm.1994.37.3.247